HE
18.5
.A34
no.
DOT
TSC
NHTSA
75-2

PB 244 309

Dept. Of Transportation
OCT 5 1975

NO. HS-801 521

ANALYSIS OF AUTOMOBILE CRASH TEST DATA AND RECOMMENDATIONS FOR ACQUIRING AND FILTERING ACCELEROMETER DATA

Frank P. DiMasi

JUNE 1975
FINAL REPORT

DOCUMENT IS AVAILABLE TO THE PUBLIC THROUGH THE NATIONAL TECHNICAL INFORMATION SERVICE, SPRINGFIELD, VIRGINIA 22161

Prepared for
U.S. DEPARTMENT OF TRANSPORTATION
NATIONAL HIGHWAY TRAFFIC SAFETY ADMINISTRATION
Research and Development
Washington DC 20590

NOTICE

This document is disseminated under the sponsorship of the Department of Transportation in the interest of information exchange. The United States Government assumes no liability for its contents or use thereof.

NOTICE

The United States Government does not endorse products or manufacturers. Trade or manufacturers' names appear herein solely because they are considered essential to the object of this report.

TA 18.5 .A54 no. DOT-TSC-NHTSA-75-2
DEC 5 1975

Technical Report Documentation Page

1. Report No.	2. Government Accession No.	3. Recipient's Catalog No.
HS-801 521		

4. Title and Subtitle	5. Report Date
ANALYSIS OF AUTOMOBILE CRASH TEST DATA AND RECOMMENDATIONS FOR ACQUIRING AND FILTERING ACCELEROMETER DATA	June 1975
	6. Performing Organization Code
7. Author(s) Frank P. DiMasi III	8. Performing Organization Report No. DOT-TSC-NHTSA-75-2
9. Performing Organization Name and Address U.S. Department of Transportation, Transportation Systems Center, Kendall Square Cambridge MA 02142	10. Work Unit No. (TRAIS) HS507/R5408
	11. Contract or Grant No.
	13. Type of Report and Period Covered Final Report July 1973-June 1974
12. Sponsoring Agency Name and Address U.S. Department of Transportation National Highway Traffic Safety Administration Research and Development Washington DC 20590	14. Sponsoring Agency Code

15. Supplementary Notes

16. Abstract

An attempt is made to define the meaningful frequency content of occupant compartment deceleration data in order to establish effective filtering guidelines which will enhance the important features of the deceleration pulse.

Acceleration and displacement spectral distributions of crash test and structural resonance data are compared to assess the presence and effects of resonances in the deceleration time history. A typical accelerometer package - floor pan configuration is modeled to characterize resonant modes associated with current accelerometer package size and mounting. Guidelines are suggested for partitioning data frequency content based on these analyses and also on the comparative effects of high and low frequency decelerations on occupant loading.

An alternative method to analog filtering of crash data, which employs a least squared error polynomial curve fitting routine, has been developed and is described. This method has the desired capability to partition the data frequency content into decelerations associated with gross vehicle crush, and residual high-frequency, low displacement amplitude decelerations associated with structural resonances, without discarding any data. Applications of the method to crash test data are presented.

17. Key Words	18. Distribution Statement
Crash Testing, Filtering Guidelines Resonance Effects, Standardized Instrumentation Methodology, Curve Fitting of Crash Data	DOCUMENT IS AVAILABLE TO THE PUBLIC THROUGH THE NATIONAL TECHNICAL INFORMATION SERVICE, SPRINGFIELD, VIRGINIA 22161

19. Security Classif. (of this report)	20. Security Classif. (of this page)	21. No. of Pages	22. Price
Unclassified	Unclassified	94	

Form DOT F 1700.7 (8-72) Reproduction of completed page authorized

PREFACE

The work described herein has been prepared at the Transportation Systems Center, Cambridge, Massachusetts, and was sponsored by the National Highway Traffic Safety Administration under Project Plan Agreements No. HS-412 entitled "Instrumentation Methodology for Automobile Crash Testing," and No. HS507 entitled "Analytical Crashworthiness." This work is directed towards the development of a standardized instrumentation methodology for the purpose of defining and obtaining maximum useful structural data from automobile crash testing.

Program direction was administered by the sponsor Program Manager, Mr. Glen Brammeier of the Research Institute's Office of Vehicle Structures Research. The TSC Task Manager was Dr. Herbert Weinstock of the Office of Engineering.

The author would like to thank Dr. Robert Wassmuth of Kentron Hawaii, Ltd. Scientific Division, Cambridge MA for his support in developing the least squared error polynomial curve fitting program and adapting it for application to crash test data. Appendix C, which describes the mechanics of the orthogonal polynomial method used and a program listing, has been provided by Dr. Wassmuth.

CONTENTS

LIST OF ILLUSTRATIONS

LIST OF ILLUSTRATIONS (CONT'D)

LIST OF ILLUSTRATIONS (CONT'D)

LIST OF TABLES

1. INTRODUCTION

A review of current automobile crash testing instrumentation methodologies and principal characteristics of automobile crash dynamics as related to occupant sruvivability was reported in Reference 1. Problems in comparing test data based on differences in test methodologies and current filtering practices were identified, and recommendations for standardized data acquisition parameters and techniques were outlined.

The motion characteristics of the occupant compartment obtained from accelerometer data are of prime importance in evaluating the crash ride-down dynamics. Because of the basic importance of this parameter, it is also valuable as a basic comparison parameter between full-scale crash tests of different vehicle structural configurations and between full scale crash tests and computer simulation model predictions. Principal characteristics of the deceleration pulse shape, such as basic pulse shape, onset rate, duration, and average and peak values, are often obscured, however, by the presence of high frequency content; this causes problems in evaluating these characteristics, as well as in comparing and interpreting the data. The character of the high frequency content has been previously examined (Ref. 1) and is attributed to localized resonances of the vehicle structure and/or accelerometer package mounting resonances.

This report attempts to define the meaningful frequency content of occupant compartment deceleration data, based on an analysis of the comparative effects of high and low frequency deceleration on occupant loading.

The size of certain accelerometer package configurations may be inducing some of the high frequency content observed. A calculation of the approximate rocking mode natural frequency for a typical accelerometer package configuration and an approximated floor pan geometry was made (Appendix A). This calculation indicates that rocking mode resonances in the range of 30 Hz are likely to exist, and that the resulting accelerations

from such a resonance can be of the same order of magnitude as the (excitation) accelerations due to vehicle gross plastic deformation.

Quantification of these effects is a necessary step in developing filtering specifications and accelerometer package and mounting configurations which will enhance the important features of the deceleration pulse by eliminating high frequency content.

1.1 SUMMARY

A spectrum analysis of occupant compartment deceleration data was performed on data from a specific crash and compared with the spectral distribution of occupant compartment accelerations taken from the same vehicle, subjected to mild structural impacts to excite structural resonances. A comparison of spectral density peak level frequencies in the crash data and structural excitation data indicates close correlation of frequencies. This correlation, in addition to the low displacement amplitudes associated with higher frequencies in crash test data, indicates that these accelerations are due to structural resonances and should be considered mechanical noise. Analysis of a typical accelerometer package/floor pan configuration (Appendix A) indicates that large accelerometer package weight and profile are probably inducing rocking mode resonances well within current filtering bandwidths and contributing to the high frequency noise problem (e.g. a 30 Hz resonance was calculated within the 115 Hz bandwidth associated with SAE j211a Class 60 filter).

Independent of the source of high frequency content (i.e. resonances and/or stepwise vehicle crush), the effect of high frequency accelerations on occupant loading has been approximated and found to be insignificant for the data analyzed when compared to the maximum ride-down loads sustained during gross vehicle crushing. A similar analysis of occupant compartment deceleration data is recommended as a guide to determine the meaningful frequency content of occupant compartment deceleration data.

A possible alternative to analog filtering, which employs a least squared error polynomial curve fitting routine with limited frequency response capability, has been developed and is described herein. Figure 1-1 illustrates the application of the curve fitting program to a typical crash test deceleration pulse. The frequency content has essentially been partitioned into residual higher frequency acclerations and a low frequency pulse, which clearly indicates principal pulse characteristics, such as pulse shape, onset rate, peak magnitude and duration. Note that data has not been discarded, but simply separated. This method has much potential in filtering applications and has many advantages when compared to current analog filtering processes.

Since the crash test data obtained for use in this analysis were necessarily retrofit data, a test plan has been outlined (Appendix B) for acquiring and analyzing a battery of crash test data from a single source. The test plan also contains recommended structural data reduction operations, which may prove valuable in assessing vehicle structural performance.

1.2 RECOMMENDATIONS

(a) Occupant compartment deceleration data should be filtered at lower frequencies than current practice. Cut-off frequencies should be determined, based on the relative effects of high and low frequency content on occupant loading as outlined herein.

(b) Accelerometer packages used in current practice appear to be too large and are probably responsible for inducing structural resonances. Lightweight, low profile accelerometer packages should be used and mounted to the stiffest possible location near the driver and passenger locations in the occupant compartment.

(c) The instrumented test vehicle should be subjected to a mild structural excitation corresponding to the direction of impact, as described below. Accelerometer outputs should be recorded and analyzed to determine the existing resonant frequencies associated with the local structure and mountings at each location. These data should aid in establishing filter

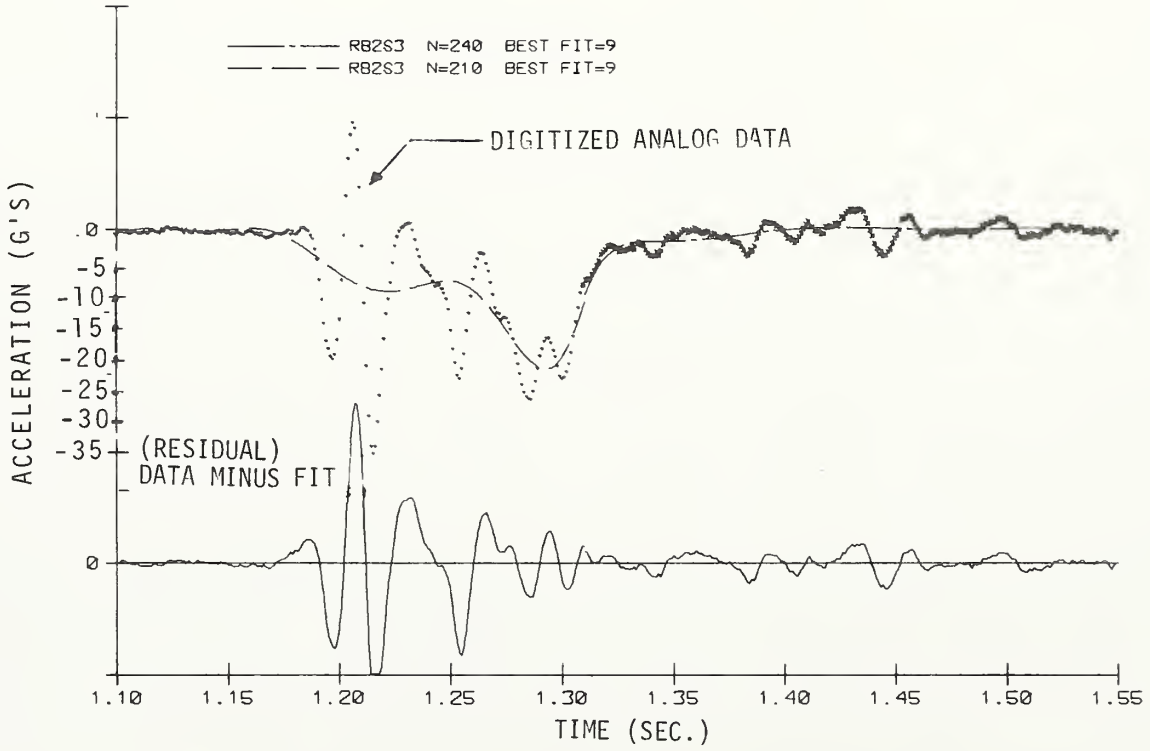

Figure 1-1. Application of Polynomial Curve Fitting Program to Crash Test Data

cut-off frequencies for the crash test data. If pre-crash data resonances are particularly strong or low in frequency these data will serve as a warning to relocate the transducer. The structural excitation should not cause plastic deformation.

The recommended method of exciting the structure is by installation of a small inertial force generating device (i.e., small electrodynamic shaker) at each normal accelerometer mounting location, and sweeping frequency until resonances are detected and noted. It may also be possible to excite the structure by mildly impacting the structures as follows:

(1) Vertically - dropping the vehicle frame onto metal (with plywood facing) or wood blocks from a height which will generate reasonalbe acceleration signal levels (e.g., 5 to 15 g's).

(2) Longitudinally - subject bumper to 5 mph pendulum test. Alternate method would be to use an adaptor fixture to excite the frame.

(3) Laterally - subject frame to 5 mph pendulum test using an adapter fixture to reach frame.

(d) As an alternative to analog filtering of occupant compartment crash test data the polynomial curve fitting method described in this report should be utilized on a trial basis. This routine effectively partitions the data into low and high frequency bands. This method provides polynomial representation and plotting of the low frequency content which describes the vehicle gross deformation during impact. Residual (i.e., filtered) high frequency data are retained and plotted separately.

(e) A test plan is outlined (Appendix B) for acquiring and analyzing test data to establish meaningful filter cut-off frequencies for occupant compartment deceleration data and assessing the effects of accelerometer package size. Recommendations are also made for reducing basic data acquisition parameters to generate quantities which may be valuable in assessing vehicle structural performance. The data from this test will be analyzed, filtered and compared with a polynomial fit to the same data.

Other recommendations (repeated from Ref.1) are:

(f) The use of a mechanical filter (i.e., an accelerometer package mounted in a C.G. vibration isolation system) should be evaluated in an experimental program, in parallel with standard accelerometer mounting/filtering practices. Such a configuration could, for example, attenuate vibratory motions above some pre-selected frequency at the rate of 12dB/octave. The accelerometer mounting system would isolate low displacement motions typically in the order of $\pm$ 0.1 inch. For motions greater than $\pm$ 0.1 inch, the isolation system stiffness should increase (by using a non-linear load-deflection curve), and the accelerometer would track the larger displacement motions. This approach offers the possibility of eliminating electronic (or digital) filtering altogether. The development of such a mechanical filter would require a moderately low investment. The consequence of the mechanical resonance of the filter would have to be investigated; however, the known relationship between the input/output characteristics of the filter at resonance may be adequate to offset this disadvantage.

(g) The use of damping material added to the structure in the area of the transducer mounting location should be considered in an experimental program. Depending on the required filtering characteristics (as determined by the test objective) it may be possible to filter out a potential resonance, or to relocate a transducer to an area which has a better frequency response. In general, the use of damping material causes transients to die out much faster, and damping materials therefore have a potentially useful function in crash testing. It is recommended that this technique be evaluated and its usefulness quantified in an experimental program.

(h) Until the requirements for filtering occupant compartment data have been adequately quantified, the emphasis on peak acceleration levels should be removed.

2. SPECTRUM ANALYSIS OF OCCUPANT COMPARTMENT ACCELEROMETER DATA

Previous examination of occupant compartment accelerometer data (Ref.1) illustrated that frequency content in excess of what is termed the filter cutoff frequency (Ref. 2) often appears in the deceleration time history. Furthermore, the small displacement amplitudes (typically ± 0.10 inches or less) associated with higher frequency acceleration components strongly implies that they are a result of small elastic resonances of the structure in the area of the accelerometer mounting. Figure 2-1, an extreme situation, illustrates the problem. This figure shows the longitudinal deceleration pulse measured at the driver and passenger floor pan locations. The data are from a 1972 Chevrolet Impala subjected to a 15 mph frontal barrier impact (Ref. 3). The floor pan area of this vehicle was described as "flimsy" and the response was interpreted to contain a floor pan resonance. Simple analysis of the nearly sinusoidal 57 Hz resonant acceleration indicates an oscillatory displacement amplitude of approximately ± 1/8 inch corresponding to the maximum peak-to-peak acceleration of 44g's (lower trace, 60-70msec). This is a clear example of the type of structural response which often confuses the interpretation of crash test data, especially when peak acceleration is used as an evaluation parameter. Figure 2-2 represents the longitudinal deceleration pulse measured at the driver and floor pan locations of a 1972 Ford Galaxy, subjected to the identical 15 mph frontal barrier impact test (Ref. 3). The features of this deceleration pulse are much more distinct. Note that the peak acceleration is only 12 g's in contrast to 20 g's in Figure 2-1. The problem of exciting structural resonances is further compounded when the impact speed range is increased from the 15 mph speed discussed here.

The effect of resonances masks such important deceleration characteristics as general pulse shape, onset range, duration, and the maximum and average decelerations associated with the gross

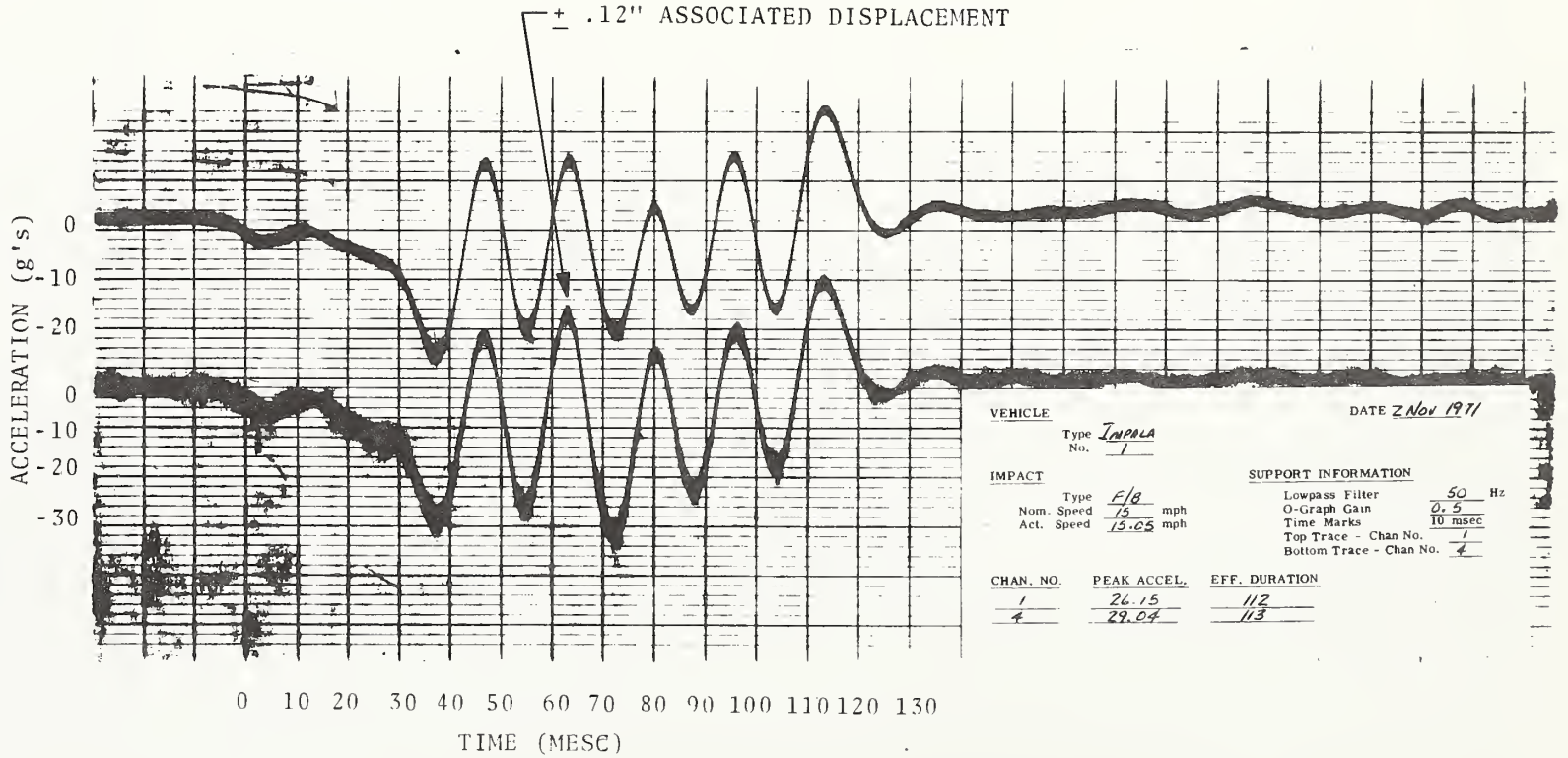

Figure 2-1. Occupant Compartment Longitudinal Deceleration, Chevrolet Impala (Ref. 3)

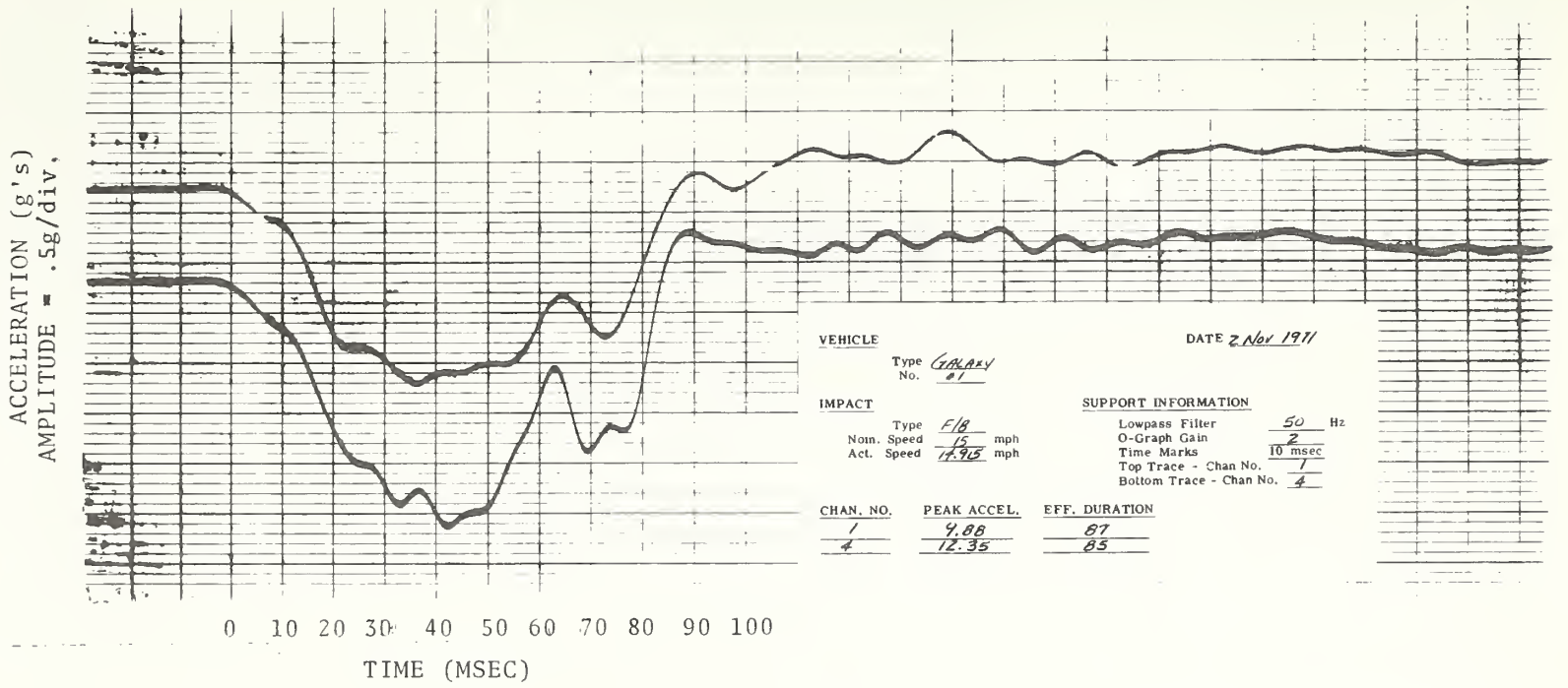

Figure 2-2. Occupant Compartment Longitudinal Direction, Ford Galaxy (Ref.3)

plastic deformation of the vehicle. Interpretation and the usefulness of deceleration data for comparison purposes are made very difficult by the presence of high frequency content. Filtering practices must be developed such that the important characteristics of the deceleration time history become more visible and low displacement amplitude noise sources are eliminated. If through analysis and/or an experimental program a definition of the source of spectral components and their relative effects on occupant loading can be accomplished, a basis will exist for specifying the desirable spectral content and the corresponding filtering characteristics.

As an example of the type of resonance which might be excited during impact, a resonance mode that is probably contributing to the problem is calculated in Appendix A. Here, the "rocking mode" (combined rotational/translational motion resulting from translational forces) resonance is approximated using an accelerometer package configuration similar to that used by Calspan and Dynamic Science, and an "equivalent effective structure" approximating the floor pan flexural rigidity. The relatively heavy package weight and high center of gravity result in a coupled longitudinal/rotational mode of vibration at approximately 32 Hz, well within the bandwidth of current filtering practices. Furthermore, the assumed 20 g impulsive excitation of the system results in an acceleration level due to the resonant motions of 20 g's peak-to-peak, i.e., of the same magnitude as the imput acceleration. The displacement amplitude associated with the resonant motion is seen to be $\pm$ 0.10 inches. Based on this analysis and the similar displacement amplitude and frequency characteristics associated with higher frequency motions observed in occupant compartment accelerometer data, accelerometer package mass and profile should be reduced relative to existing configurations. Also, the package should be mounted to the stiffest structural location near the occupant locations. General Motors (SRDL) uses a triaxial accelerometer package weighing approximately 5 oz, which also has a very low profile. The package is mounted on the side sills, forward of the front seat edge at the driver and front

passenger locations. The combination of a much smaller accelerometer package and what appears to be a substantially stiffer location should produce a much cleaner representation of vehicle kinematics due to gross plastic deformation. In order to help establish appropriate filtering characteristics, it is strongly recommended that the instrumented vehicle be subject to a mild pre-impact excitation similar to that which it will experience in the impact test. Accelerometer output data should be analyzed to determine the existance of low frequency resonances and allow modifications in transducer location or mounting to be made prior to impact, in order to reduce the effect of resonances.

The following steps are generally required to develop appropriate filtering practices for each acquisition parameter:

(a) Principal characteristics of the data as related to evaluation of a test objective must be defined.

(b) Frequency content associated with the principal evaluation characteristics should be defined by identifying the kinematic features (i.e., displacement velocities and accelerations) associated with the principal characteristics. Identification of noise sources must also be identified in this manner.

(c) Having made the above determinations, a basis exists for tailoring appropriate filtering characteristics to each data acquisition parameter.

A spectrum analysis of crash test data and structural excitation data has been performed to relate various frequency components in the deceleration time history with physical events in the structure. Occupant compartment deceleration data, a principal data acquisition parameter, are considered here. A typical frontal barrier impact of an unmodified full size car will have a duration of approximately 100 ms. and the vehicle will crush a distance which is approximately proportional to impact speed. Filtering characteristics for this parameter should be such that the kinematics associated with gross vehicle crush are separated from those due to noise.

Noise should be defined as frequency content, which has little or no effect on vehicle ride-down displacement (crush) time history or on occupants. For the configuration of a frontal barrier crash, which simplifies the analysis process, it is readily apparent that the only forces acting on the occupant are applied through the restraint system (assuming second collisions do not occur) as a result of relative motions between vehicle and occupant during crash ride-down. Forces resulting from displacements associated with gross vehicle deformation are much greater than those associated with high frequency displacements. The force transmissibility characteristics of seatbelts is another consideration. Typical belt compliance (as much as 20 inches of static deflection for upper torso and pelvic restraints when subjected to a combined 4000 lb tensile load, Ref. 4) is such that it acts as a filter when subjected to small, high frequency relative displacements. Figures 2-3 through 2-7 (Refs.5 and 6) show some typical seatbelt load time histories from crashes where second collisions did not occur. The responses shown are basically half-sine or haversine in nature, with a period corresponding to 6 to 10 Hz depending on how the sine wave approximation is made. A similar characterization of seatbelt response has been made in Ref. 7. The "equivalent" period was approximated by extending the downward slope of the seatbelt data through the zero intercept of the abscissa. The "quarter period" associated with the pulse was taken as a difference in time between the zero crossing and the peak load. The approximated response calculated (Ref.7) was 9.3 Hz for the data presented in that report. Approximating the "quarter period" associated with the seatbelt response data for Figure 2-7, $t/4 \simeq (1.25 \text{ div})\ (.02 \text{ sec/div}) = .025$ sec. The corresponding response frequency is about 10 Hz. This approximation is meaningful because it can be used as a guide to assessing the transmissibility characteristics of typical lap/shoulder belt systems. Using the figures derived above, the belt will filter frequencies higher than 1.41 times the natural frequency, i.e. 14 Hz. This cursory approximation is useful in assessing the frequency range

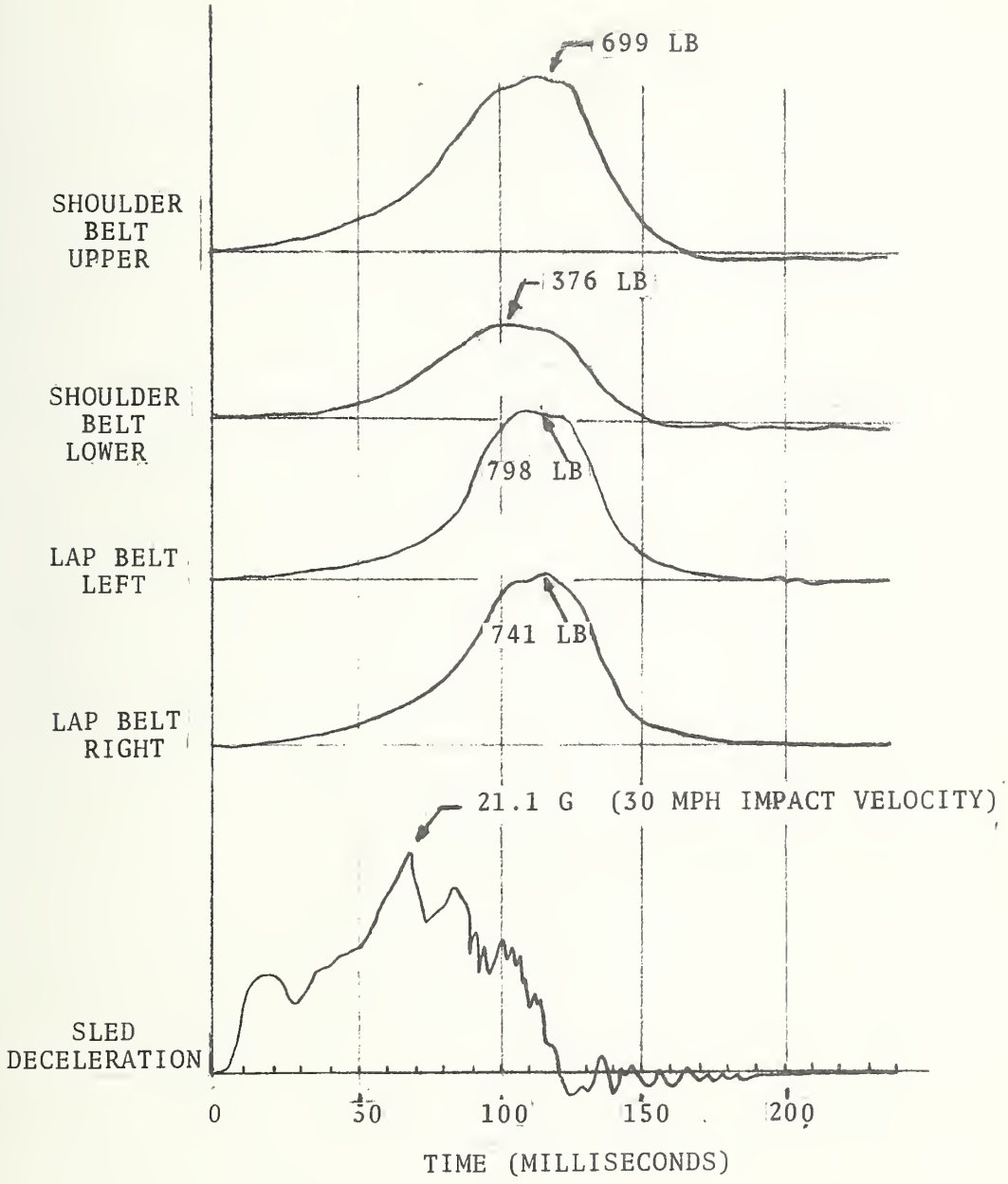

Figure 2-3. Seatbelt Loads and Deceleration Profile Corresponding to Sled Testing with Human Volunteers (Ref. 5)

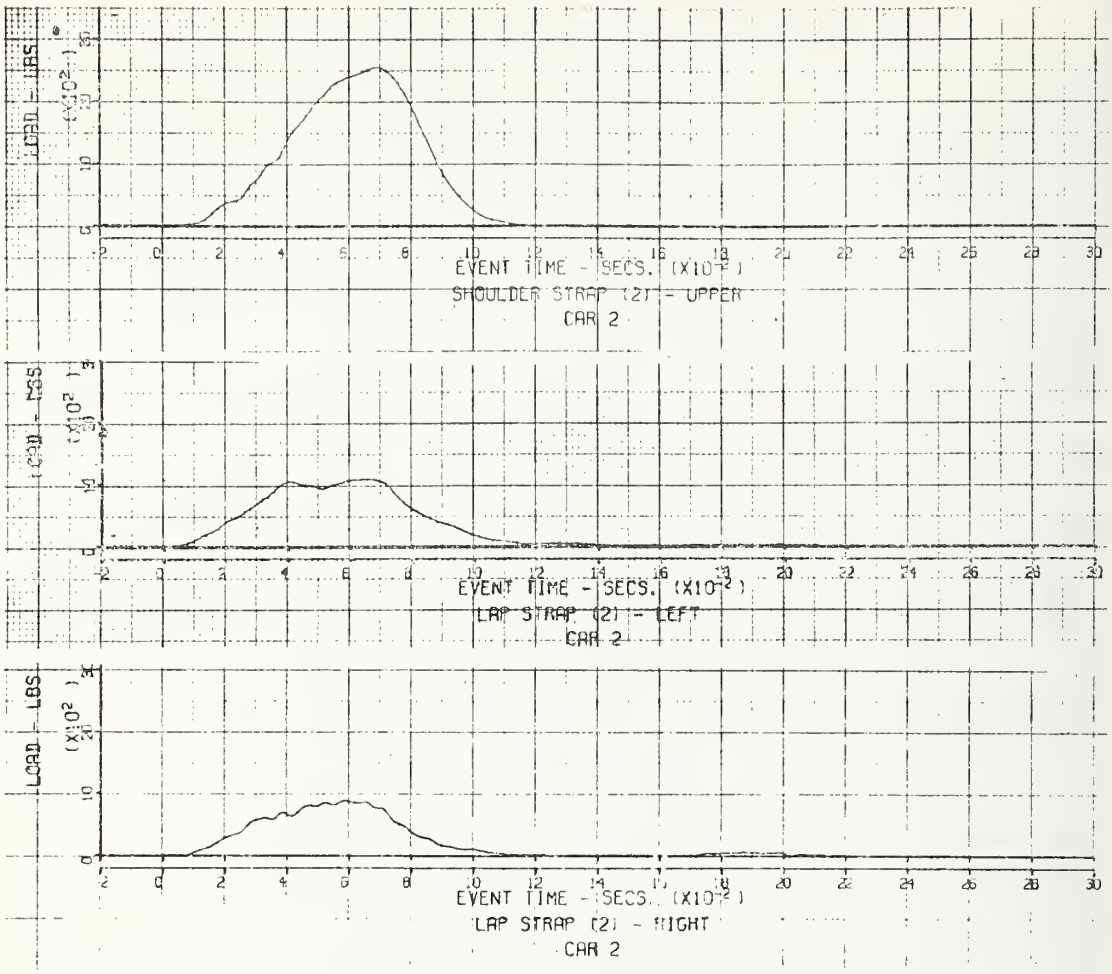

RESTRAINT SYSTEM FORCES

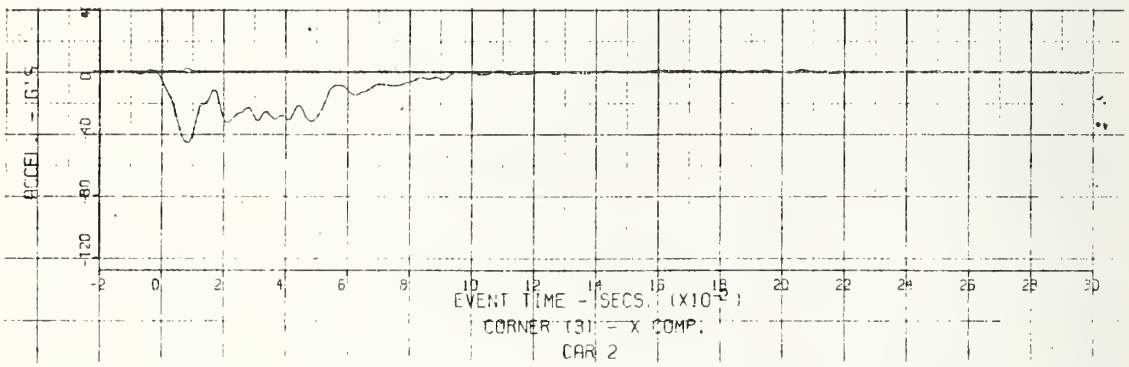

PASSENGER COMPARTMENT ACCELERATION

Figure 2-4. Seatbelt Loads and Deceleration Profile - Test No. 88, Frontal Car-Car, 80 MPH Closing Speed, Modified '72 Ford (Ref. 6)

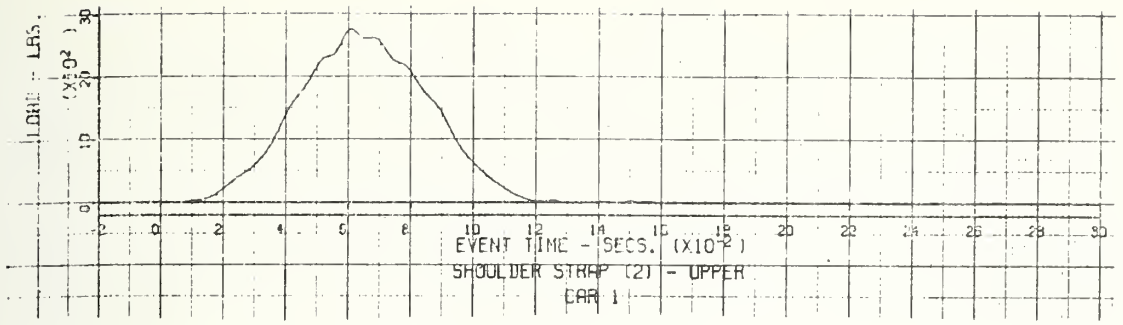

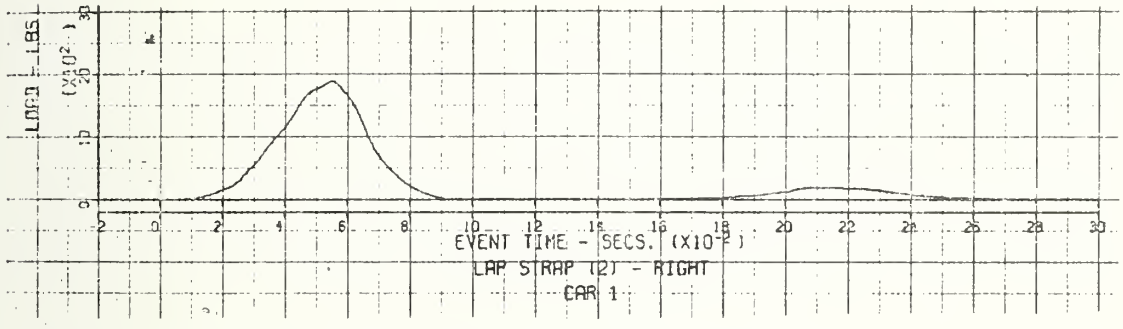

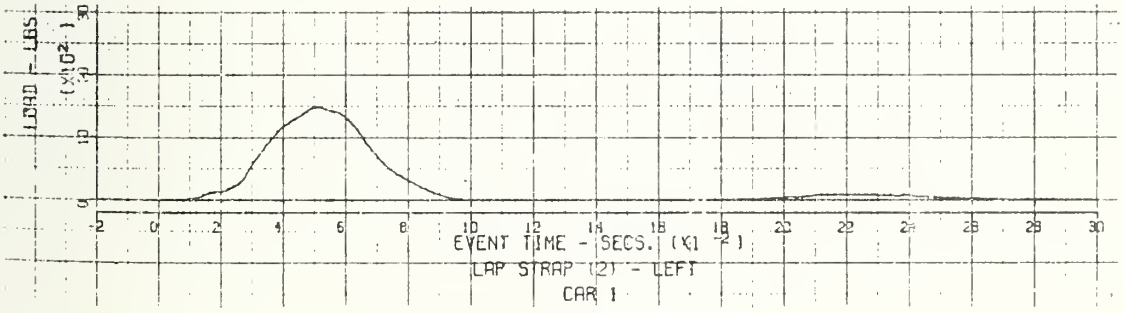

RESTRAINT SYSTEM FORCES

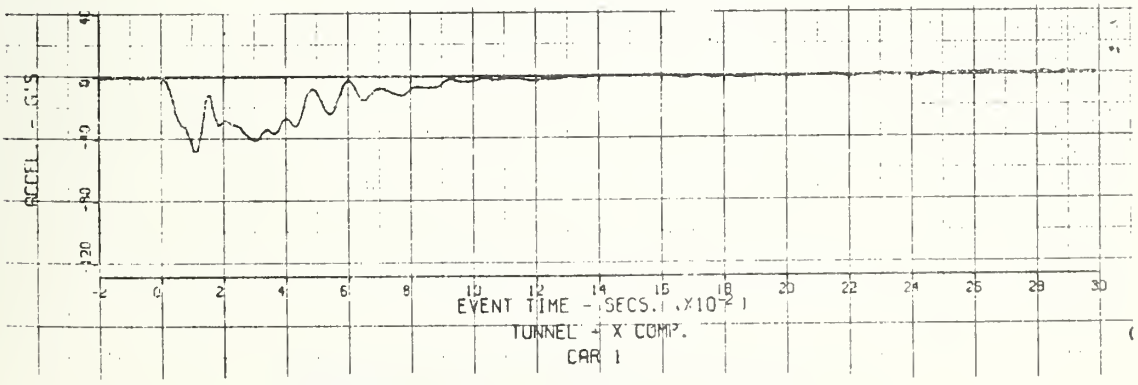

PASSENGER COMPARTMENT ACCELERATION

Figure 2-5. Seatbelt Loads and Deceleration Profile - Test No. 81, Frontal Car-Car, 80 MPH Closing Speed, Modified '72 Ford (Ref. 6)

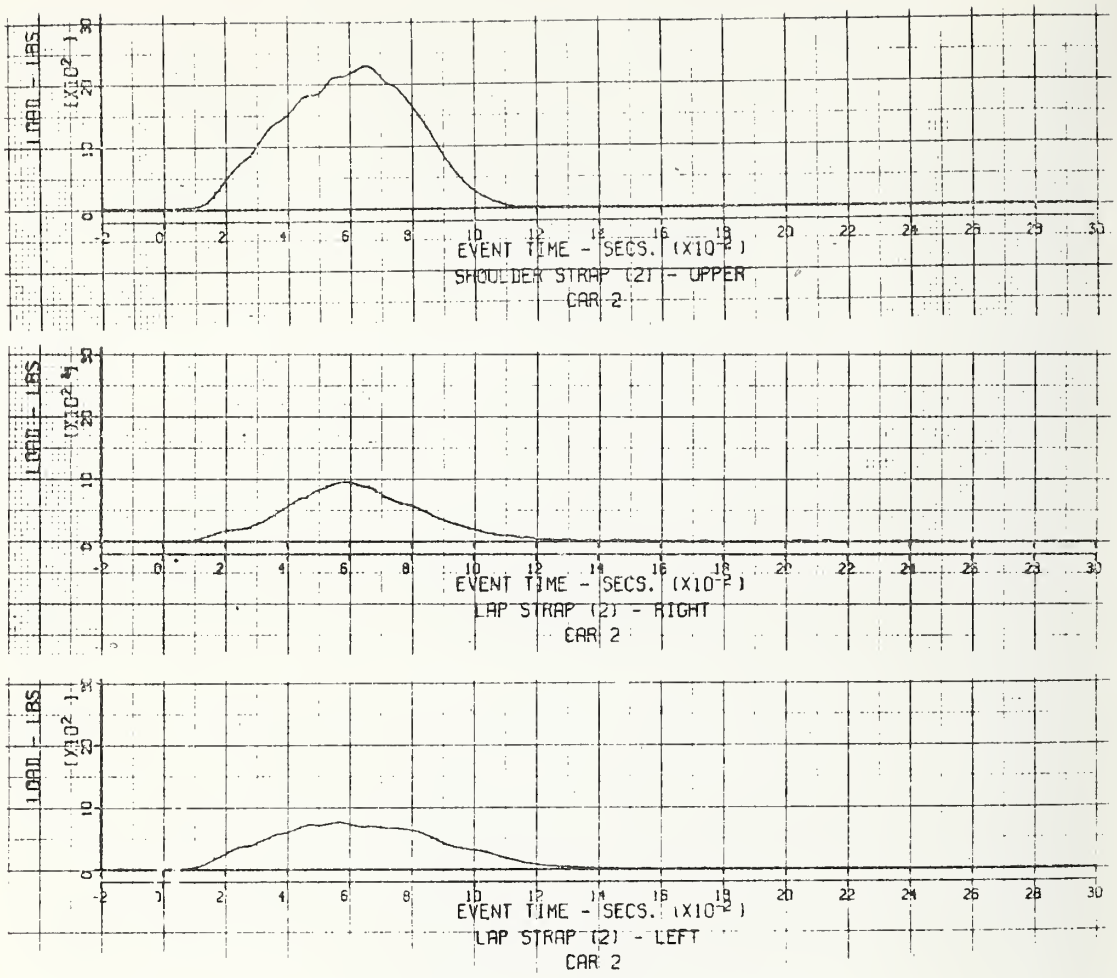

RESTRAINT SYSTEM FORCES

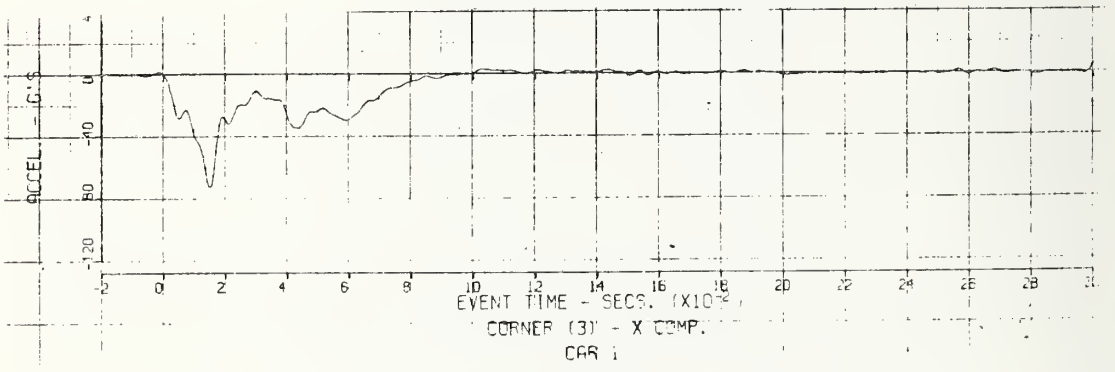

PASSENGER COMPARTMENT ACCELERATION

Figure 2-6. Seatbelt Loads and Deceleration Profile - Test No. 86, Frontal Car-Car, 80 MPH Closing Speed, Modified '72 Ford (Ref. 6)

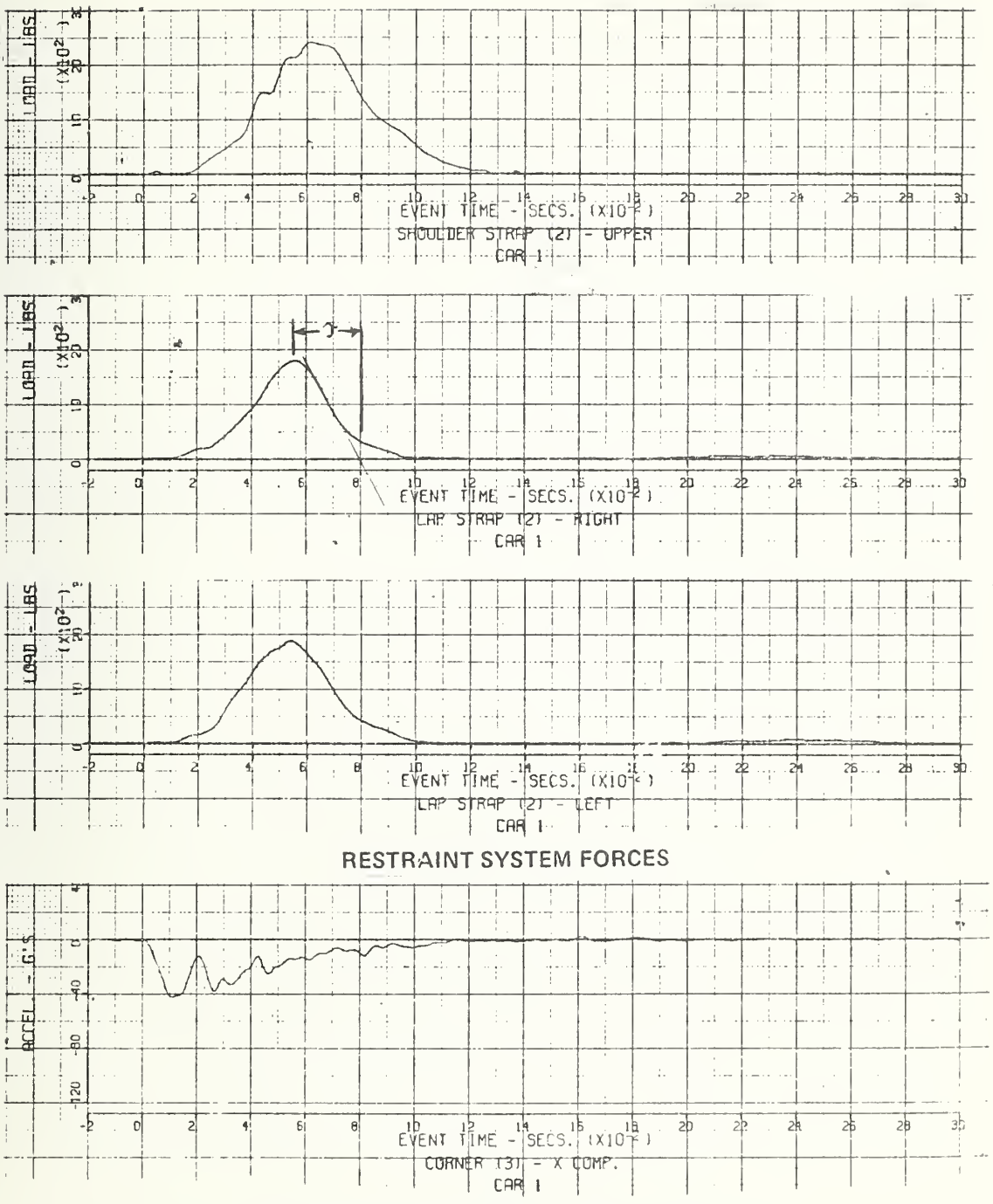

Figure 2-7 Seatbelt Loads and Deceleration Profile - Test No. 83, Frontal Car-Car, 80 MPH Closing Speed, Modified '72 Ford (Ref. 6)

of motions to which an occupant may be subjected, which in turn will be a useful input to specifying filtering characteristics for occupant compartment acceleration. Another factor affecting the transmission of oscillatory forces through the belts is the lag between peak vehicle and occupant decelerations resulting from seatbelt slack and stretching. Considering an airbag system, the occupant is, of course, completely decoupled from the vehicle structure, and high frequency content in the deceleration time history is even less significant.

A spectrum analysis of crash test data and of corresponding structural resonance data has been performed to analyze the frequency content of typical deceleration time history pulses. The object is to relate frequency content to gross vehicle deformation or to elastic resonances of the structure and to calculate displacements associated with these motions.

For this purpose, crash test and structural excitation data have been purchased on magnetic tape from Calspan Corporation. The data consist of structural acceleration response data taken from various locations on the vehicle, with emphasis on occupant compartment data. Responses to both the crash environment and to mild excitations of the structure, intended only to excite structural resonances, have been obtained. Guidelines for selecting and preparing crash test data for analysis were as follows:

(a) data from an unmodified production type vehicle was preferred to data from structurally modified vehicles;

(b) test mode was to be frontal and symmetrical with respect to the vehicle longitudinal axis, and impact speed was to be such that gross vehicle deformations would be limited to the front structure with little or no deformation of the occupant compartment occuring; and

(c) all data were to be supplied in raw, unfiltered form and recorded on one inch, fourteen channel magnetic tape using IRIG intermediate band format.

The primary requirement was (b), because this configuration limits large plastic deformation to the front structure and displacements within the occupant compartment to small elastic motions. Occupant compartment deceleration data from opposite sides of the vehicle, but at the same longitudinal station, can be analyzed for this situation to establish the in-phase and out-of-phase spectrum content. In-phase components are those associated with the overall vehicle ride-down motions, while out-of-phase components are attributed to localized, low displacement amplitudes structural resonances.

An ideal test configuration for the above conditions would involve a full size standard vehicle subjected to a frontal barrier test at approximately 30 mph. This would provide the deformation pattern described above with an apprecialbe amount of front structure crush (approximately two feet). The data for this analysis were somewhat limited, however, since the results of only a few crash tests of this nature were available. In addition to provide post-test structural resonance data it was necessary that the crashed vehicle be intact and undamaged in the transducer location areas (especially the occupant compartment) and in the possession of the vendor. The more ideal methodology would be to obtain pre-crash resonance data in the manner developed with Calspan (to be described) for a specified crash configuration. Appendix B contains a suggested test plan for obtaining and analyzing crash test data in a more precise manner. This is intended to be performed in parallel with a scheduled frontal barrier test, such as an FMVSS 208 compliance test. Enough data have been collected and analyzed in this report, however, to establish that substantial structural resonances exist within the bandwidth of current structural data filtering practices.

Data were obtained from Calspan for two frontal impact situations. Data from a 1970 Ford impacting an AMF modified Hornet in a side impact test at 25 mph were obtained. The 1970 Ford experienced only a few inches of crush in this test, and because of the low level of deformation, structural resonance data

were obtainable from this vehicle. Accelerometer packages were re-installed in the crashed vehicle at the four corner locations of the occupant compartment and at the tunnel (i.e. c.g.) and engine locations. The structure was excited in the longitudinal direction using a 5 mph bumper pendulum test, and in the vertical direction by raising the vehicle frame over four wooden blocks and dropping the vehicle onto the blocks. Photographs of the impact configuration and front structure damage to the 1970 Ford are shown in Figure 2-8. Figure 2-9 describes the location of the accelerometer packages within the occupant compartment and the setup for exciting the vehicle in the longitudinal and vertical directions. Longitudinal and vertical accelerations resulting from the mild structural excitations were measured at all locations (6 total) and recorded on magnetic tape for purposes of analysis. Crash test data are shown in Table 2-1.

Data from a second crash test were also obtained from Calspan. In this test, another 1970 Ford, which had been modified to essentially reproduce the front structure developed for full size automobiles during Canspan's Basic Research in Crashworthiness project, was subjected to a 50 mph frontal barrier test. The overall vehicle crush distance associated with this crash was 33-3/4 inches. The occupant compartment experienced moderate deformation as a result of this test, as described in Table 2-2, which indicates approximately 7-1/2 inches of crush in the front section and virtually zero crush in the rear section of the occupant compartment. Unfortunately, good photographic descriptions of occupant floor deformation were not available. Photographs depicting overall crash damage are included in Figure 2-10. Crash test data obtained from this test data are described in Table 2-3.

The analog operations (i.e., averaging, differences, and integrations) contained in Tables 2-1 and 2-3 were included to assess effects of signal averaging and to determine the in-phase spectral components. For the symmetrical (with respect to vehicle longitudinal axis) frontal test situation motions associated with gross vehicle ride-down must necessarily be in-phase when there

(a)

(b)

Figure 2-8. Crash Configuation and Resulting Structual Damage to 1970 Ford

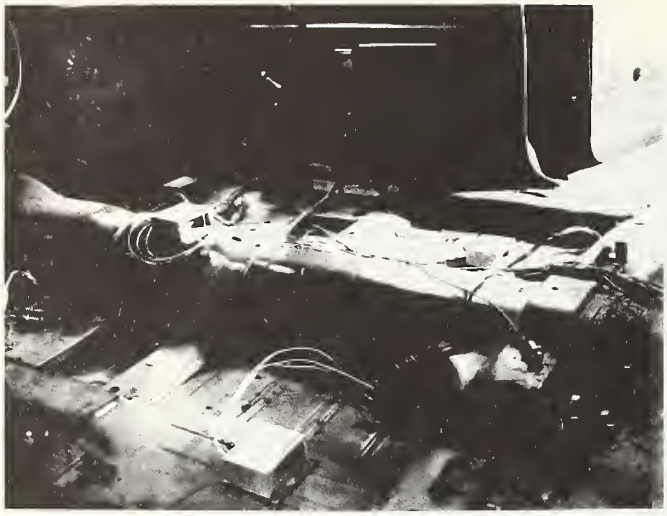

(a) Accelerometor Package Locations and Mounting Configuration

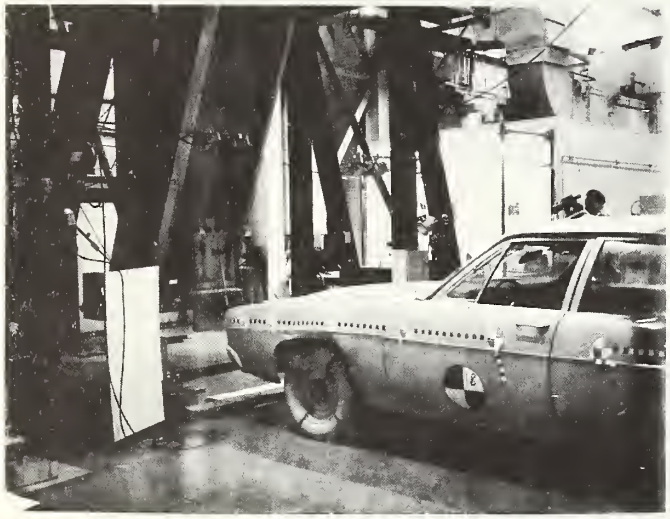

(b) Vehicle Logitudinal Structural Excitation with Pendulum

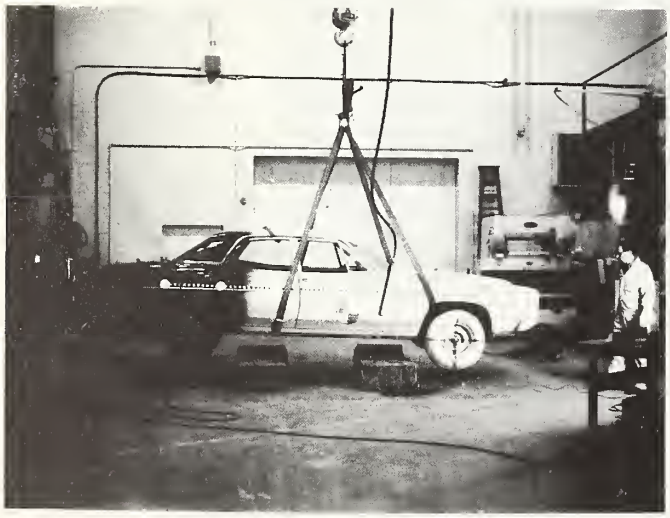

(c) Vehicle Vertical Structural Excitation Configuration

Figure 2-9. Structural Excitation of 1970 Ford

TABLE 2-1. CRASH TEST DATA: 1970 FORD SIDE IMPACTING AMF MODIFIED HORNET AT 25 MPH

Tape Channel No.	Tape Segment Number					
	1	2	3	4	5	6
1	$C_1 \dddot{X}_1$	$C_1 \dddot{X}_V$	$T\dddot{X}_1$	$C_2 \dddot{X}_1$	$C_2 \dddot{X}_V$	$E\dddot{X}_1$
2	$C_3 \ddot{X}_1$	$C_3 \ddot{X}_V$	$T\ddot{X}_V$	$C_4 \ddot{X}_V$	$C_4 \ddot{X}_V$	$E\ddot{X}_V$
3	$C_1 \dot{X}_1$	$C_1 \dot{X}_V$	$T\dot{X}_1$	$C_2 \dot{X}_1$	$C_2 \dot{X}_V$	$E\dot{X}_1$
4	$C_3 \dot{X}_1$	$C_3 \dot{X}_V$	$T\dot{X}_V$	$C_4 \dot{X}_1$	$C_4 \dot{X}_V$	$E\dot{X}_V$
5	$C_1 X_1$	$C_1 X_V$	TX_1	$C_2 X_V$	$C_2 X_V$	EX_1
6	$C_3 X_1$	$C_3 X_V$	TX_V	$C_4 X_1$	$C_4 X_V$	EX_V
7	SYNCH	SYNCH	SYNCH	SYNCH	SYNCH	SYNCH
8	$(C_1-C_3) \ddot{X}_1$	$(C_1-C_3) \ddot{X}_V$	BLANK	$(C_2-C_4) \ddot{X}_1$	$(C_2-C_4) \ddot{X}_V$	BLANK
9	$\left(\frac{C_1+C_3}{2}\right) \ddot{X}_1$	$\left(\frac{C_1+C_3}{2}\right) \ddot{X}_V$	BLANK	$\left(\frac{C_2+C_4}{2}\right) \ddot{X}_V$	$\left(\frac{C_2+C_4}{2}\right) \ddot{X}_V$	BLANK
10	$(C_1-C_3) \dot{X}_1$	$(C_1-C_3) \dot{X}_V$	BLANK	$(C_2-C_4) \dot{X}_1$	$(C_2-C_4) \dot{X}_V$	BLANK
11	$\left(\frac{C_1+C_3}{2}\right) \dot{X}_1$	$\left(\frac{C_1+C_3}{2}\right) \dot{X}_V$	BLANK	$\left(\frac{C_2+C_4}{2}\right) \dot{X}_1$	$\left(\frac{C_2+C_4}{2}\right) \dot{X}_V$	BLANK
12	$(C_1-C_3) X_1$	$(C_1-C_3) X_V$	BLANK	$(C_2-C_4) X_V$	$(C_2-C_4) X_V$	BLANK
13	$\left(\frac{C_1+C_3}{2}\right) X_1$	$\left(\frac{C_1+C_3}{2}\right) X_V$	BLANK	$\left(\frac{C_2+C_4}{2}\right) X_1$	$\left(\frac{C_2+C_4}{2}\right) X_V$	BLANK
14	$C_1 \ddot{X}_V$	$C_3 \ddot{X}_1$	BLANK	$C_2 \dot{X}_V$	$C_4 \ddot{X}_1$	BLANK

C_1 C_2 C_3 C_4 = corners 1 thru 4, occupant compartment location

T = tunnel location

E = engine location

1 = longitudinal direction

V = vertical direction

TABLE 2-2. DIMENSIONAL CHANGES (DECREASES) FROM HIGH SPEED (50 MPH) BARRIER IMPACT OF 1970 FORD

INTERIOR			
LOCATION	LEFT SIDE	VEHICLE CENTER	RIGHT SIDE
A-PILLAR TO B-PILLAR – FLOOR LEVEL – 9" ABOVE FLOOR – 22" ABOVE FLOOR (AT WINDOW SILL)	1 3-1/2 7-3/8		1-1/4 4 7-1/2
B-PILLAR TO C-PILLAR – FLOOR LEVEL – 9" ABOVE FLOOR 22" ABOVE FLOOR (AT WINDOW SILL)	0 0 1/4		0 0 1/8
FIRE WALL TO REAR DECK (APPROXIMATELY 12" ABOVE FLOOR)	5-3/4	7-1/2	6-1/8
FIRE WALL TO REAR SEAT-BACK SUPPORT (AT FLOOR LEVEL)	2	5-3/4	1-1/2
REAR MOST POINT ON DASH PANEL TO REAR SPEAKER DECK		8-3/8	
DASH PANEL/WINDSHIELD INTERFACE TO REAR SPEAKER DECK	7-1/4	8-1/2	6-1/4

EXTERIOR	
LOCATION	AVERAGED DIMENSION
FRONT BUMPER (FLAT BARRIER) TO ENGINE RAMP	20-3/4
TO FIRE WALL	22-7/8
TO FRONT/REAR DOOR INTERFACE	30-3/4
TO REAR AXLE	31-1/4
TO REAR BUMPER (OVERALL VEHICLE CRUSH)	33-3/4
WHEELBASE	11-1/2

(a)

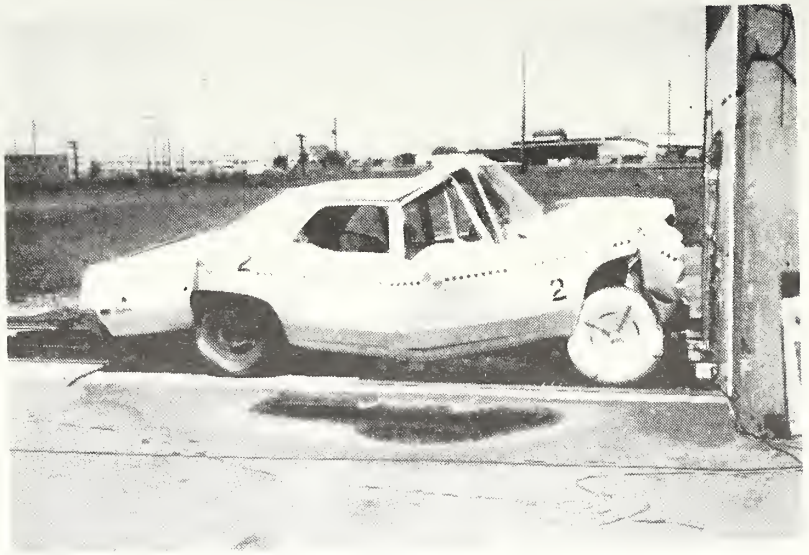

(b)

(c)

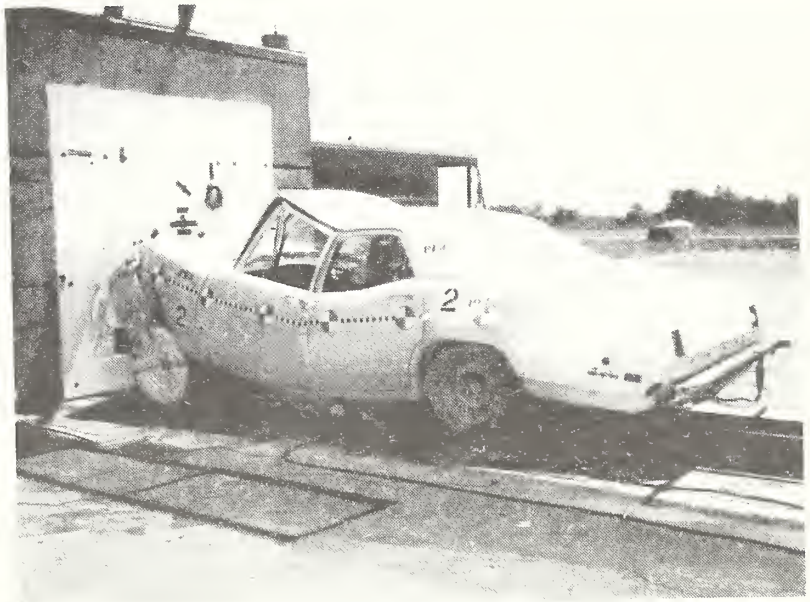

(d)

Figure 2-10. Before and After Test Photographs - High Speed (50 MPH) Barrier Test of 1970 Ford

TABLE 2-3. CRASH TEST DATA: 1970 FORD, FRONTAL BARRIER IMPACT TEST AT 50 MPH

Tape Channel No.	Tape Segment No. 1	2	3	4	5
1	$C_1 \ddot{X}_1$	$C_1 \ddot{X}_v$	$C_3 \ddot{X}_1$	$C_3 \ddot{X}_v$	$T \ddot{X}_1$
2	$C_2 \ddot{X}_1$	$C_2 \ddot{X}_v$	$C_4 \ddot{X}_1$	$C_4 \ddot{X}_v$	$T \ddot{X}_v$
3	$C_1 \dot{X}_1$	$C_1 \dot{X}_v$	$C_3 \dot{X}_1$	$C_3 \dot{X}_1$	$T \dot{X}_1$
4	$C_2 \dot{X}_1$	$C_2 \dot{X}_v$	$C_4 \dot{X}_1$	$C_4 \dot{X}_v$	$T \dot{X}_v$
5	$C_1 X_1$	$C_1 X_v$	$C_3 X_1$	$C_3 X_v$	$T X_1$
6	$C_2 X_1$	$C_2 X_v$	$C_4 X_1$	$C_4 X_v$	$T X_v$
7	SYNCH	SYNCH	SYNCH	SYNCH	SYNCH
8	$(C_1-C_2) \ddot{X}_1$	$(C_1-C_2) \ddot{X}_x$	$(C_3-C_4) \ddot{X}_1$	$(C_3-C_4) \ddot{X}_v$	BLANK
9	$\left(\frac{C_1+C_2}{2}\right) \ddot{X}_1$	$\left(\frac{C_1+C_2}{2}\right) \ddot{X}_v$	$\left(\frac{C_3+C_4}{2}\right) \ddot{X}_1$	$\left(\frac{C_3+C_4}{2}\right) \ddot{X}_v$	BLANK
10	$C_1-C_2) \dot{X}_1$	$C_1-C_2 \dot{X}_v$	$C_3-C_4 \dot{X}_1$	$C_3-C_4 \dot{X}_v$	BLANK
11	$\left(\frac{C_1+C_2}{2}\right) \dot{X}_1$	$\left(\frac{C_1+C_2}{2}\right) \dot{X}_v$	$\left(\frac{C_3+C_4}{2}\right) \dot{X}_1$	$\left(\frac{C_3+C_4}{2}\right) \dot{X}_v$	BLANK
12	$(C_1-C_2) X_1$	$(C_1-C_2) X_v$	$(C_3-C_4) X_1$	$(C_3-C_4) X_v$	BLANK
13	$\left(\frac{C_1+C_2}{2}\right) X_1$	$\left(\frac{C_1+C_2}{2}\right) X_v$	$\left(\frac{C_3+C_4}{2}\right) X_1$	$\left(\frac{C_3+C_4}{2}\right) X_v$	BLANK
14	$C_1 \ddot{X}_v$	$C_2 \ddot{X}_1$	$C_3 \ddot{X}_v$	$C_4 \ddot{X}_1$	BLANK

C_1 C_2 C_3 C_4 = corners 1 thru 4, occupant compartment location

T = Tunnel location

1 = longitudinal direction

v = vertical direction

is no deformation within the occupant compartment. When dynamic (accelerometer) measurements of these motions are taken at the same station, but on opposite sides of the vehicle with respect to the longitudinal centerline or the vehicle, one would expect to obtain the same results from each transducer. When the two signals are subtracted and analyzed, the in-phase spectral content should subtract out, while the out-of-phase components will remain. The out-of-phase components are attributed to structural resonances associated with elastic motions of the vehicle structure. Spectral analysis of this "difference" signal has potential for partitioning the spectral content of occupant compartment acceleration data into low frequency (high displacement amplitude) in-phase components associated with plastic deformations and high frequency (low displacement amplitude) out-of-phase components associated with elastic motions.

A spectrum analysis of longitudinal passenger compartment accelerometer data, including averaged and difference signals, has been performed on the crash test and structural excitation data. Of particular interest is a comparison of frequencies corresponding to peak spectral density levels for the 25 mph crash test data and the corresponding structural excitation data taken from the same vehicle. This data has been organized in Table 2-4, which shows a definite correlation in the acceleration energy frequency content for the passenger compartment locations C1, C2, and C3, as defined by Figure 2-11 (structural excitation data for C4 was faulty). Results also show that the longitudinal structural response of the tunnel location contains less high frequency content than the corner locations for this test. Tunnel acceleration spectral density data is shown in Figure 2-12, and structural excitation acceleration spectral densities at locations C1 and C3 resulting from structural excitation are shown in Figures 2-13 and 2-14, respectively.

TABLE 2-4. CORRELATION OF CRASH TEST DATA (25 MPH TEST) AND STRUCTURAL RESONANCE DATA, BASED ON PEAK LEVELS IN ACCELERATION SPECTRAL DENSITY DATA

Location	Peak Level Frequencies (Hz)	
	Crash Test Data	Structural Resonance Data
C_1 (long)	4, 28, 56, (72-80)	4, 28, 56, 76 (pt)
C_3 (long)	4, 32, 58, 72	4, 24, 58 (pt)
C_1-C_3 (long)	28, 52, 80	10, 28, 54 (pt)
$\frac{C_1+C_3}{2}$ (long)	4, 22, 56, 70	4, 22, 56 (pt)
TUN (long)	4, 22	4, (pt)
C_2 (long)	4, 24, 30	4, 30 (pt)
C_4 (long)	4, 24	data not available
C_2-C_4 (long)	28, 40, 80, 106	data not available
$\frac{C_2+C_4}{2}$ (long)	4, 24, 40	data not available
C_2 (vert)	16	12, 50, 80 (dt)
C_4 (vert)	10, 30, (58-70)	12, 36, (60-84) (dt)
TUN (vert)	10, 30 (58-70)	12, 36, (60-84) (dt)

excitation mode: (pt) = pendulum test, (dt) = drop test

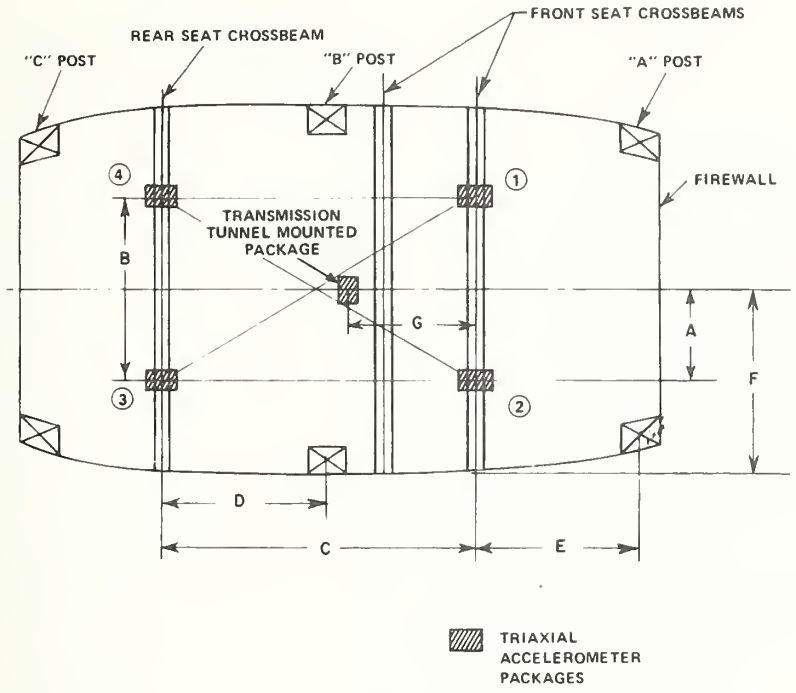

Figure2-11.Schematic of Passenger Compartment Showing Accelerometer Locations

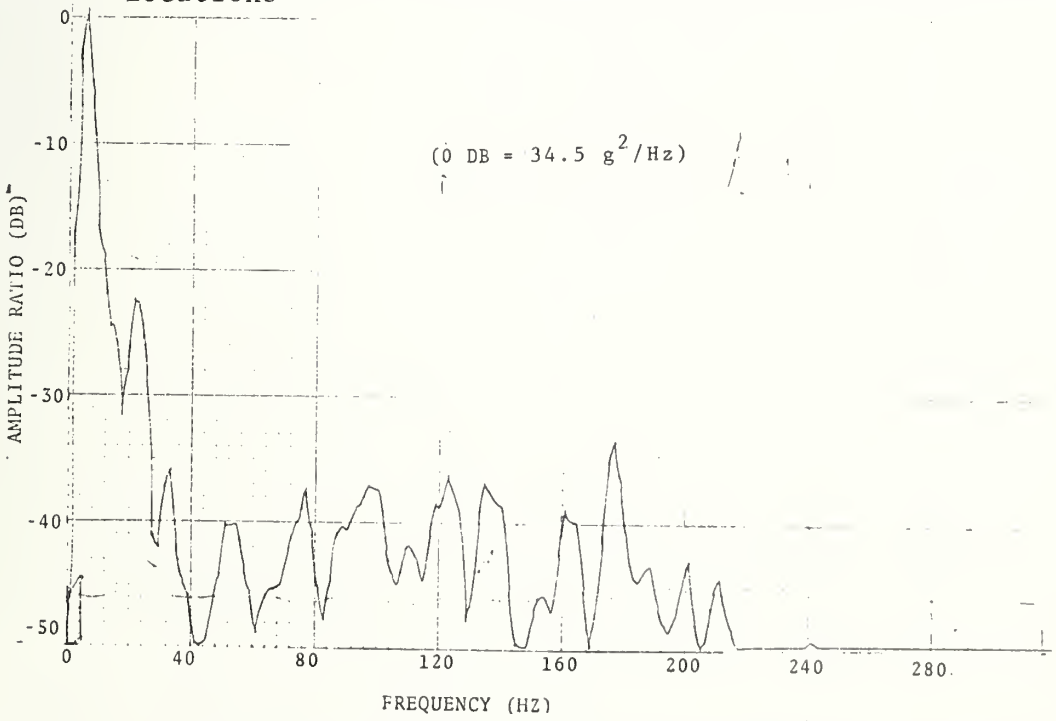

Figure 2-12. Longitudinal Acceleration Spectral Density, Tunnel Location (Ref. Fig. 2-11), Low Speed Impact of 1970 Ford

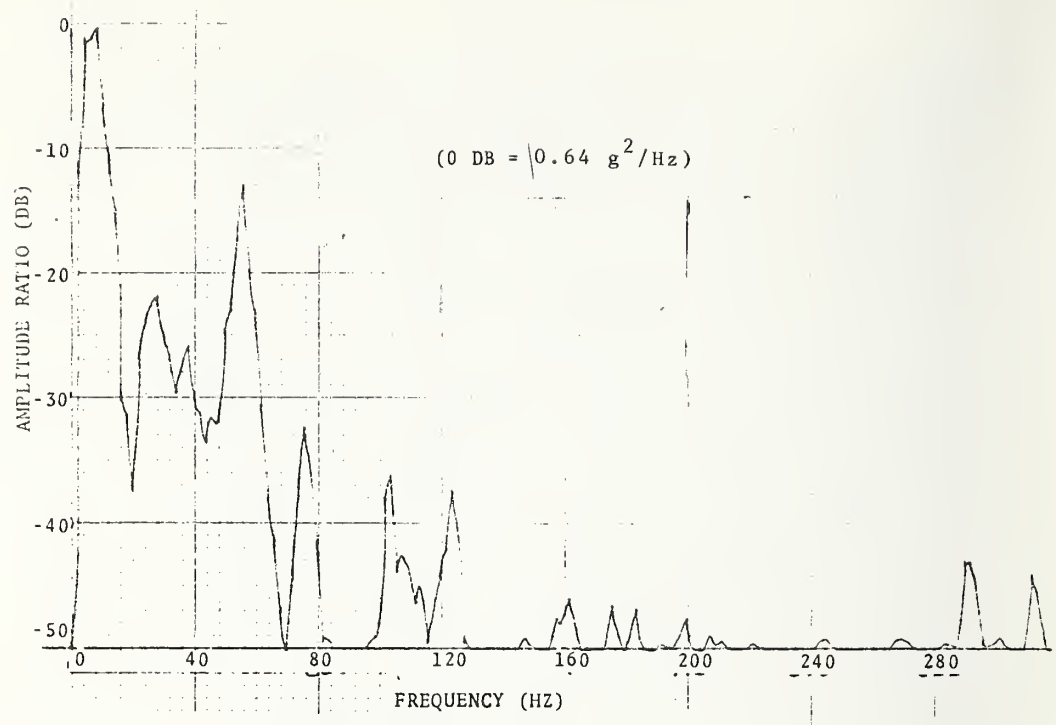

Figure 2-13. Longitudinal Acceleration Spectral Density, Corner 1 Location (Ref. Fig. 2-11) Corresponding to Pendulum Excitation Test

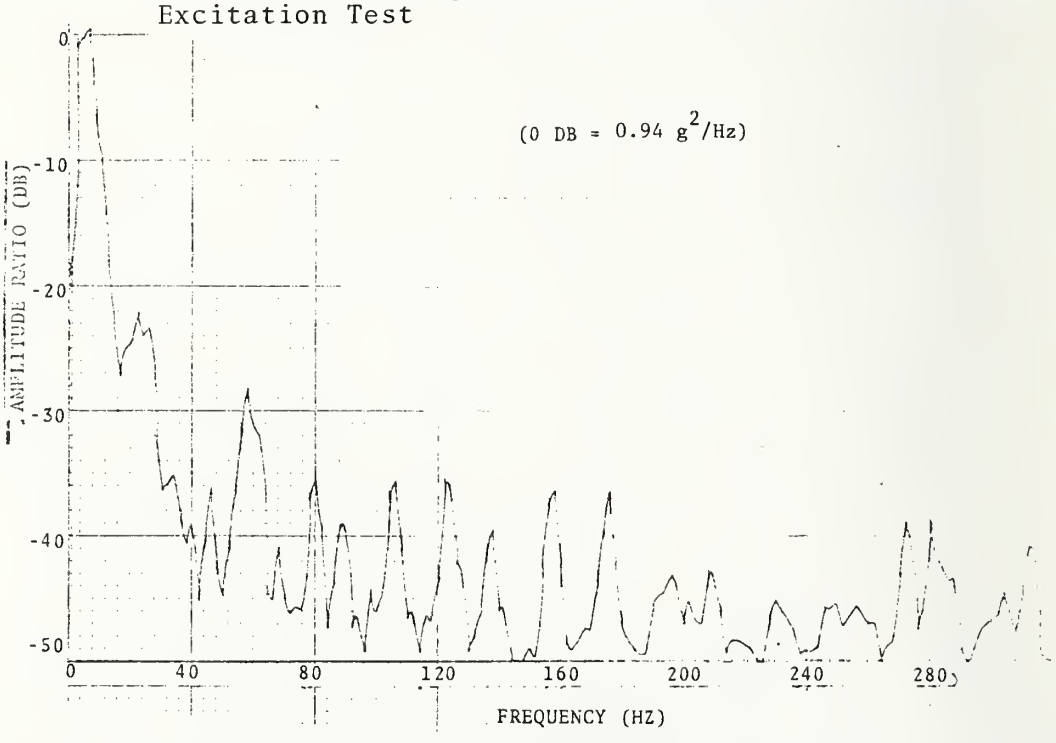

Figure 2-14. Longitudinal Acceleration Spectral Density - Corner 3 Location (Ref. Fig 2-11) Corresponding to Pendulum Excitation Test

To provide insight into the relative importance of spectral components, equivalent displacement spectral-content of selected signals has been calculated. Figures 2-15a and 2-15b are the displacement spectral contents calculated from the corner 1 and 3 longitudinal acceleration spectrum shown in Figures 2-16 and 2-17. This indicates that displacement levels associated with frequencies above 25 Hz are essentially negligible in this case when compared with the displacement levels below 25 Hz. In Figure 2-16, for example, there are three distinct relatively high level peaks in the acceleration spectrum occuring at 4, 28, and 56 Hz. This data, which was derived from the corner 1 location at the occupant compartment longitudinal deceleration pulse from the 25 mph crash test, contains substantial acceleration energy content in the mid-frequency range (using the SAE j211a Class 60 filter bandpass limit of approximately 115 Hz as a reference). The acceleration time history of the pulse is shown in Figure 2-18a.

The average and difference signals have been analyzed for acceleration data from (diagonal) corners 1 and 3 of the occupant compartment. (Corner 1 and corner 2 accelerations would have been preferable for this purpose, but it was not possible to obtain the data in the desired format). For the 25 mph test, plastic deformation of the structure was limited to the front bumper area. If the accelerometers located in corners 1 and 3 have equal sensitivities and the entire occupant compartment was decelerated without deformation (as was the case) then the difference between the two acceleration signals should be zero, or at least diminished if all motions are in-phase. Figure 2-19 is the acceleration spectral distribution for the difference signal, $(C1-C3)\ddot{X}$, and shows that the 4 Hz component is essentially eliminated. The components at 28 and 56 Hz, however, have actually increased in magnitude, indicating that a significant phase difference exists between the two motions at these frequencies. Figure 2-20 is the acceleration spectral distribution for the averaged

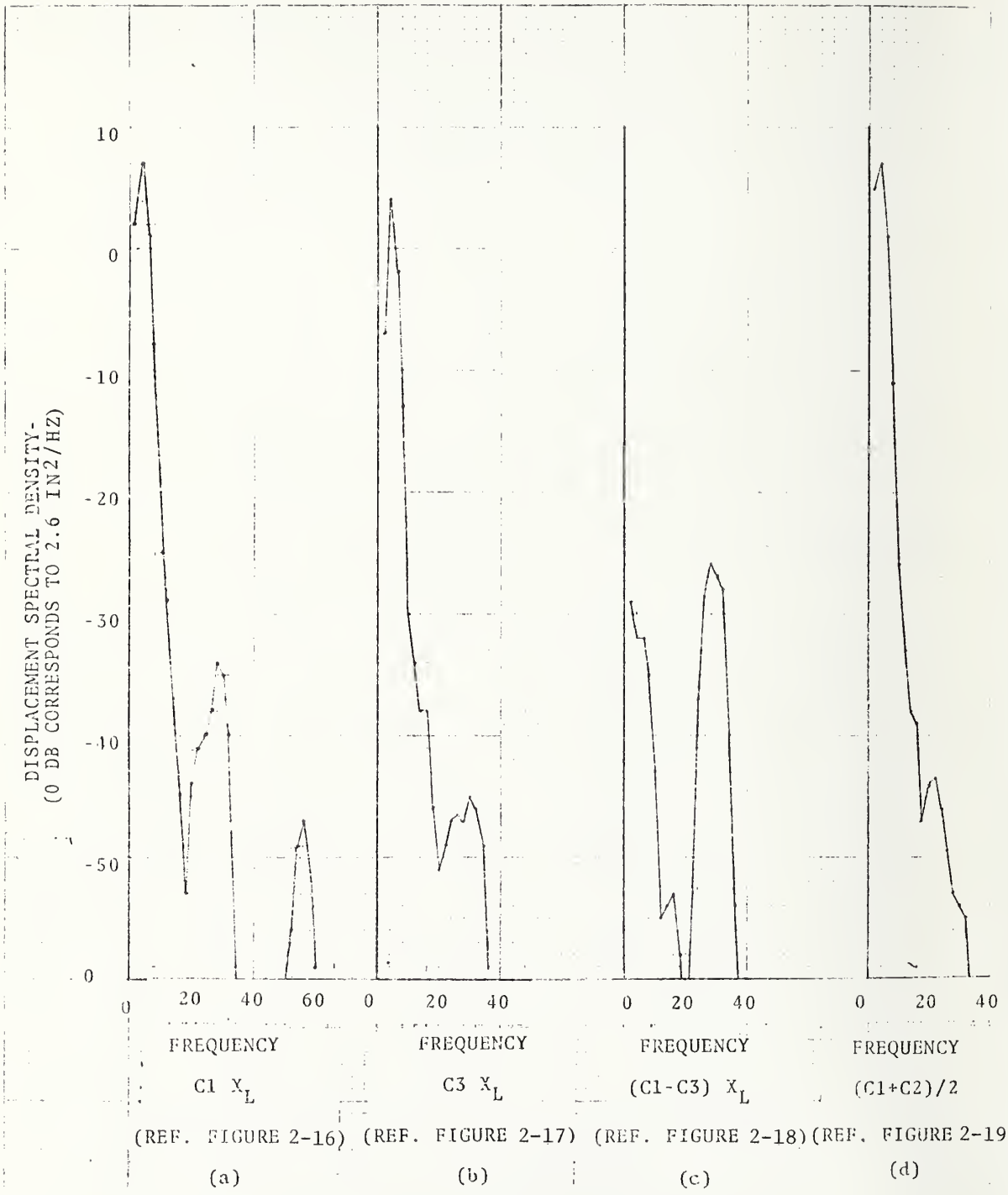

Figure 2-15. Occupant Compartment Displacement Spectral Densities

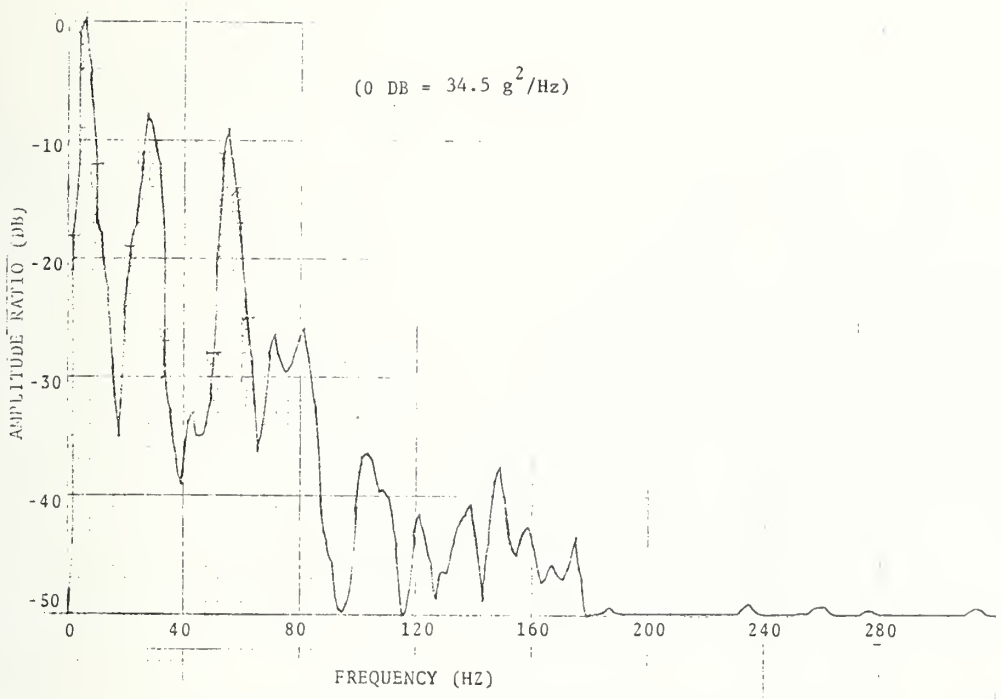

Figure 2-16. Longitudinal Acceleration Spectral Density - Corner 1 Location (Ref. Fig. 2-11) Low Speed Impact of 1970 Ford

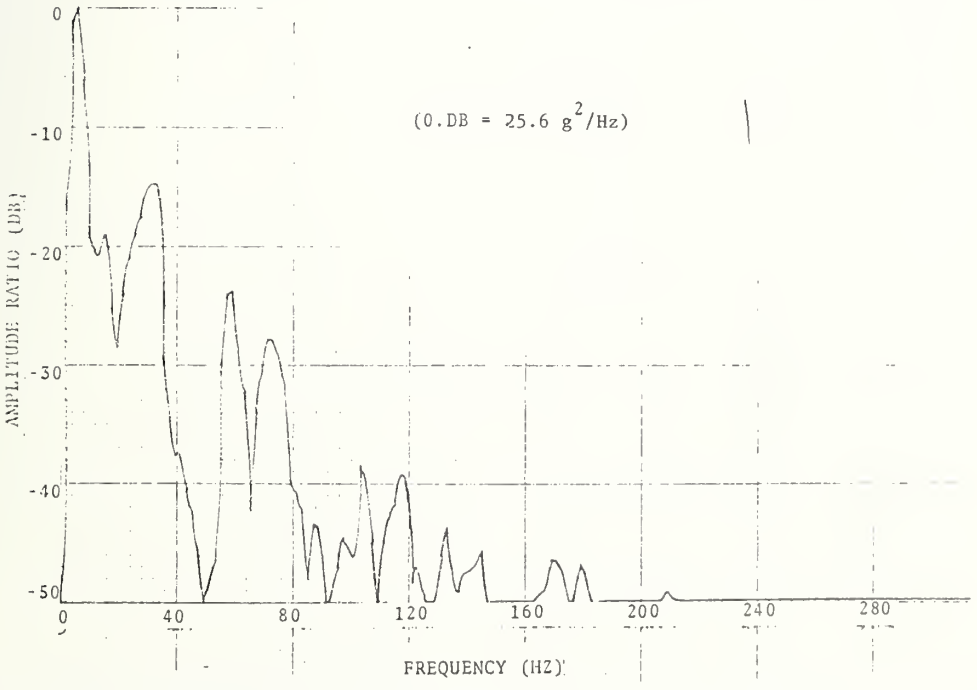

Figure 2-17. Longitudinal Acceleration Spectral Density - Corner 3 Location (Ref. Fig. 2-11) Low Speed Impact of 1970 Ford

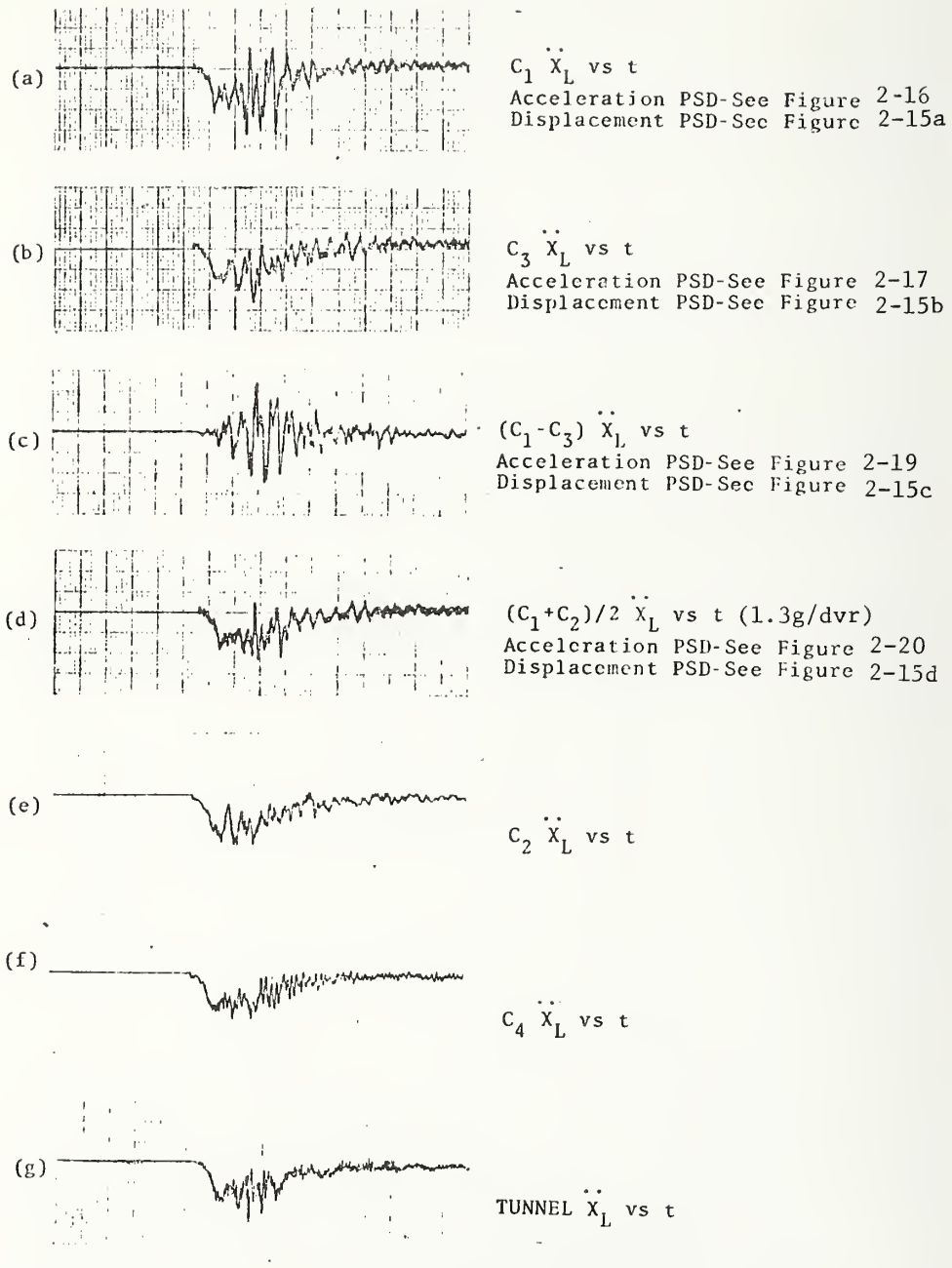

Figure 2-18. Occupant Compartment Acceleration-Time Histories, Low Speed Impact of 1970

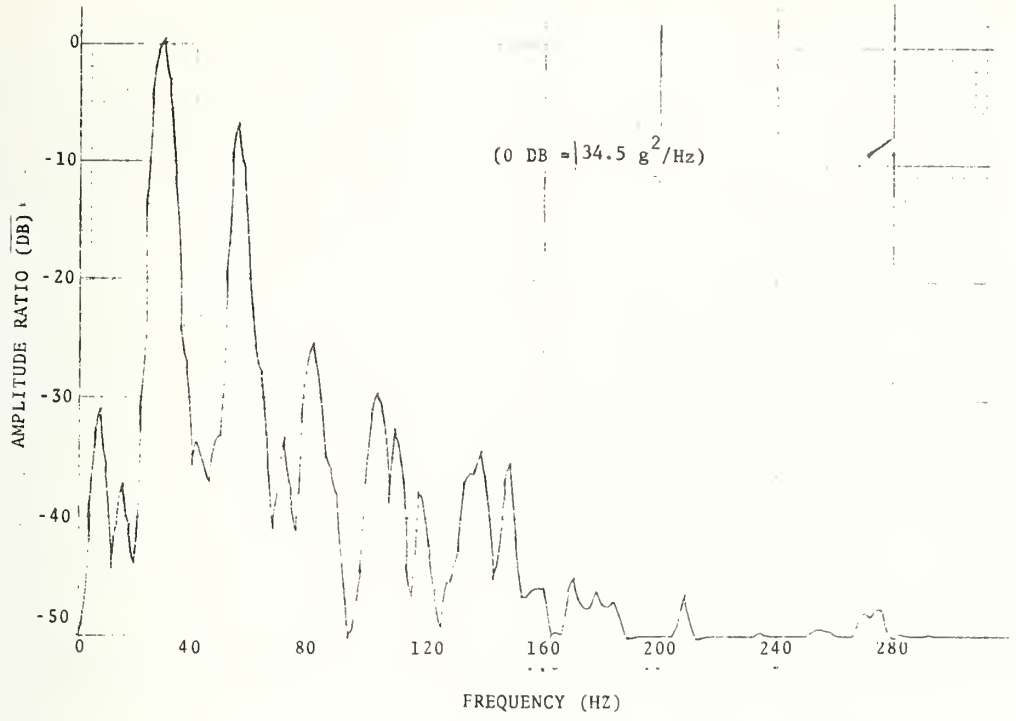

Figure 2-19. Longitudinal Acceleration Spectral Density - Corner 1 Minus Corner 3 Accelerations (Ref. Fig. 2-11) Low Speed Impact of 1970 Ford

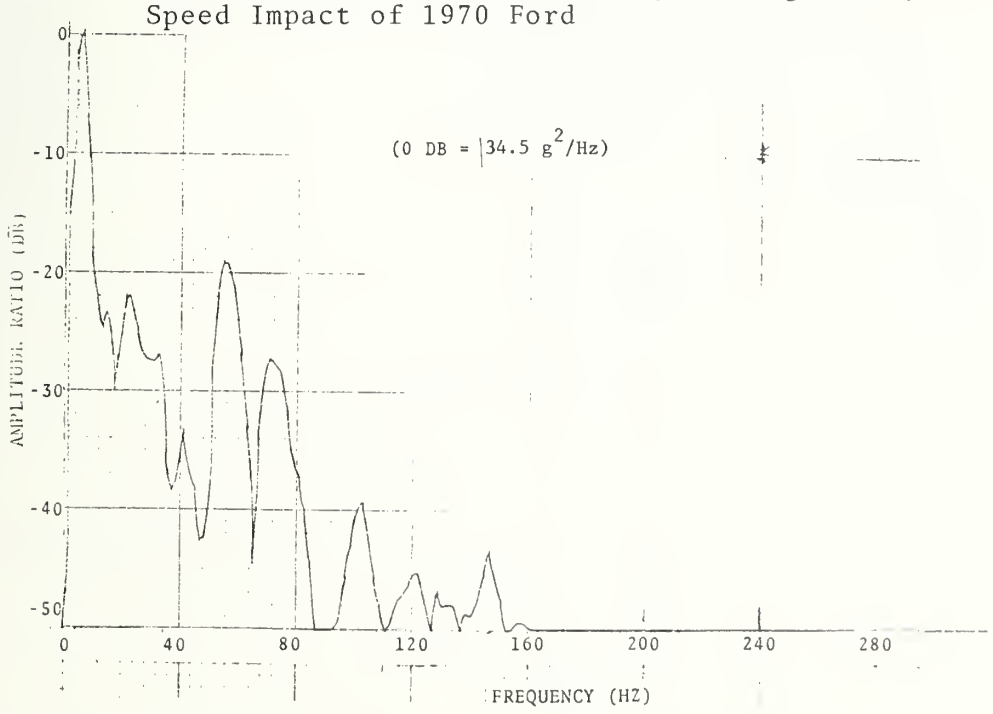

Figure 2-20. Longitudinal Acceleration Spectral Density - Arithmetic Average of Corner 1 and Corner 3 Accelerations (Ref. Fig. 2-11) Low Speed Impact of 1970 Ford

acceleration signals, $(C1+C3)\ddot{X}/2$, which shows a decrease in magnitude at 28 and 56 Hz. This effect also indicates that a phase difference exists between the two motions. The corresponding effect of the difference and averaging operations on displacement spectral distributions is shown in Figure 2-15c and 2-15d.

A similar analysis has been performed on the 50 mph crash test data. Figures 2-21 through 2-24 are longitudinal acceleration spectral densities for corner 1 (C1), corner 2 (C2), the difference signal (C1-C2), and the average signal (C1+C2)/2. The trends are much the same as discussed for the 25 mph test, although there is substantially more high frequency energy present (as expected for the more dynamic impact).

The results of these analyses indicate that the high frequency motions observed are characterized by a resonance-like behavior and are considered to be structural resonances.

From Figure 2-15a, the following "displacement energy" values have been calculated (for the 25 mph crash test data):

Peak Level	Peak Displacement Level ($inches^2/Hz$)	Peak Acceleration Level (G^2/Hz-Fig. 2-16)
4 Hz	13	34.5
28 Hz	1×10^{-3}	5.5
56 Hz	5.2×10^{-5}	4.3

Also, the areas under each of the three frequency peaks have been approximated to estimate the rms displacement levels associated with each peak.

Peak Level Frequency	Approximate RMS Displacement (in)	Approximate RMS Acceleration (g)
4 Hz	6.1	12.2
28 Hz	0.078	5.3
56 Hz	0.016	4.2

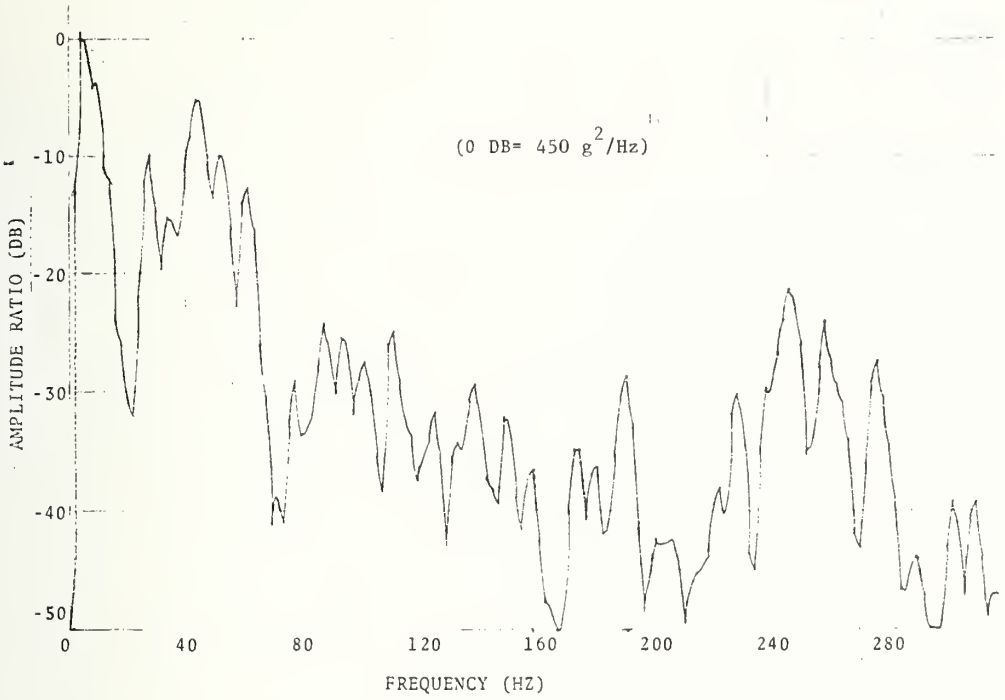

Figure 2-21. Longitudinal Acceleration Spectral Density - Corner 1 Location (Ref. Fig. 2-11) High Speed Impact of 1970 Ford

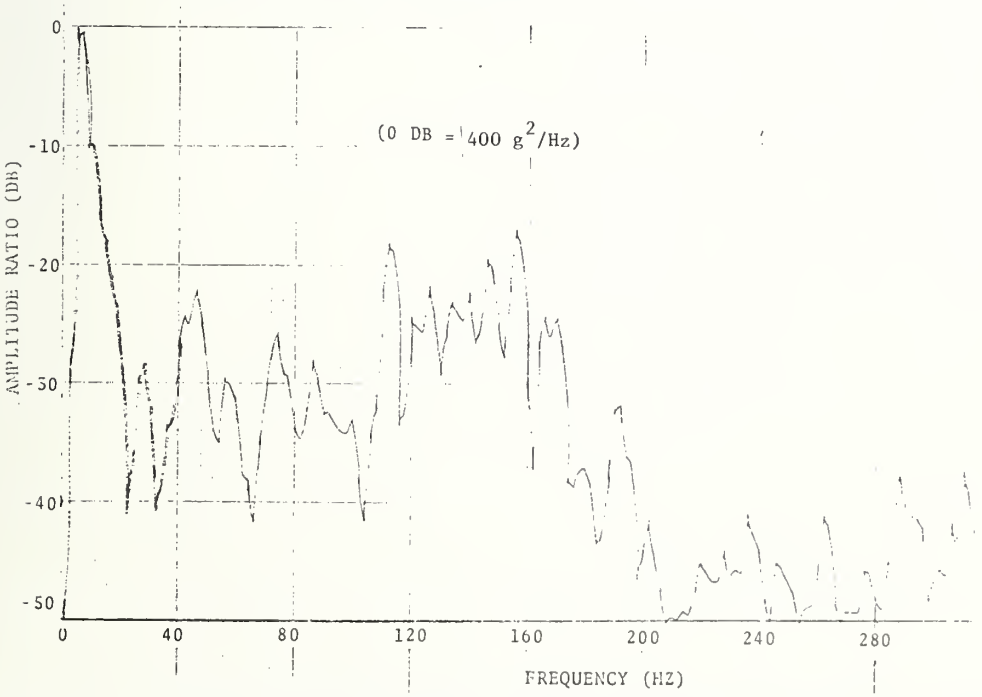

Figure 2-22. Longitudinal Acceleration Spectral Density - Corner 3 Location (Ref. Fig. 2-11) High Speed Impact of 1970 Ford

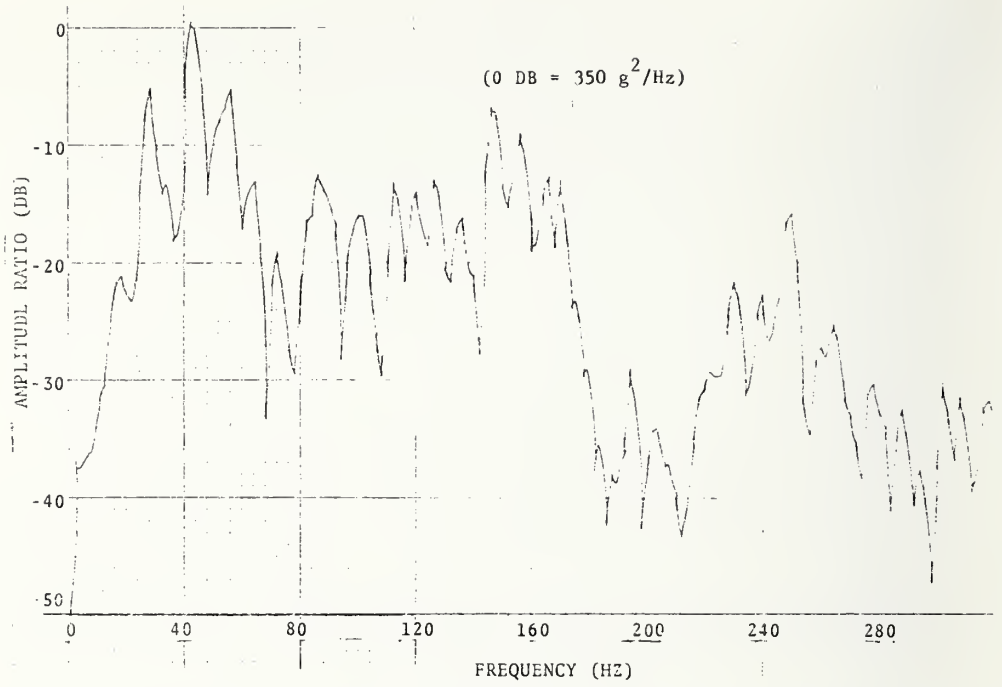

Figure 2-23. Longitudinal Acceleration Spectral Density - Corner 1 Minus Corner 3 Accelerations (Ref. Fig. 2-11) High Speed Impact of 1970 Ford

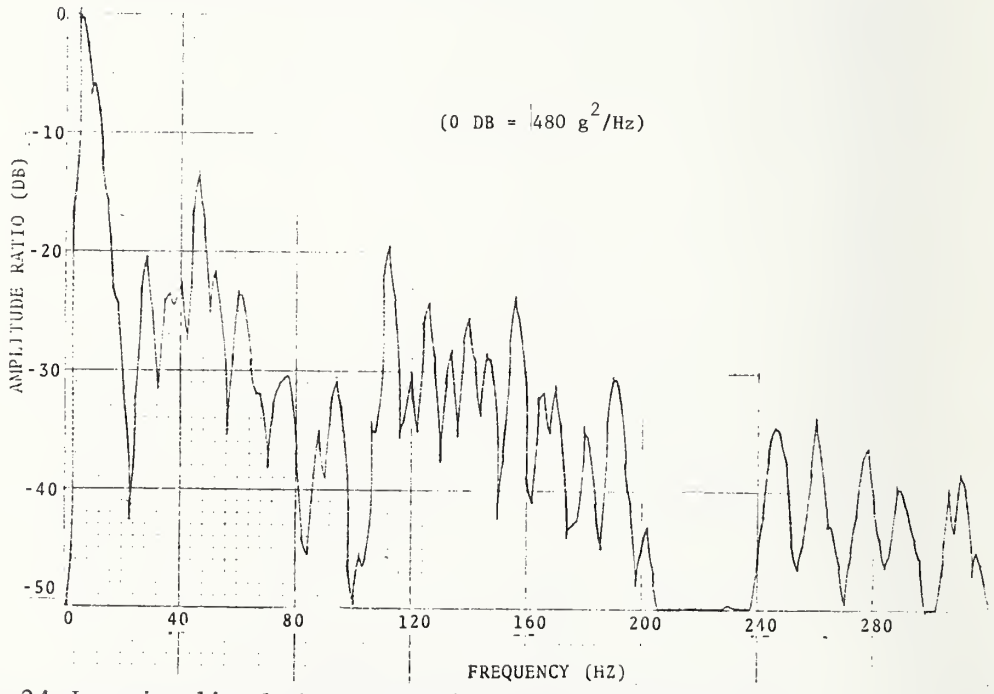

Figure 2-24 Longitudinal Acceleration Spectral Density - Arithmetic Mean of Corner 1 and Corner 3 Accelerations (Ref. Fig. 2-11) High Speed Impact of 1970 Ford

The acceleration amplitudes associated with the three principal frequencies are fairly close in magnitude, while the corresponding displacement amplitudes indicate a dramatic difference. The relative amplitudes of the rms displacements are useful in assessing the effects of various frequency components on occupant loading and on motion characteristics of the structure. This, in turn, is useful in specifying filtering characteristics. If it were assumed that the high frequency displacements occuring in the occupant compartment were not localized structural resonances, but were overall vehicle motions, they would represent a displacement excitation of the restraint system. If the lap/shoulder belt restraint system can be characterized as a 10 Hz single degree of freedom system based on the earlier belt system characterization, having a damping ratio of 1/3, the force transmission characteristics associated with the 28 and 56 Hz components are:

$$T(28Hz) = (.32)$$

$$T(56Hz) = (.14)$$

Applied to the rms displacements calculated, the magnitudes of the high frequency displacements which the belt system can transmit to the occupant frequency are:

at 28 Hz, rms displacement = (0.078) (.32) = .025 in rms

at 56 Hz, rms displacement = (.016) (.14) = .0022 in rms

The loads transmitted to the occupant as a result of restraint system transmissibility and dynamic load deflection characteristics can now be approximated. Representative values of restraint system dynamic load deflection characteristics are reproduced from Reference 8 in Figure 2-25. Seatbelt load data for the 25 mph crash test was not available, but can be approximated using the deceleration pulse of Figure 2-18b and Figure 2-25. Assuming a 180 lb occupant, from Figure 2-18d the "sustained" deceleration is approximately 9 g's. The seatbelt webbing load is approximately 1600 lb. From Figure 2-25, the dynamic stiffness of the webbing at a deflection corresponding to 1600 lb is 450 lb/in, assuming a 50 in belt length. The incremental forces

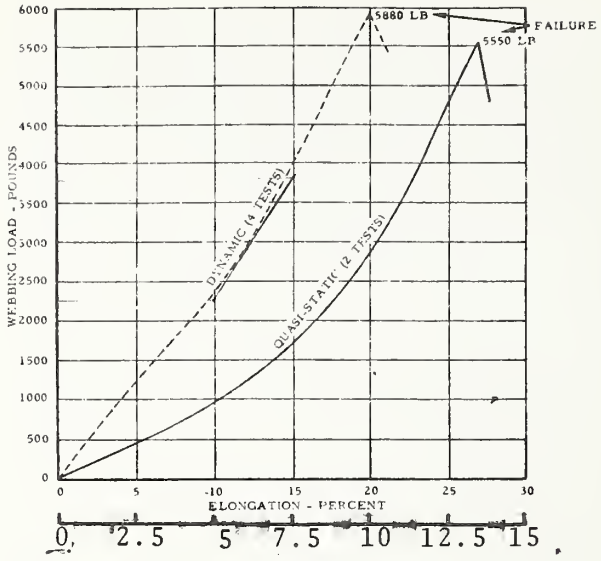

Figure 2-25. Seatbelt Webbing Static and Dynamic Load Deflection Curves (Ref. 8)

developed on the occupant due to displacements such as those associated with the 28 and 56 Hz components can be approximated by the belt system dynamic stiffness and the relative motion between the occupant and vehicle (basically the vehicle displacement at high frequencies). The average incremental forces which could develop as a result of the 28 and 56 Hz displacements are:

28 Hz Force = 450# in (.025) (1.41) in = 16 lb

56 Hz Force = 450# in (.0022) (1.41) in = 1.4 lb

These forces are neglibible when compared to the belt loading of the occupant associated with the low frequency nature of the crash dynamics (about 1%). These levels are in the range of expected instrumentation error.

This analysis is cursory, but it does represent an approach to analyzing the effects of occupant compartment deceleration frequency components on the occupant. The conclusion is that high frequency motions (e.g., greater than 20 Hz for the data analyzed herein) do not effect the occupant, regardless of whether these motions are

resonances or due to stepwise vehicle crush, and should be filtered out of the data.

Based on the preceding discussion, a possible filtering criterion which might be applied to occupant compartment deceleration data would be to eliminate small oscillatory displacement amplitudes (determined through spectrum analysis), which would cause a loading of the occupants equal to or less than 3% of the peak seatbelt loading associated with gross vehicle plastic deformation. (The 3% value is somewhat arbitrary, and might be set higher.)

This procedure would achieve the desired goal of separating "signal" vs. "noise" in the vehicle crash deceleration response, based upon a definition of the desired characteristics. It would also, however, have the adverse affect of requiring that an even greater variation in filtering characteristics be utilized. This procedure would initially be awkward to implement, since it would require continuously analyzing the spectral content of the deceleration crash pulse and calculating loading components on the occupant. Although somewhat complicated, this process is necessary. After a number of applications, however, it is reasonable to expect that a "partition" frequency will result which would allow the establishment of a uniform filtering specification. Based on the data analysis performed in this report, that "partition" frequency would be approximately 20 Hz (3dB down). This is much lower than current practice (J211a), which has a 3 dB down point of approximately 115 Hz.

An alternative to the above data analysis for determination of filtering characteristics is discussed in the following section. An analytical approach is described that has the propensity to enhance the low frequency content. Initial exercising of this technique has provided results which partition the frequency content in a very desirable manner.

3. APPLICATION OF AN ANALYTICAL CURVE FITTING AND FILTERING PROCEDURE TO CRASH TEST DATA

The previous discussion outlined a procedure for using spectrum analysis of crash test data to assess the transmissibility effects of high frequency accelerations in the crash response through seatbelt restraint systems to occupants. This approach represents a procedure which would partition the frequency content into occupant threatening and non-threatening ranges, thus forming a criterion for specifying filtering characteristics. Based on the previously analyzed data the partition frequency is 20 Hz and high rolloff filtering should begin at 20 Hz (i.e. 3 dB down at 20 Hz).

The low frequency pulse contains occupant threatening (high loading) components and is associated with large relative displacements between the occupant and vehicle during ride-down (i.e. large seatbelt elongations). The high frequency residual components do not represent threatening high relative displacement motions and therefore have only minimal effect on occupant loading.

The spectrum analysis approach for defining filtering characteristics as described above would be, at least initially, cumbersome to implement. Other difficulties could arise if the spectral distribution did not show discrete frequencies aside from the frequency peak associated with gross plastic deformation. This situation can be expected, and partitioning the frequency content as previously outlined could be more difficult. Another initial difficulty in analog and/or digital filtering of the data would be the necessity to construct different filters, each having a tailored frequency response for a particular piece of data. Also, requirements for sharp rolloffs at frequencies such as 20 Hz may introduce undesirable phase shifts at low frequencies when analog filters are used.

A possible alternative to analog filtering of crash test data to eliminate high frequency peaks from accelerometer data may be to fit the data with a least squared error polynomial curve. This is accomplished by digitizing the analog data which is to be filtered and using the digitized points as input to a computer program fitting routine. This routine applies on orthogonal polynomial least squared error subroutine to the data to generate a polynomial function of the acceleration time history of the form: $\ddot{X} = a_0 + a_1 t + a_2 t^2 + \ldots a_n t^n$ where n is the order of the fit. A discussion of the mechanics of the orthogonal polynomial method used and a program listing are contained in Appendix C.

The character of the curve fitting program is such that it has limited frequency reproduction capability, and for this reason, it effectively acts as a filter on the data. The resulting effect is that the digitized analog data is fitted with a basic low frequency pulse shape (i.e. half-sine, haversine triangular, etc.) in a least squared error sense, and this eliminates high frequency components from the data. The curve fitting routine effectively automates the spectrum analysis and filtering operations and provides the desired frequency partitioning effects without discarding any of the original data.

Computer output includes polynomial data (order and coefficients of fit) and a plotted description of the fit. Plotted information presently includes the points taken from the digitized crash pulse data, a plot of the fitted curve through these points, and a plot of the residual (i.e., the difference between the data points and the fitted curve). When applied to occupant compartment deceleration data, the residual can be analyzed in the same manner as the high frequency spectrum analysis content was analyzed to determine its effect on occupant loading. All parameters are plotted versus time.

3.1 CHARACTERIZATION OF FREQUENCY RESPONSE OF THE ANALYTICAL CURVE FITTING ROUTINE

The frequency response characteristics of the curve fitting routine are dependant upon the following curve fitting parameters: the order (n) of the polynomial used to fit the data, the number of segments (i.e., the number of applications or an n^{th} order polynomial fit within a given interval), and the amount of overlap between segments. The number of data points selected within a segment of data will affect the smoothness of the fitted curve, but has little influence on frequency response. In preliminary applications of the routine to crash test data, a ratio of 100 points per segment and an overlap of 20 points on either side of the 100 points has worked well. The overlap of 20 points serves as a "weighting" function to match the endpoints and slopes of the fitted curve at either end of the segment with the adjacent data.

To quantify the effects of the above mentioned parameters on the routine's ability to fit a curve, the routine was applied to a constant amplitude sinusoid input signal which varied in frequency from 4 to 40 Hz in 1 Hz increments. Odd sinusoidal input signals (i.e. $f(x) = -f(-x)$) were used for fitting odd polynomials (n = 5, 7 and 9), and even sinusoidal input signals (i.e. $f(x) = f(-x)$) were used for even polynomials (n = 6 and 8). Each input signal frequency was fitted with a fifth through ninth order polynomial and the "goodness" of the fit was determined by computing and summing the least squared error between the signal and fitted curves at each data point, averaged over the number of points in the interval. The rms ratio between the fitted curves and signal were also computed for assessing the filtering chracteristics of the routine. The least squared error will vary between 0.000 for a perfect fit at low frequencies and approximately 0.500 (the mean squared value of a unity amplitude sinusoid) for higher frequencies, indicating that the fit is virtually insensitive to the signal frequency. To determine the effects of various overlap lengths, this proceedure was repeated for interval/overlap ratios of (100/10), (100/20), and (100/30) milliseconds. The

relationship between least squared error and frequency for various order polynomials is shown in Figure 3-1 for the 100 msec interval, with a 10 msec overlap. The relationship between least squared error values and the quality of the fit can be judged from Figures 3-2 and 3-3 which show fifth through ninth order fits of 18 and 21 Hz sinusoids for a 100 msec interval, with a 10 msec overlap. Based on these curve fits, a least squared error (LSE) of 0.003 or less is qualitatively judged as the minimum acceptable fit (refer to the 8^{th} order fit of Figure 3-2). Based on this LSE criterion, the maximum frequencies which various orders of polynomials will adequately fit for the 100 msec interval with various overlaps were determined and tabulated in Table 3-1. The relationships between least squared error and frequency for the 100/20 and 100/30 interval/overlap ratios are shown in Figures 3-4 and 3-5, respectively. The oscillations or "waviness" in the curves at higher frequencies (about the amplitude LSE/100*N = 0.50) are due to end point phase relationships, which are a consequence of fitting an even or odd sinusoidal signal (about t=50 msec), varying in frequency, in a fixed time interval.

Within a given interval (e.g. 100 msec), the maximum frequency can be extended by increasing the number of applications of the routine within the interval. This amounts to a simple scaling problem; for example, using two applications of an 8^{th} order polynomial within a 100 msec interval (50 msec per application) and using a ratio of interval to overlap length of 100/10 for each sub-segment, the maximum (LSE=0.00) frequency would be increased from 19 Hz to 38 Hz (Reference Table 3-1).

In order to quantify the filtering characteristics of the curve fitting routine, the rms ratios between the fitted and signal curves have been computed and plotted versus frequency for various interval/overlap ratios and various order polynomials. The results are shown in Figures 3-6 through 3-8 for interval/overlap ratios of 100/10, 100/20, and 100/30.

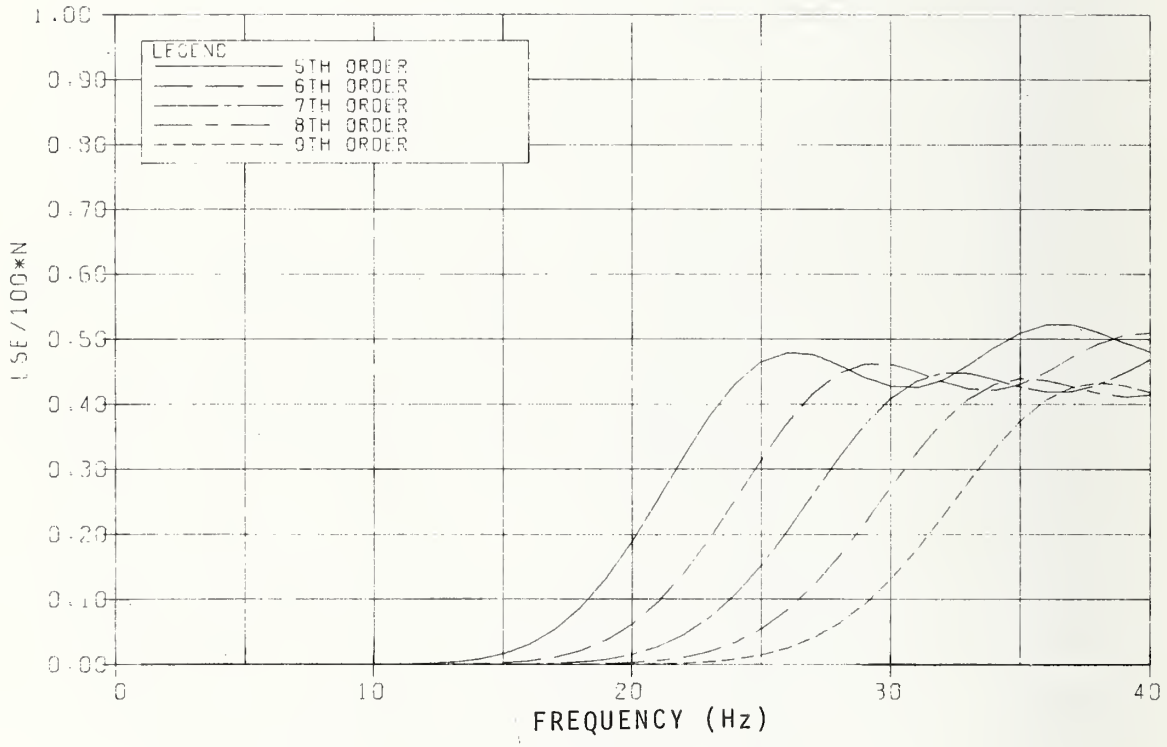

Figure 3-1. Relationship Between Least Squared Error and Frequency for an Interval/Overlap Ratio of (100/10)

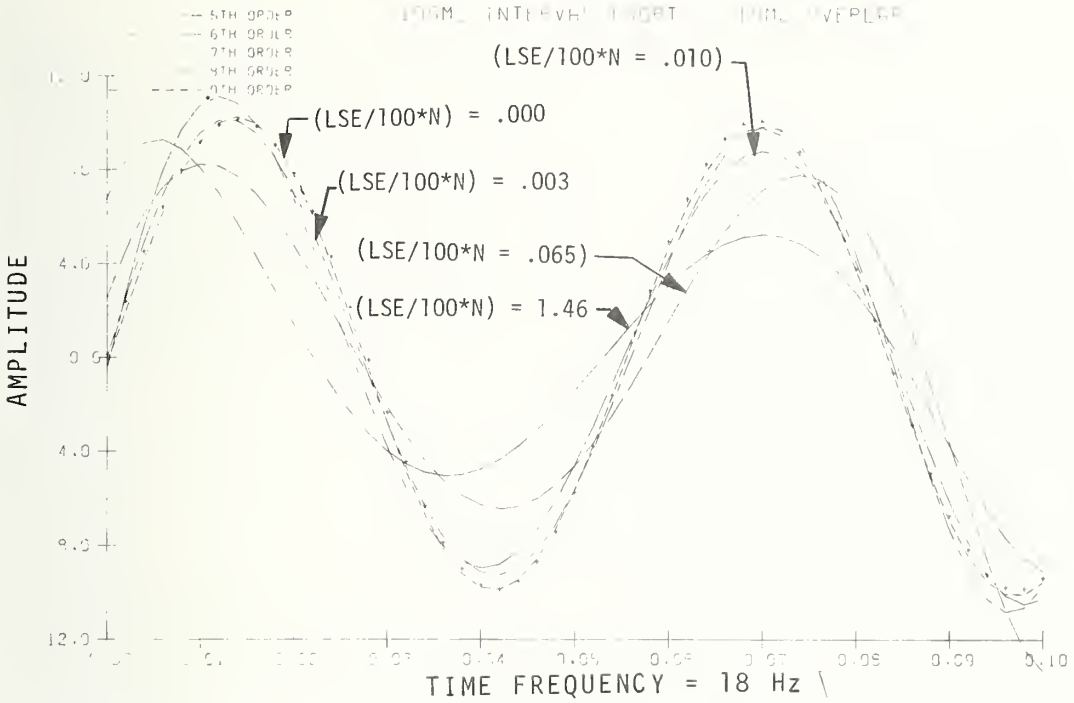

Figure 3-2. Fifth through Ninth Order Fits on an 18 Hz Sinusoid from an Interval/Overlap Ratio of (100/10)

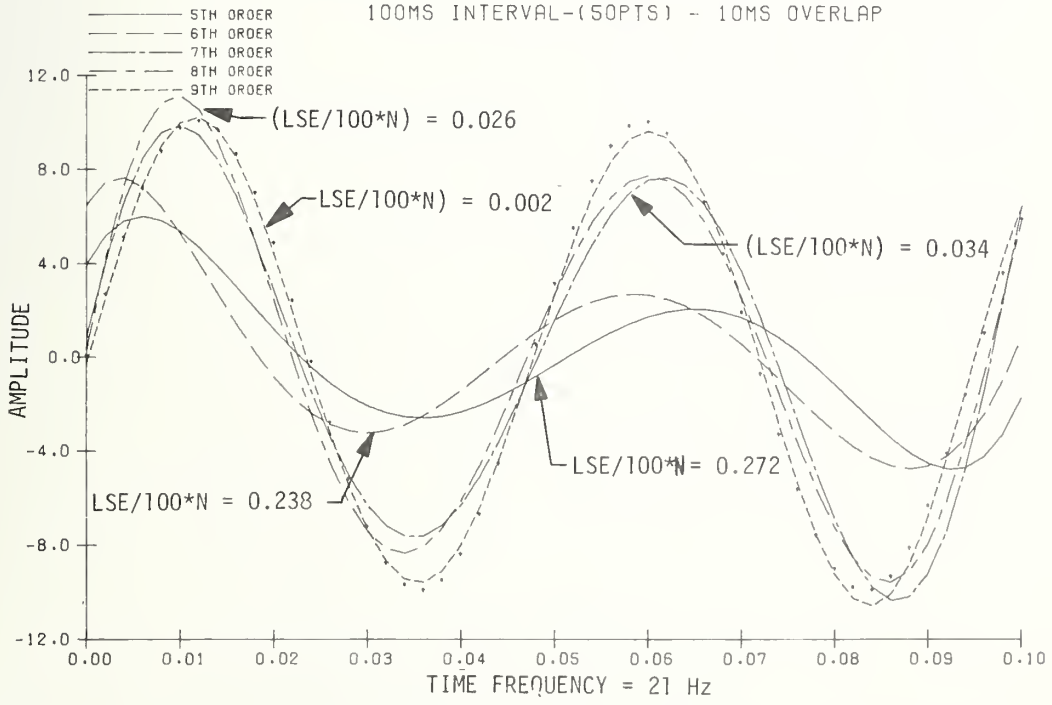

Figure 3-3. Fifth through Ninth Order Fits of a 21 Hz Sinusoid for an Interval/Overlap Ratio of (100/10)

TABLE 3-1. RELATIONSHIP BETWEEN ORDER OF POLYNOMIAL INTERVAL/OVERLAP RATIO AND MAXIMUM FREQUENCY REPRODUCTION CAPABILITY (BASED ON LSE<.003 CRITERION)

ORDER OF POLYNOMIAL	MAXIMUM FREQUENCY INTERVAL OVERLAP RATIO		
	100/10	100/20	100/30
5	12	10	9
6	15	12	11
7	17	15	13
8	19	17	15
9	22	19	16

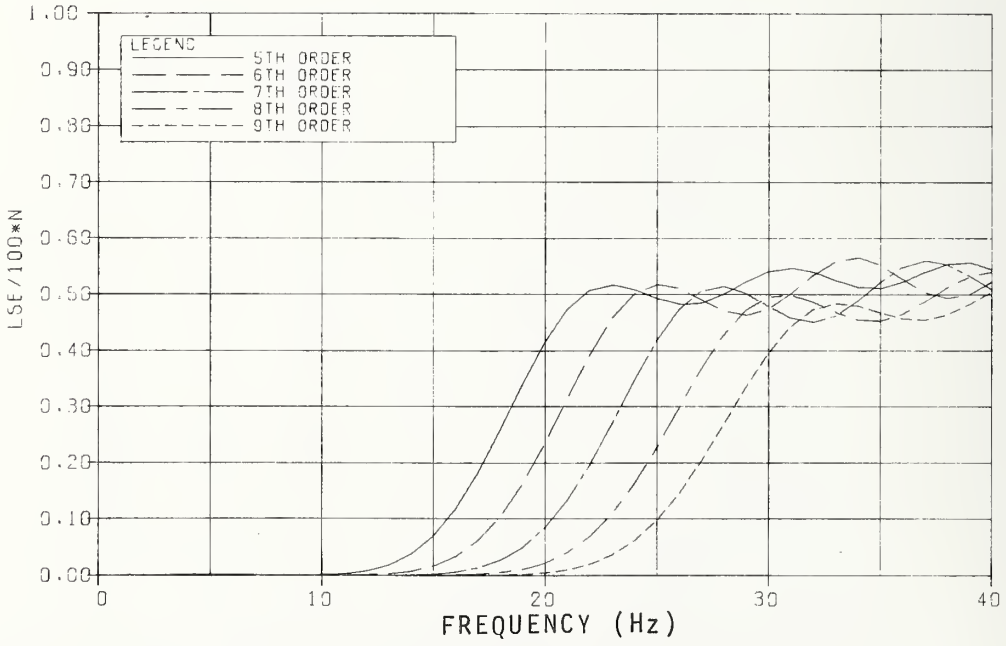

Figure 3-4. Relationship Between Least Squared Error and Frequency for an Interval/Overlap Ratio of (100/20)

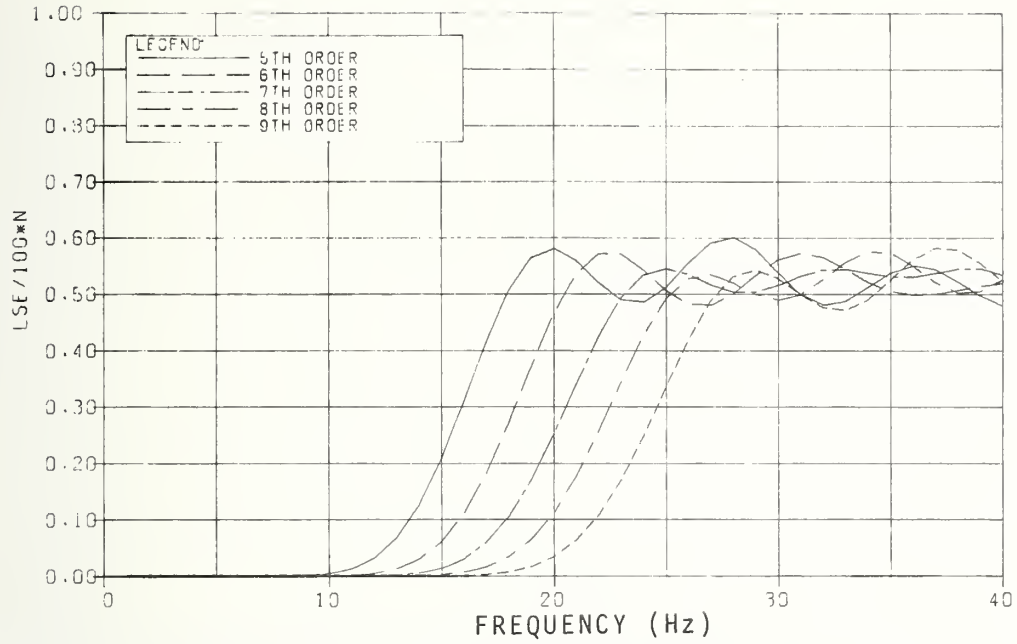

Figure 3-5. Relationship Between Least Squared Error and Frequency for an Interval/Overlap Ratio of (100/30)

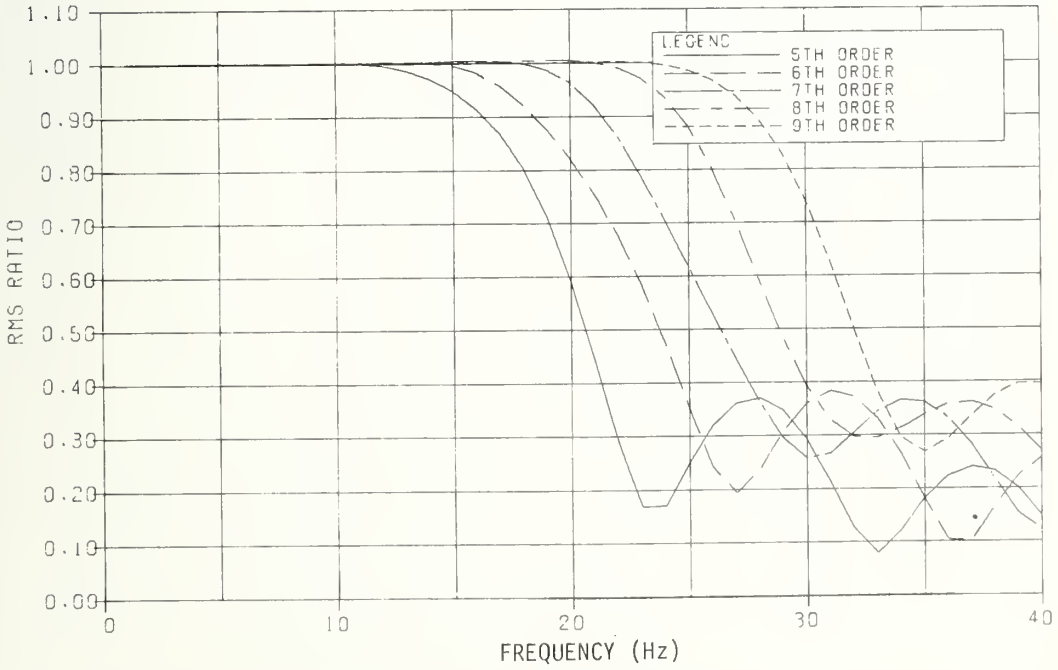

Figure 3-6. Amplitude Ratio Frequency Response of Curve Fitting Routine for Interval/Overlap Ratio of (100/10)

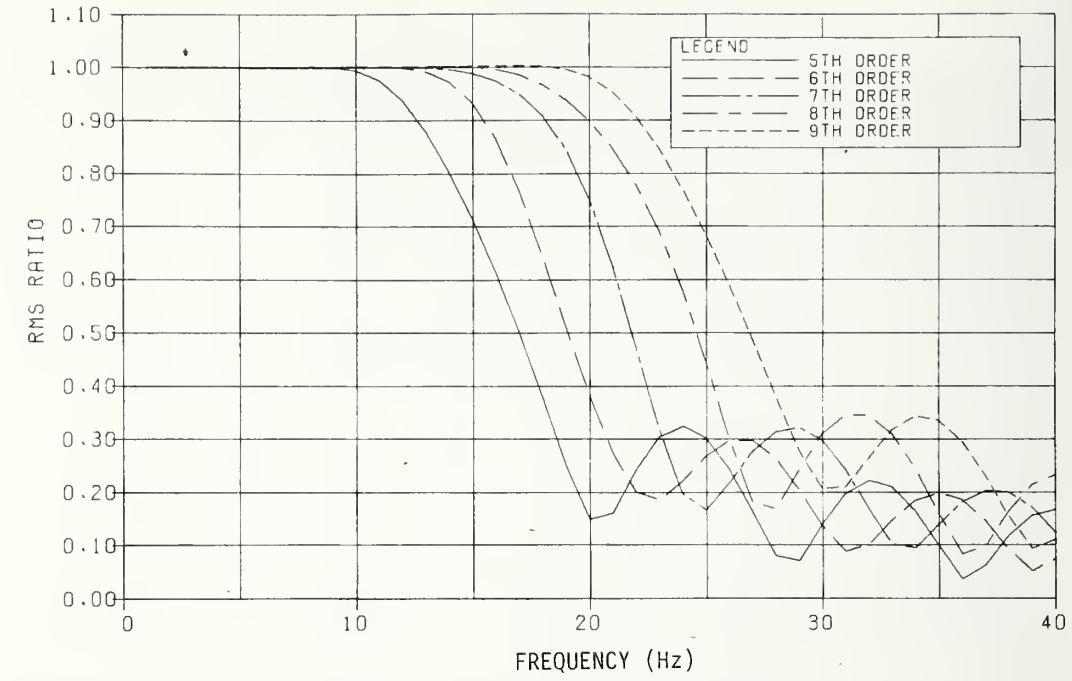

Figure 3-7. Amplitude Ratio Frequency Response of Curve Fitting Routine for Interval/Overlap Ratio of (100/20)

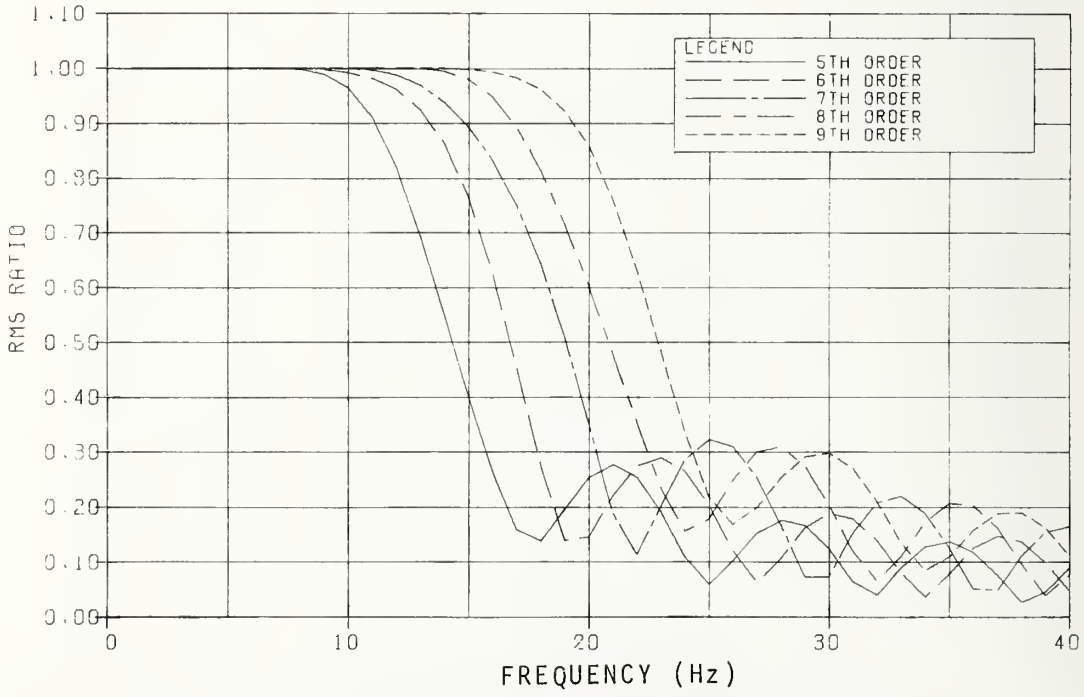

Figure 3-8. Amplitude Ratio Frequency Response of Curve Fitting Routine for Interval/Overlap Ratio of (100/30)

The "waviness" in the curves at higher frequencies is, again, a result of end point phase relationships, as previously described for the LSE curves. Figures 3-6 through 3-8 show that approximately 70% filtering can be obtained within 5 to 10 cycles of the "cutoff" frequency. To provide an estimate of filtering capability the "rolloff" rate of the 6th order curve of Figure 3-7 has been approximated as 22 db/oct using the straight line segment shown.

In practice, the set of curves presented in Figures 3-6 through 3-8 and observed frequency content in the crash data will be used as a guide for selecting initial curve fitting parameters. Parameters will then be varied to increase or decrease frequency reproduction capability, based upon an analysis of the residual accelerations (i.e. the difference between the input data and the fitted curve). This procedure is illustrated in the next section. The polynomial representation and presentation of crash test data has excellent potential for:

(a) Providing a more valuable description of the crash ride-down dynamics by emphasizing the low frequency content of the data and partitioning the high frequency residual accelerations from the low frequency content without discarding data;

(b) Presenting test results in a completely described analytical form via generation of a polynomial curve fit;

(c) Allowing rapid hand calculations to be performed on the data, such as integrated parameter descriptions by either the test organization or report readers;

(d) Stimulating the exchange of crash test data among test organizations for comparison and evaluation purposes by simplifying handling and utilization problems;

(e) Providing a standard, uniform means of filtering, describing and reporting crash test data; and

(f) Providing complete description of the "filtering" applied to the data by specification of the input parameters to the curve fitting program.

3.2 DEVELOPMENTAL APPLICATIONS OF THE ANALYTICAL CURVE FITTING PROCEDURE

Figures 3-9 through 3-11 show the application of the curve fitting procedures to a segment of digitized accelerometer data filtered at 250 Hz. The longitudinal deceleration time history data used in this exercise is from the C.G. or tunnel location of a Plymouth Fury barrier impacted at 30 mph. The digitized data has been divided into one, two and three segments (Figures 3-9, 3-10, and 3-11, respectively) and fitted with a polynomial curve for each segment. The coefficients for the various fitted segments in Figures 3-9 through 3-11 are tabulated in Table 3-2. The quality of the fit can be judged by the residual curve plotted in each figure, and it is apparent that the residual is reduced for the two and three segment fits. The differences between these residuals (Figures 3-10 and 3-11), however, is small, which indicates that dividing the digitized data into more than three segments will not have much effect on improving the fit. There is a small discontinuity at $t=1.25$ sec. in Figure 3-11 (the end of the first segment and the start of the second), which can be eliminated with heavier weighting of the endpoints.

To approximate the displacements associated with the basic low frequency curve fit to the data and the maximum contained in the residual, an integration operation was performed. The curve fit of Figure 3-10 was approximated by straight line segments, and the two largest peaks in the residual were approximated by a half-sinusoids (see Figure 3-10). The displacement amplitude associated with peak 1 was found to be approximately 0.08 inches vector (from an acceleration amplitude of 25 g's and a half period of .0097 sec) and from peak 2, 0.14 inches vector (from an acceleration amplitude of 10 g's and a half period of .019 sec). The displacement associated with the straight line approximation to the low frequency curve of Figure 3-10 was calculated to be approximately 34 inches. The maximum displacements associated with the residual were approximately 0.4% of the displacement associated with gross vehicle crush. This indicates that useful data is not being eliminated by use of the curve fitting/filtering

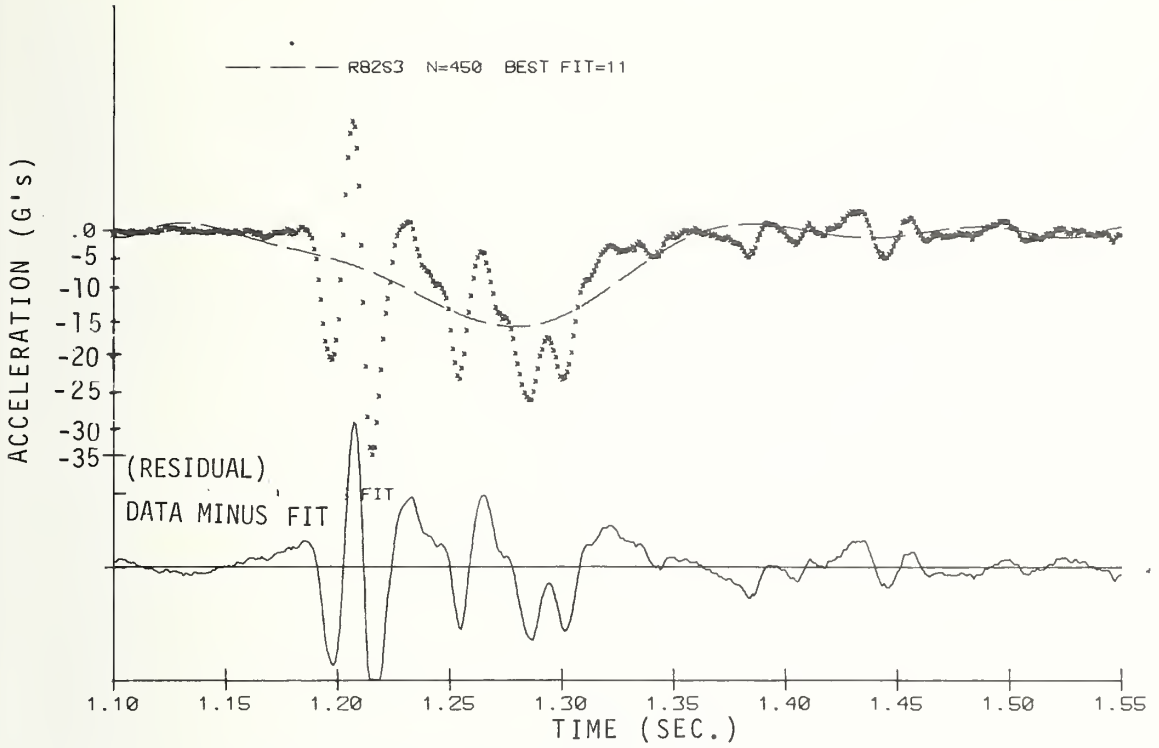

Figure 3-9. Application of Curve Fitting Program to Crash Test Data - One Segment Fit

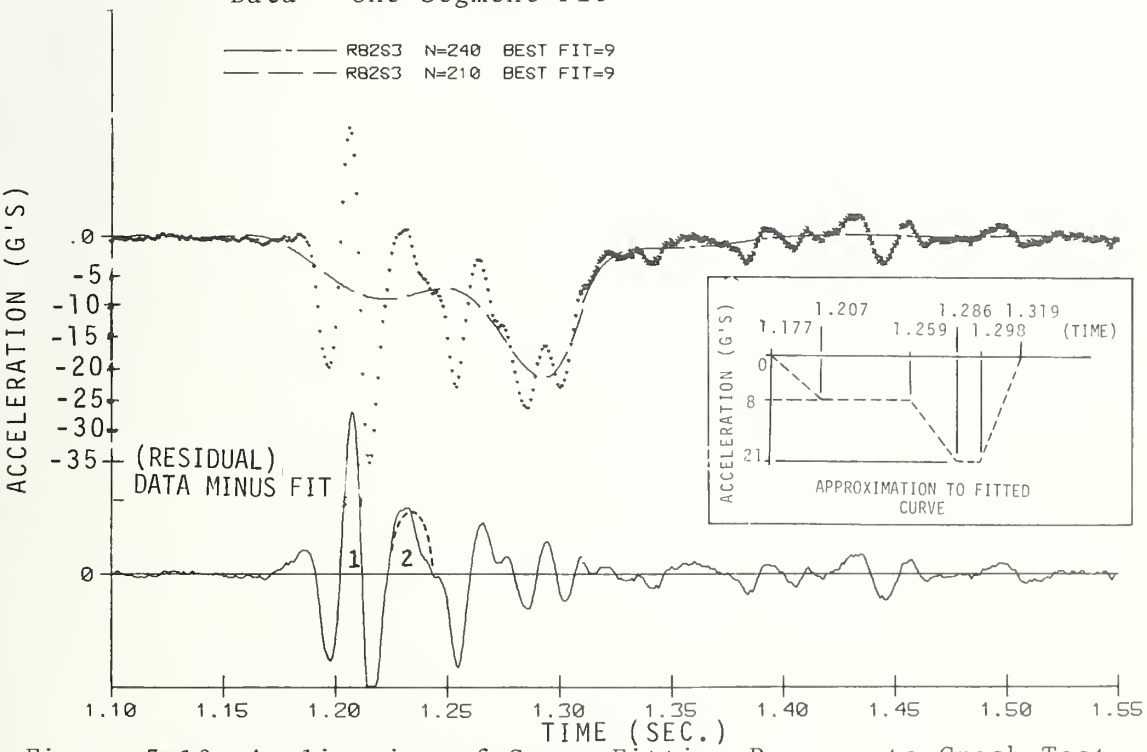

Figure 3-10. Application of Curve Fitting Program to Crash Test Data - Two Segment Fit

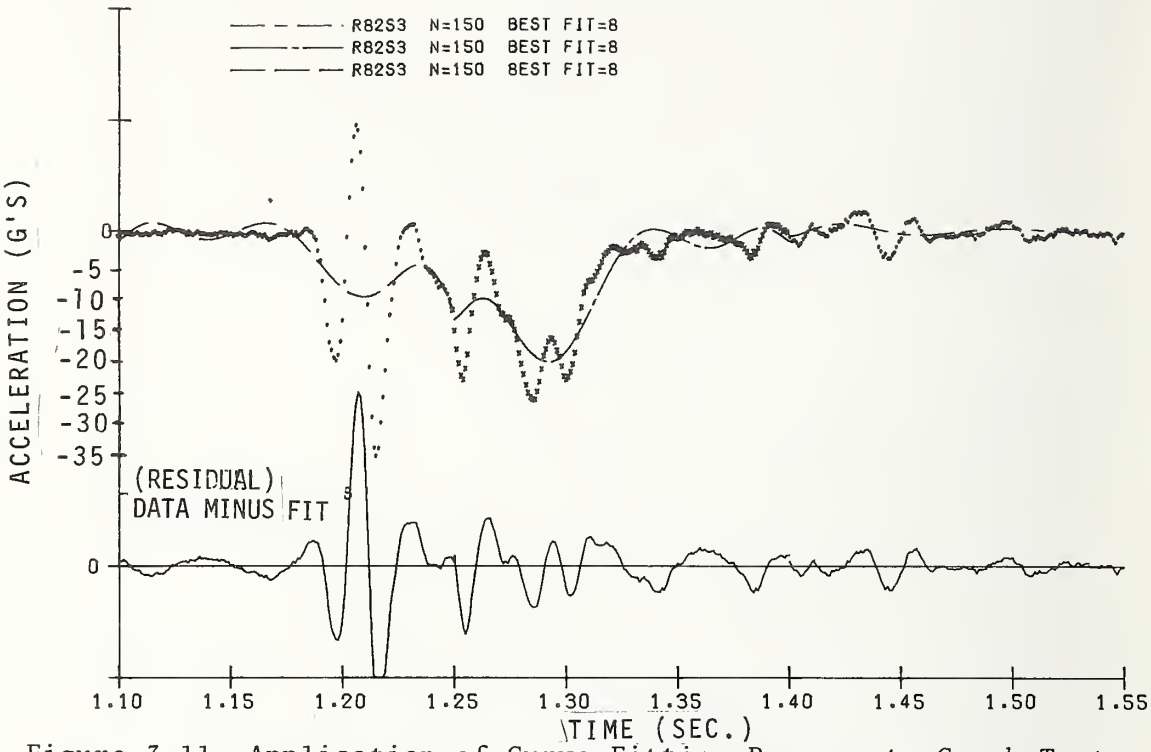

Figure 3-11. Application of Curve Fitting Program to Crash Test Data - Three Segment Fit

TABLE 3-2. POLYNOMIAL COEFFICIENTS FOR THE CURVE FITS OF FIGURES 3-9, 3-10 AND 3-11

COEFFICIENT	FIGURE 3-9	FIGURE 3-10		FIGURE 3-11		
	SEGMENT 1	SEGMENT 1	SEGMENT 2	SEGMENT 1	SEGMENT 2	SEGMENT 3
A_0	$.2319 \times 10^{12}$	$.5188 \times 10^{12}$	$-.1082 \times 10^{12}$	$.3788 \times 10^{12}$	$.1416 \times 10^{13}$	$.3284 \times 10^{12}$
A_1	$-.1956 \times 10^{13}$	$-.3914 \times 10^{13}$	$.6769 \times 10^{12}$	$-.2588 \times 10^{13}$	$-.8546 \times 10^{13}$	$-.1772 \times 10^{13}$
A_2	$.7490 \times 10^{13}$	$.1312 \times 10^{14}$	$-.1882 \times 10^{13}$	$.7732 \times 10^{13}$	$.2256 \times 10^{14}$	$.4184 \times 10^{13}$
A_3	$-.1718 \times 10^{14}$	$-.2563 \times 10^{14}$	$.3050 \times 10^{13}$	$-.1320 \times 10^{14}$	$-.3402 \times 10^{14}$	$-.5644 \times 10^{13}$
A_4	$.2622 \times 10^{14}$	$.3218 \times 10^{14}$	$-.3179 \times 10^{13}$	$.1407 \times 10^{14}$	$.3206 \times 10^{14}$	$.4757 \times 10^{13}$
A_5	$-.2797 \times 10^{14}$	$-.2691 \times 10^{14}$	$.2208 \times 10^{13}$	$-.9596 \times 10^{13}$	$-.1933 \times 10^{14}$	$-.2565 \times 10^{13}$
A_6	$.2127 \times 10^{14}$	$.1199 \times 10^{14}$	$-.1022 \times 10^{13}$	$.4089 \times 10^{13}$	$.7281 \times 10^{13}$	$.8644 \times 10^{12}$
A_7	$-.1154 \times 10^{4}$	$-.5369 \times 10^{13}$	$.3042 \times 10^{12}$	$-.9954 \times 10^{12}$	$-.1567 \times 10^{13}$	$-.1664 \times 10^{12}$
A_8	$.4374 \times 10^{13}$	$.1121 \times 10^{13}$	$-.5279 \times 10^{11}$	$.1060 \times 10^{12}$	$.1475 \times 10^{12}$	$.1401 \times 10^{11}$
A_9	$-.1104 \times 10^{13}$	$-.1040 \times 10^{2}$	$.4071 \times 10^{10}$	-	-	-
A_{10}	$.1668 \times 10^{12}$	-	-	-	-	-
A_{11}	$-.1144 \times 10^{11}$	-	-	-	-	-

technique. Note that the peak acceleration associated with the fitted curve is approximately 21 g's at end of the crush pulse, while the maximum associated with the crash data is 35 g's and occurs early in the pulse. The peak value associated with the fitted curve is a truer representation of the acceleration levels to which the occupant is actually subjected. As expected, the residual content has an average value which appears to be very close to zero (Figure 3-10). This indicates that the integrated value of the polynomial curve (i.e. velocity changes) is the same or very close to the value of the integrated crash pulse acceleration (velocity change). Integration of the straight line segment approximation of the curve fit yielded values of 31 mph for a velocity change and a displacement of approximately 34 inches. These values compare very closely with the 30 mph test impact velocity and longitudinal displacement values of approximately 3 feet derived from integrating accelerometer data from several locations on the vehicle.

The curve fitting program has also been applied to a segment of digitized structural resonance data generated by a vehicle structural excitation test to illustrate its response to nearly pure high frequency data content. The results are shown in Figure 3-12. The frequency of the damped, quasi-sinusoidal resonance is approximately 40 Hz, and the polynomial curve is essentially a straight line through the resonance data, indicating that the curve fitting routine is insensitive to this high frequency content, as desired.

The procedure utilized in the spectrum analysis (see Section 2) of crash test data could be largely automated by computer procedures to assess the effects of high frequency components on occupants. For example, the displacement time history calculated from the residual acceleration curve would represent a displacement-forcing function to an occupant/seatbelt model, and together with seatbelt dynamic load deflection and transmissibility characteristics, could be used to calculate occupant dynamic loading resulting from the residual deceleration curve.

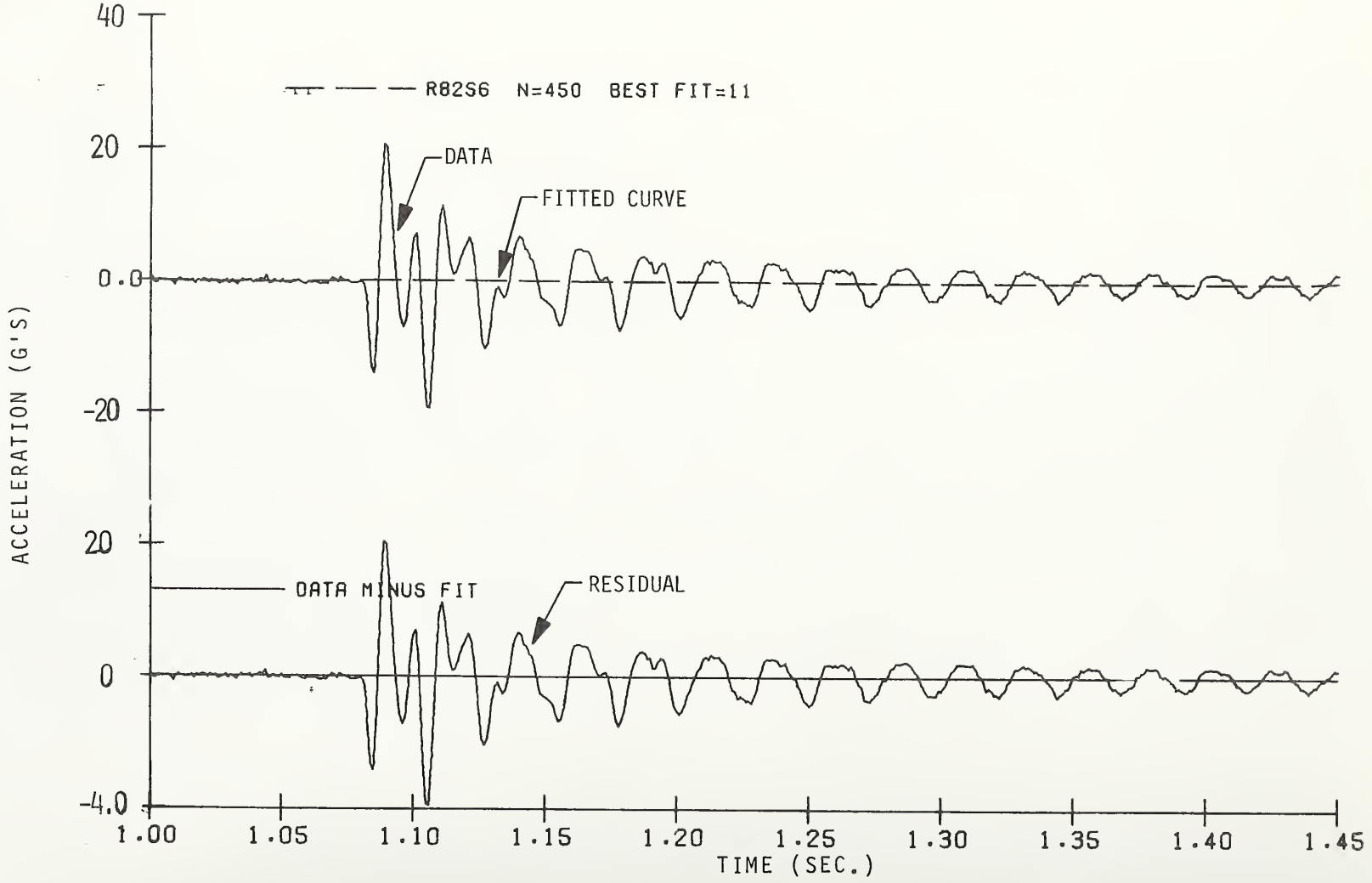

Figure 3-12. Application of Curve Fitting Routine to Structural Resonance Data

These loads would be compared with peak seatbelt loads due to the low frequency deceleration content of the crash response to assess their relative effects and importance.

If the calculated loads are insignificant when compared to the low frequency response loads, the residual decelerations will have been shown to be non-influential to occupant loading. The fitted curve can then be interpreted as representative of gross vehicle plastic deformation and the prime forcing function for deceleration of the occupants.

3.3 DIAGNOSTIC APPLICATIONS OF THE ANALYTICAL CURVE FITTING PROGRAM TO BASIC PULSE SHAPES

To determine the program's capability to fit various pulse shapes, the curve fitting program has been applied to basic pulse shapes, such as triangular, square-wave, trapezoid and half-sine. The results of fitting these shapes with various order polynomials are shown in Figures 3-13 through 3-16. The residual between the pulse shape and the fitted curve is also plotted. These results indicate that the curve fitting routine has an excellent tracking capability when applied to relatively low frequency basic pulse shapes, as desired.

The final diagnostic (and developmental) exercise performed was to apply the curve fitting routine to an analytical function of mixed sinusoids (Figure 3-17). Frequency components of 5, 15, 50 and a fourth frequency of 140 Hz (Figure 3-17) were mixed, and the curve fitting program was applied to this function. The fitted curve was then compared to the four component sinusoidal function and then to the same function minus the highest frequency. Figure 3-17 indicates that for the curve fitting parameters chosen, the curve reproduces the 5, 15, and 50 Hz components and "filters" the 140 Hz components. This demonstrates the program's ability to separate frequency components in various frequency ranges.

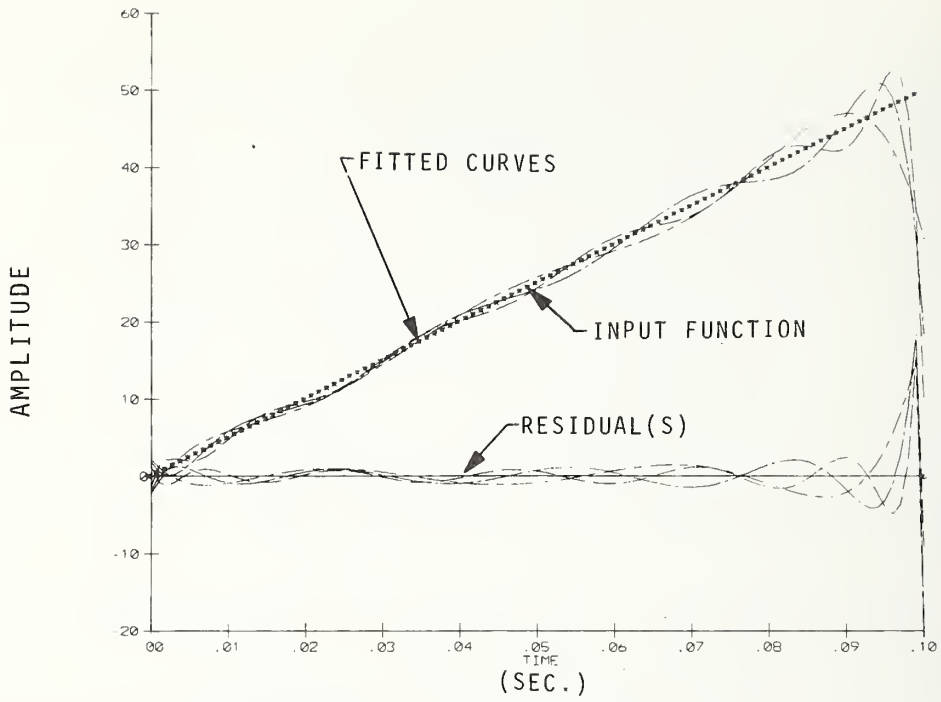

Figure 3-13. Application of Curve Fitting Program to a Triangular Pulse Shape

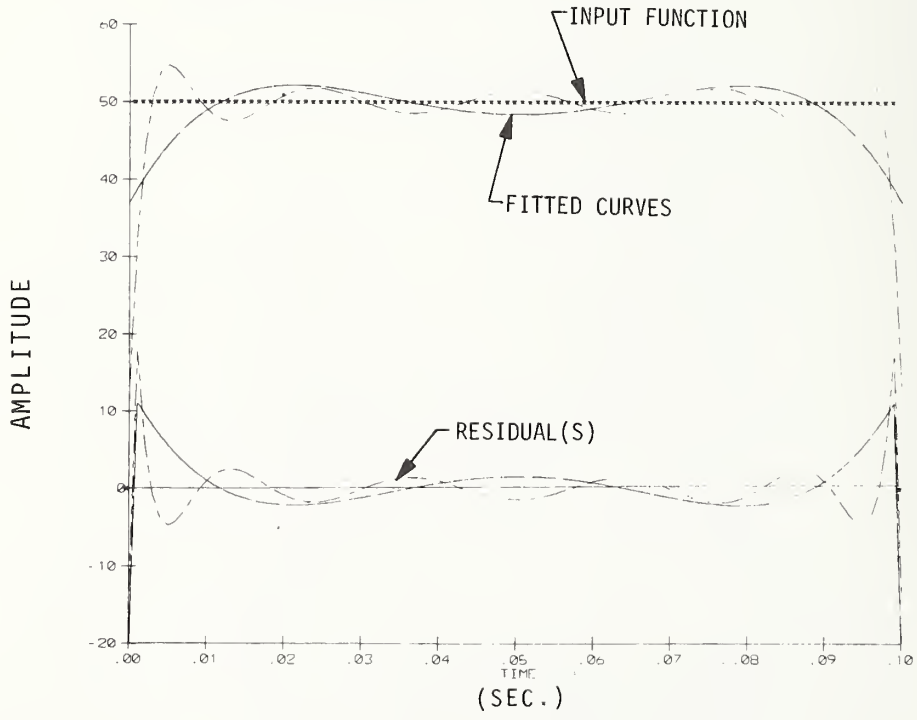

Figure 3-14. Application of Curve Fitting Program to a Square Wave Pulse Shape

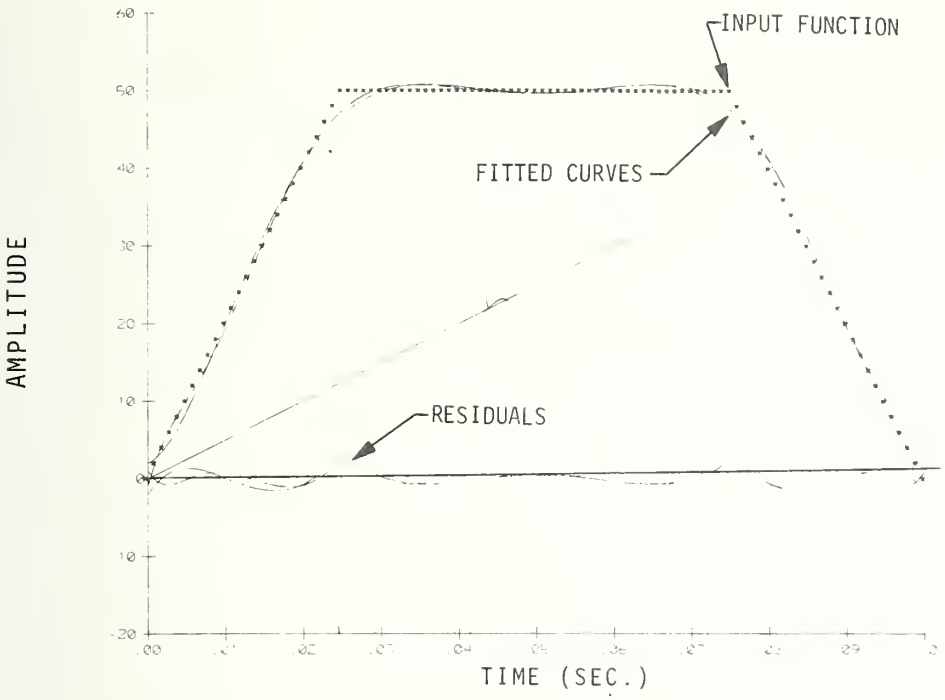

Figure 3-15. Application of Curve Fitting Program to a Trapezoidal Pulse Shape

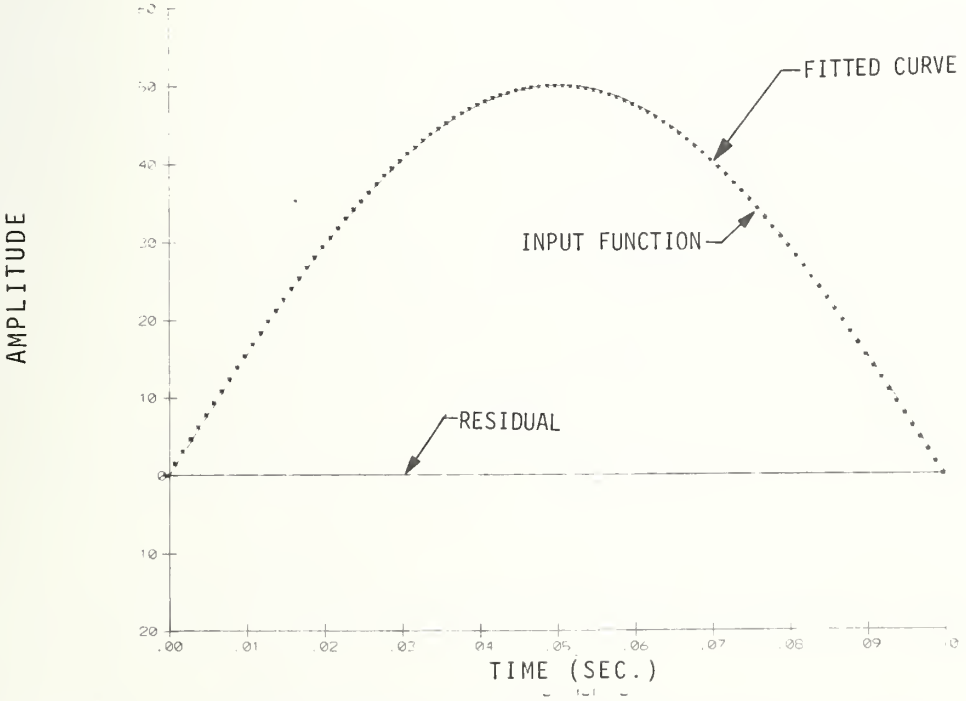

Figure 3-16. Application of the Curve Fitting Program to a Half-Sinusoidal Pulse Shape

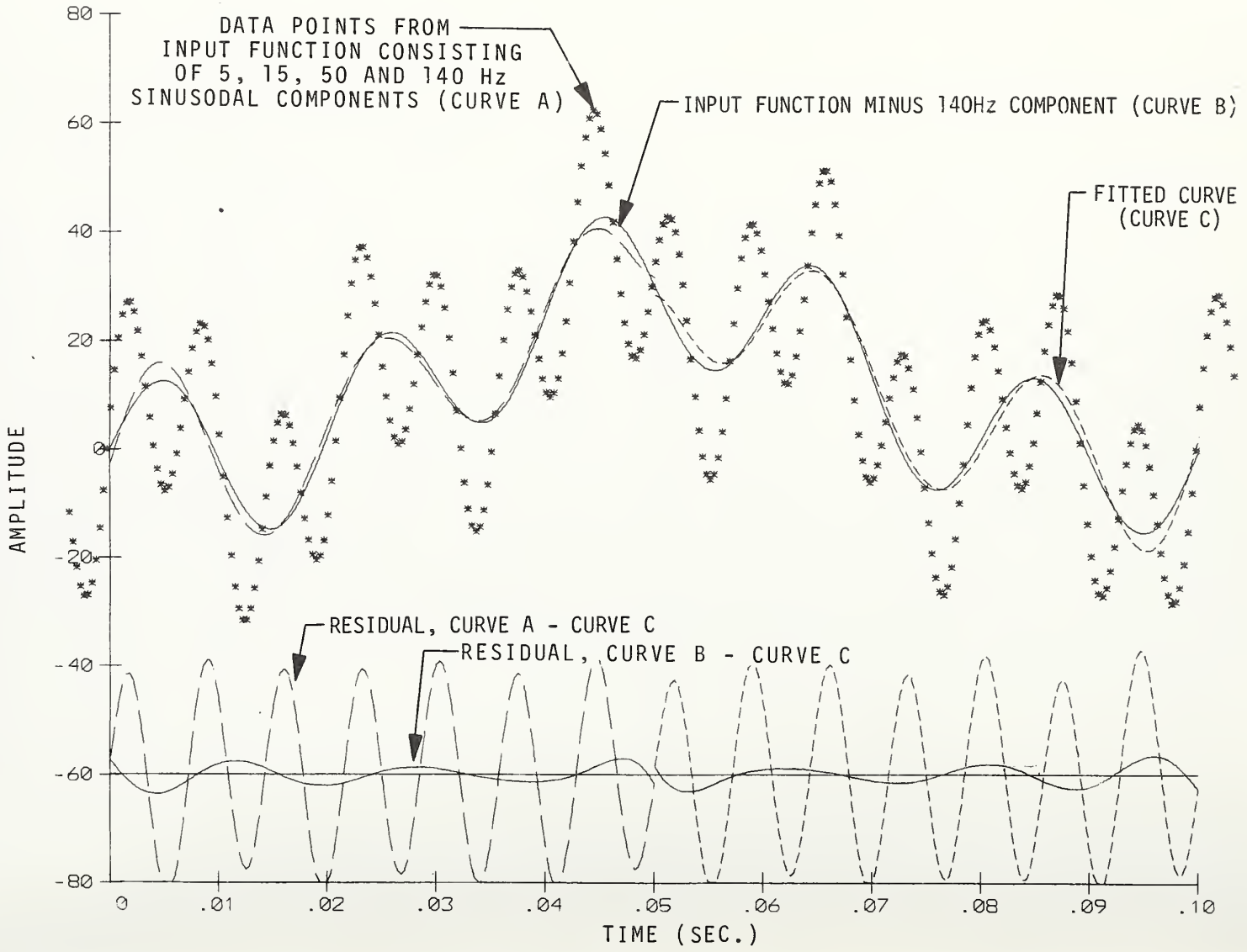

Figure 3-17. Application of Curve Fitting Program to a Mixed Sinusoid Function

REFERENCES

1. DiMasi, F. P.,"Instrumentation Methodology for Automobile Crash Testing," Interim Report, No. DOT-TSC-NHTSA-74-1 (HS-801211) August 1974.

2. Anon., Society of Automotive Engineers Recommended Practice J211a, "Instrumentation for Barrier Collision Tests," 1972.

3. Anon., "Insurance Institute for Highway Safety, 1972 Low Speed Vehicle Impact Testing" Volume II, Prepared for the Insurance Institute by EG&G Inc., EG&G Technical Report No. 336, Dec. 1971.

4. Glenn, T.H.,"Anthropomorphic Dummy and Human Volunteer Testing of Advanced and/or Passive Belt Restraint Systems." SAE Conference Proceedings, Third International Conference on Occupant Protection, Troy, Michigan, July 10-12, 1974.

5. Miller P. M., "Basic Research in Crashworthiness II- Further Refinement in Engine Deflection Concept" Calspan Corportation, Report No. YB-2987-V-18, April 1973.

6. Davis, S.,"Application of the Shock Spectrum to Some Automotive Crashworthiness Problems" Society of Automotive Engineers, Paper No. 720071, Jan. 1972.

7. Federal Motor Vehicle Safety Standard 209, "Seat Belt Assemblies - Passenger Cars, Multipurpose Passenger Vehicles, Trucks and Buses." Code of Federal Regulations, Title 49, Part 571; S209, April 1971.

8. Haley, J. L., "Effects of Rapid Loading Rates on the Stress Strain Properties of Restraint Webbings," Proceedings of the Tenth Stapp Car Crash Conference, Paper No. 660798, Nov. 1966.

9. Roark, R. J., "Forumulas For Stress and Strain," Third Edition, Copyright 1954, McGraw-Hill Book Co., New York.

APPENDIX A
CALCULATION OF APPROXIMATE ROCKING MODE NATURAL FREQUENCY OF A TYPICAL ACCELEROMETER PACKAGE, VEHICLE FLOOR PAN INTERFACE

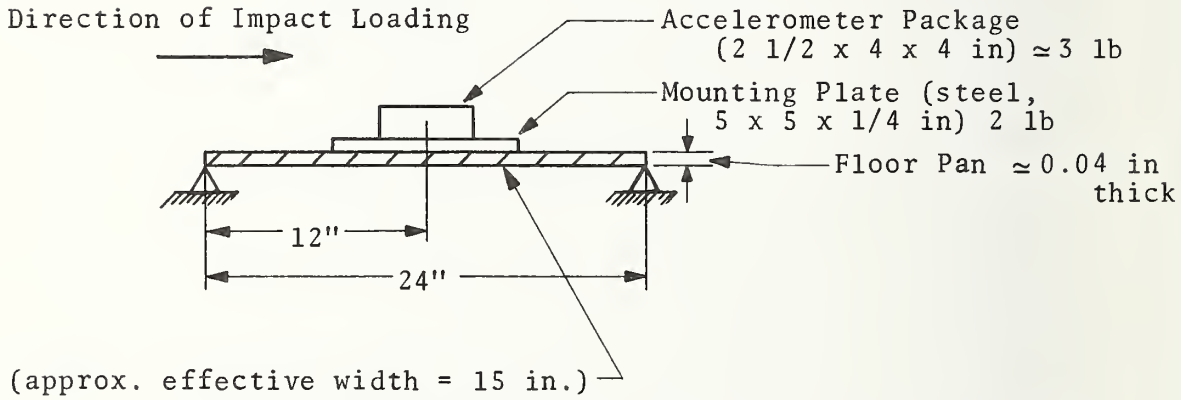

Approximate "equivalent effective floor pan stiffness model

Load Rotational Inertia (Assume Homogeneous Masses)

About Load CG:

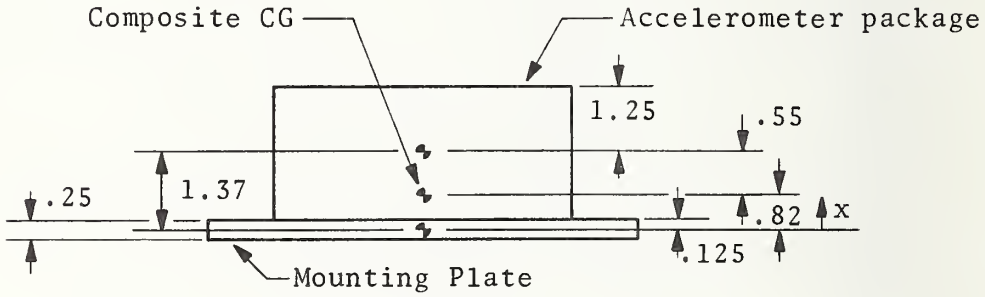

Locate center of Gravity: $\sum M_{cg} = 0$

(2 lb) (x) = (3 lb) (1.37-x)

x = 0.82 in

$$I_{cg} = \sum_{3} \frac{m}{12} (a^2 + b^2) + m r^2$$

$$I_{CG} = \frac{3}{(306)\ (12)}\ (2.5^2 + 4^2) + \frac{3}{386}\ (.55)^2 \quad \text{(accelerometer package)}$$

$$+ \frac{2}{(386)\ (12)}\ (.25^2 + 5^2) + \frac{2}{386}\ (.82)^2 \quad \text{(mounting plate)}$$

$$I_{CG} = .015 + .002 + .011 + .004 \simeq .03 \text{ in lb-sec}^2$$

"Equivalent Beam" Rotational Stiffness:

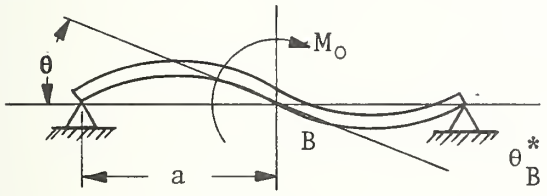

$$\theta_B^* = \left(a - \frac{a^2}{\ell} - \frac{\ell}{3}\right)$$

$$K_\theta = \frac{M_O}{\theta_B} = \frac{EI}{\left(a - \frac{a^2}{\ell} - \frac{\ell}{3}\right)}$$

$$E \text{ (Steel)} = 30 \times 10^6$$

$$I_A = bt^3/12 \text{ (b = 15 in = "effective" width, t = .04 in)}$$

$$I_A = \frac{(15)\ (.04)^3}{12} = 80 \times 10^{-6}$$

$$EI = 2400 \text{ \# in}^2$$

$$K_\theta = (12)\ (2400)/(24) = 1200 \text{ in \#/rad.}$$

Approximate Natural Frequency:

$$f_n = \frac{1}{2\pi}\sqrt{\frac{K_\theta}{I_{CG}}} + \frac{1}{2\pi}\sqrt{\frac{1200}{.03}} \simeq \underline{32 \text{ HZ}}$$

---

*Reference 3, Table III, Formula No 20

Under a dynamic load of e.g. 20 g, having a large period compared with 1/32 sec the moment developed on the beam is approximated by

$$M = (\ddot{X})\ (m)\ (\delta)$$

where δ = offset distance between load CG and the floor pan which is subjected to 20 g deceleration

$$M \simeq (20\ g)\left(\frac{5\#}{g}\right)(.13 + .82) = 95\ \text{in-lb}$$

The resulting rotation of the floor pan support at $\ell/2$ is:

$$\theta = \frac{M}{EI}\left(\frac{\ell}{12}\right) = \frac{95}{2400}\left(\frac{24}{12}\right) \simeq .08\ \text{rad}$$

The resulting translational motion in the longitudinal direction is (assuming longitudinal accelerometer axis is located 1 in. above mounting plate surface):

$$X_\ell = \theta(h) = (.08)\ (1.25) = 0.10\ \text{in}$$

(where h is the distance from the floor pan surface to the longitudinal accelerometer axis)

The acceleration developed by an oscillatory motion of ± 0.10 at the system natural frequency of 32 Hz is

$$\ddot{X} = \frac{x\ (2\pi f^2)}{386\ \text{in/sec}^2/g} = \frac{0.1\ [(2\pi)\ (32)]^2}{386},$$

$$\ddot{X} \simeq 10\ \text{g's (vector)}$$

or 20 g's (peak to peak)

Note that the induced oscillatory acceleration is equal in magnitude to the relatively long duration 20 g input.

APPENDIX B
RECOMMENDATIONS FOR AN EXPERIMENTAL TEST PROGRAM

The object of this experimental test program is to provide crash test data from a single source specifically suited to allow a more detailed analysis than the cursory analysis of Section 2, which used pieces of data from several sources. These analyses include spectrum analysis of occupant compartment accelerometer data and dynamic response characteristics of occupant seatbelt load-time histories. These analyses are intended to provide insight into the effects various frequency components in the vehicle deceleration time history may have on occupant loading. This information is necessary in order to specify appropriate filtering characteristics for occupant compartment accelerometer data. Another objective of the test plan is to quantify the effects of accelerometer package size. The calculations made in Appendix A indicate that large accelerometer packages (in order of 5 lb total) in conjunction with typical floor pan stiffness can induce structural resonances well within the bandwidth of current filtering practices.

The data required to meet these objectives could be obtained by providing additional instrumentation to a scheduled vehicle compliance test, such as an FMVSS 301/208/212 test for fuel tank integrity, occupant protection and windshield retension. The 30 mph frontal barrier compliance test represents a desirable test configuration, as described in Section 2, in that structural damage is basically limited to the front structure with little or no deformation of the occupant compartment. The occupant compartment should remain rigid throughout the crash ride-down and longitudinal accelerometer data measured at any two rigid points in the occupant compartment should be identical, if structural resonances did not occur.

Data acquisition for this test will basically consist of the four corner accelerations (as defined by Figure 2-11 in Section 2.) two side-sill, tunnel, engine, and rear deck accelerations and seatbelt load cell data. Barrier force time history and dynamic and static crush distances are desirable pieces of data, but not

essential to the test plan. Calibration voltages should preceed each data parameter, and each data segment should be synchronized to a standardized time base.

The four corner accelerometer packages should consist of longitudinal and vertical accelerometers and should be mounted in the standard Calspan manner. This consists of a 5x5x1/4 in steel plate welded to the floor pan, with the accelerometer package attached using bolts and the threaded holes in the welded base plate. After installation of accelerometers and associated electronic support equipment, the vehicle should be excited in the longitudinal direction using a 5 mph bumper pendulum test and in the vertical direction by dropping the vehicle from a height of several inches onto four wooden blocks under the main frame. The actual drop height should be selected such that reasonable acceleration signal levels are generated, as discussed in Section 2. Accelerometer outputs due to these excitations should be recorded on one-inch 14 channel IRIG format intermediate band magnetic tape. No filtering of the data should be applied unless specified, and all data should be recorded on magnetic tape and reproduced in a specified format on a second magnetic tape per Table B-1 (segments 1 through 4). Associated with Table B-1 is a set of notes which describes how each data parameter is to be used in the analysis. The analog processing operations indicated in Table B-1 should be performed on the raw data. Dimensional and weight information on the accelerometer package physical components should be made available and the standard (biaxial) accelerometer package should be subjected to a vibration test along both principal direction(s) in order to experimentally determine the resonant modes of vibration of the accelerometer package. The transmissibility plot should be included as part of the data package.

The second phase of structural excitation testing is intended to quantify the effects of using lighter accelerometer packages having lower profiles. The four corner and tunnel and rear deck accelerometer packages should be replaced by a minimum weight and profile bracket, which is to be mounted to the structure using the same welded steel plate. The new mounting configuration

will be basic, simple and will not be furnished with "protective covers." The vehicle will again be subjected to identical pendulum and drop tests as in part one, and unfiltered data is to be recorded as described in Table B-1, segments 5 through 8 having the same format as segments 1 through 4. The minimum weight accelerometer configuration should also be subjected to a vibration test to identify resonances associated with this package along principal axes. The transmissibility plot(s) should be included with the data package.

The final phase of testing involves data acquisition corresponding to the 30 mph frontal barrier impact test. The required basic raw data for meeting the primary data analysis objectives is outlined in Table B-1, segments 9,10 and 11. In the full scale test, it is desirable to obtain accelerometer data from opposite sides of the vehicle at a particular station for the case where the standard size accelerometer package is mounted on one side of the vehicle and the smaller, low profile configuration is used on the opposite side. The accelerometers located at corners 3 and 4 and/or the accelerometer located on the rear deck are recommended for this purpose. This data will be analyzed in the manner described in Section 2 to determine the meaningful frequency content of occupant compartment data. The frequency distribution of signal and noise components shall be used to determine filter characteristics. Digital filtering is preferable because of zero phase shift characteristics and the flexibility in constructing roll-off characteristics (using the fast Fourier transform "straight line" filter and inverse Fourier transform technique). The curve fitting routine shall also be applied to the unfiltered occupant compartment data for comparison purposes.

Segments 12 through 15 contain additional recommended data reduction operations on basic data acquisition parameters for use in generating quantities that may prove valuable in assessing vehicle structural performance. Energy dissipation versus time and the time integral of this quantity are processed in segment 12. Relative and absolute velocities and displacements can be

generated from segment 13 and segment 14 data. Cross plotted data is listed under segment 15 and contains occupant compartment acceleration versus crush distance, barrier force data versus occupant compartment displacement, and integrated structural energy dissipation associated with front structure crush and engine decelerations, plotted versus crush distance. The mechanics of assembling this battery of vehicle evaluation parameters will illustrate the feasibility of making such measurements and allow further assessment of their usefulness.

Dynamic load deflection data of the seatbelt webbing used in the test is another necessary piece of information for the analysis. This data, however, is almost certain to be available from seatbelt webbing manufacturers and need not be obtained from special laboratory tests.

Other related test objectives which might be considered in a similary program might include an assessment of the effect of mechanical filtering of acceleration data (i.e. the mounting of accelerometer packages in a "tuned" vibration isolation system), and the effects of adding damping material to the structure in the transducer mounting area.

TABLE B-1. CRASH TEST DATA ACQUISITION PARAMETERS FOR ANALYTICAL TEST PROGRAM

	SEGMENT 1(pt)		SEGMENT 2(pt)		SEGMENT 3(dt)		SEGMENT 4(dt)		SEGMENT 5(pt)	
CHANNEL	PARAMETER	NOTE	PARAMETER	NOTE	PARAMETER	NOTE	PARAMETER	NOTE	PARAMETER	NOTE
1	C1 $\ddot{X}_{\ell}$	1	C1 $\ddot{X}_{v}$	4	C1 $\ddot{X}_{\ell}$	5	C1 $\ddot{X}_{v}$	5	↑	6
2	C2 $\ddot{X}_{\ell}$	1	C2 $\ddot{X}_{v}$	4	C2 $\ddot{X}_{\ell}$	5	C2 $\ddot{X}_{v}$	5		
3	C3 $\ddot{X}_{\ell}$	1	C3 $\ddot{X}_{v}$	4	C3 $\ddot{X}_{\ell}$	5	C3 $\ddot{X}_{v}$	5		
4	C4 $\ddot{X}_{\ell}$	1	C4 $\ddot{X}_{v}$	4	C4 $\ddot{X}_{\ell}$	5	C4 $\ddot{X}_{v}$	5		
5	T $\ddot{X}_{\ell}$	1	T $\ddot{X}_{v}$	4	T $\ddot{X}_{\ell}$	5	T $\ddot{X}_{v}$	5		
6	RDR $\ddot{X}_{\ell}$	1	RDR $\ddot{X}_{v}$	4	RDR $\ddot{X}_{\ell}$	5	RDR $\ddot{X}_{v}$	5		
7	RDR $\ddot{X}_{\ell}$	1	RDL $\ddot{X}_{v}$	4	RDL $\ddot{X}_{\ell}$	5	RDL $\ddot{X}_{v}$	5		
8	(C1-C2) $\ddot{X}_{\ell}$	2	BLANK	-	BLANK	-	BLANK	-		
9	(C1+C2)/2 $\ddot{X}_{\ell}$	3	↓		↓		↓		Same as Segment 1	
10	(C3-C4) $\ddot{X}_{\ell}$	2								
11	(C3+C4)/2 $\ddot{X}_{\ell}$	3								
12	(C1+C2+C3+C4)/4 $\ddot{X}_{\ell}$	3								
13	(RDR-RDL) $\ddot{X}_{\ell}$	2								
14	SYNCH	-	SYNCH		SYNCH		SYNCH			—

TABLE B-1. CRASH TEST DATA ACQUISITION PARAMETERS FOR ANALYTICAL TEST PROGRAM (CONT'D)

	SEGMENT 6(pt)		SEGMENT 7(dt)		SEGMENT 8(dt)		SEGMENT 9		SEGMENT 10	
CHANNEL	PARAMETER	NOTE	PARAMETER	NOTE	PARAMETER	NOTE	PARAMETER	NOTE	PARAMETER	NOTE
1	C1 $\ddot{X}_v$	6	Same as Segment 3	6	Same as Segment 4	6	Same as Segment 1	7	C1 $\ddot{X}_v$	4
2	C2 $\ddot{X}_v$							7	C2 $\ddot{X}_v$	4
3	C3 $\ddot{X}_v$							7,8	C3 $\ddot{X}_v$	4
4	C4 $\ddot{X}_v$							7,8	C4 $\ddot{X}_v$	4
5	T $\ddot{X}_v$							7	T $\ddot{X}_v$	4
6	SS1 $\ddot{X}_\ell$							7	E $\ddot{X}_\ell$	9
7	SS2 $\ddot{X}_\ell$							7	E $\ddot{X}_v$	9
8	(SS1-SS2)$\ddot{X}_\ell$							2	SS1 $\ddot{X}_\ell$	10
9	(SS1+SS2)/2$\ddot{X}_\ell$							3	SS2 $\ddot{X}_\ell$	10
10	SS1 $\ddot{X}_v$							2	(SS1-SS2)/$\ddot{X}_\ell$	2
11	SS2 $\ddot{X}_v$							3	(SS2+SS2)/2$\ddot{X}_\ell$	3
12	BLANK							3	SS1$\ddot{X}_v$	4
13	"							2	SS2$\ddot{X}_v$	4
14	SYNCH	-				-		-	SYNCH	-

TABLE B-1. CRASH TEST DATA ACQUISITION PARAMETERS FOR ANALYTICAL TEST PROGRAM (CONT'D)

	SEGMENT 11		SEGMENT 12		SEGMENT 13		SEGMENT 14		SEGMENT 15	
CHANNEL	PARAMETER	NOTE	PARAMETER	NOTE	PARAMETER	NOTE	PARAMETER	NOTE	PARAMETER	NOTE
1	SBD-1	11	TBF	14	C1 $\dot{X}_\ell$	19	C1 X_ℓ	14	C1 $\ddot{X}_\ell$ vs C1 X_ℓ	21
2	SBD-2	11	C1 X_ℓ	14	C2 $\dot{X}_\ell$		C2 X_ℓ		C3 $\ddot{X}_\ell$ vs C3 X_ℓ	21
3	SBD-3	11	E $\ddot{X}_\ell$	14	C3 $\dot{X}_\ell$		C3 X_ℓ		RDL $\ddot{X}_\ell$ vs RDL X_ℓ	21
4	SBP-1	11	E X_ℓ	14	C4 $\dot{X}_\ell$		C4 X_ℓ		TBF vs C1 X_ℓ	20
5	SBP-2	11	C2 X_ℓ	14	T $\dot{X}_\ell$		T X_ℓ		TBF vs C3 X_ℓ	20
6	SBP-3	11	E X_V	14	RDR $\dot{X}_\ell$		RDR X_ℓ		TBF vs RDL $\ddot{X}_\ell$	20
7	C3 $\ddot{X}_\ell$	11	(TBF)(C1X_ℓ)	15	RDL $\dot{X}_\ell$		RDL X_ℓ		$\int_0^{C1X_\ell}$ (TBF)(C1X_ℓ) vs C1X_ℓ	17
8	C4 $\ddot{X}_\ell$	11	(TBF)(C2X_ℓ)	15	E $\dot{X}_\ell$		E X_ℓ		$\int_0^{EX_\ell}$ (EX_ℓ)(EX_ℓ) vs C1X_ℓ	17
9	T $\ddot{X}_\ell$	11	($\ddot{EX}_\ell$)(EX_ℓ)	16	BLANK	-	BLANK	-	BLANK	-
10	SBD1+SBD2+SBD3	11,12	$\ddot{EX}_V$	14						
11	SBP1+SBP2+SBP3	11,12	($\ddot{EX}_V$)(EX_V)	16						
12	SBD1+SBD3	11,13	$\int_0^t$ (TBF)(C1X_ℓ)	17						
13	SBP1+SBP3	11,13	$\int_0^t$ ($\ddot{EX}_\ell$)(EX_ℓ)	18						
14	SYNCH	-	SYNCH	-	SYNCH		SYNCH			

Notes Corresponding to Table B-1

(1) For a mild, 5 mph pendulum impact, spectrum analysis of this parameter is useful in identifying longitudinal structural resonant frequencies and other noise sources associated with the structure or instrumentation package. Accelerometer packages should be installed in their normal corner locations and normal configurations.

(2) This analog operation further isolates noise sources by subtracting out the low frequency in-phase components. Evaluate using spectrum decomposition.

(3) This analog operation will assess the effects of averaging data from symmetrically located transducers to reduce the noise level using spectrum decomposition techniques.

(4) A similar response in terms of spectral composition of the vertical response to a longitudinal excitation can be expected if a coupled "rocking mode" resonance exists in the transducer mounting configuration. Comparison of vertical and longitudinal spectral components can be used to assess this occurance.

(5) Spectrum analysis of longitudinal and vertical structural response to vertical excitation at a particular location can be used to determine if coupled motion responses exist. This data is easy to obtain and should be acquired for completeness, although it is of secondary importance relative to longitudinal excitation data.

(6) This data is to be acquired for the purpose of assessing the effects of using minimum weight and profile accelerometer packages on the structural response to the 5 mph pendulum test and on the drop test. Analog functions will be evaluated as described in notes 2 and 3, and the effects on "rocking mode" coupling will be evaluated per note 4. As before, the response to vertical excitation is easy to obtain, although it is of secondary importance relative to longitudinal excitation data.

(7) This data is taken from the barrier crash testing phase of the test program; accelerometer data will be spectrum analyzed to determine if peak levels of high frequency components correlate with peak frequencies in the spectrum analysis of pendulum test excitation data. Standard accelerometer package configurations are to be used for this measurement. The data will be analyzed to determine suitable filtering characteristics, which will make the important features of the pulse more visible. Pulse shape rise time, average and peak values of the basic pulse are the principal parameters of interest. These characteristics can be optimized for the available crush distance of a certain vehicle and for tailoring restraint system characteristics to the crash ride-down pulse.

Integrated accelerometer data is also used to provide vehicle velocity and displacement profiles which may be used in conjunction with other data acquisition parameters to construct vehicle-structural evaluation parameters (to be discussed).

(8) Accelerometer data from this vehicle station should be acquired using the standard accelerometer package on the driver side and a minimum weight and profile accelerometer on the opposite side (corners 3 and 4). This data will be spectrum analyzed to quantify the effects of the lighter accelerometer package under impact conditions.

(9) The motion characteristics of the large concentrated engine transmission mass have an important effect on vehicle ride-down in terms of effecting available crush space.

(10) This data should be acquired using the minimum weight and profile accelerometer packages. The locations are the side sills, just forward of the front seat edge at the driver and front passenger locations as used in the GM methodology. The combination of smaller accelerometer package size and what appears to be a substantially stiffer location is expected to show a much cleaner deceleration pulse. The data will be spectrum analyzed and compared with data from C1 and C2 locations.

(11) Seatbelt load-time history data will be analyzed to characterize the seatbelt/dummy system as a one degree of freedom, second order system. The response will be compared with the acceleration data at corners 3 and 4 and tunnel locations to determine if high frequency oscillations at these locations are inducing oscillatory belt loads. Spectrum analysis of seatbelt data and characterizing the seatbelt/dummy system as described above will provide a means of estimating transmitted forces to the occupant due to high frequency motions.

(12) This parameter represents total belt force loading of the occupant.

(13) This parameter represents the summation of outboard seatbelt loads, driver and passenger locations.

(14) This parameter is used with other basic data acquisition parameters to produce derived data which characterizes vehicle performance during impact.

(15) This parameter is constructed from basic data parameters and represents the energy dissipation time history between the point of impact for a frontal crash and front seat passenger locations. This parameter characterizes the energy absorption behavior of the front structure.

(16) This parameter is proportional to the approximate energy dissipation time history associated with deceleration of the engine/transmission mass.

(17) This parameter represents the total energy dissipated by the structure over the duration of the crash. This parameter may be plotted versus time or versus crush, and together with other parameters, such as front end structure, dynamic stiffness and available crush distance, may be used to approximate the maximum energy absorption capability and therefore to approximate the maximum survivable crash speed of a vehicle.

(18) This parameter represents total energy dissipation associated with decelerating the engine/transmission mass. This parameter is of secondary interest, but may be useful in approximating the energy dissipation ratio between decelerating the engine transmission mass relative to the total energy dissipated in the crash (i.e. the effect of engine size and weight).

(19) Although no planned use for this parameter exists this data is easy to provide and should be included for completeness.

(20) This parameter may be useful in establishing a dynamic load deflection curve for the front structure.

(21) This parameter is useful for the visualization of structural crush/deceleration characterizations, indicating the buildup and level of accelerations as a function of vehicle crush and the efficient utilization of available crush distance.

APPENDIX C

COMPUTATIONAL METHODOLOGY OF LEAST SQUARED ERROR POLYNOMIAL CURVE FITTING ROUTINE

Dr. K. H. Wassmuth

Least squared error polynomial fitting is accomplished by finding the polynomial which minimizes the sum of the squares of the differences between the observed data values and their corresponding polynomial values. The normal method of finding this polynomial produces a set of m+1 linear equations, where m is the order of the polynomial desired. In practice, the solution of this set of of equations, when m becomes larger than about five, tends to become difficult, since the determinant of the equations is often very small. This leads to round off errors in the computer which can often produce erroneous results.

One method of overcoming this computational difficulty is to use orthogonal polynomials in the calculation of the least squared error polynomial. The use of orthogonal polynomials leads to a set of equations for which all the terms of the main diagonal are zero; hence the solution is direct and trivial. Now, however, the set of orthogonal polynomials must be calculated.

The curve fitting routine described in this report uses the three term recurrence relation necessary for all orthogonal polynomials to generate a set of orthogonal polynomials from the data which is then combined to find the coefficients of the simple polynomial of order m.*

---

*Reference: Hamming, R. W., Numerical Methods for Scientists and Engineers, "Interactional Series in Pure and Applied Mathematics," Chapter 18, p. 245, 1962.

Any three consecutive orthogonal polynomials are related by

$$P_{n+1}(x) = (A_n x + B_n)P_n(x) - C_n P_{n-1}(x).$$

This relationship can be rewritten as

$$P_0(x) = 1$$

$$P_1(x) = xP_0(x) - \alpha_1 P_0(x)$$

$$P_J(x) = xP_{J-1}(x) - \alpha_J P_{J-1}(x) - \beta_J P_{J-2}(x) \qquad J>1 \qquad \text{(eq. C.1)}$$

where α_J and B_J are to be determined.

Using some of the properties of orthogonal polynomials

$$\alpha_{J+1} = \frac{\sum_{k=1}^{n} x_k P^2_J(x_k)}{\sum_{k=1}^{n} P^2_J(x_k)} \qquad \text{(eq. C.2)}$$

and

$$\beta_{J+1} = \frac{\sum_{k=1}^{n} y_k P_J(x_k)\, P_{J-1}(x_k)}{\sum_{k=1}^{n} P^2_{J-1}(x_k)} \qquad \text{(eq. C.3)}$$

where n is the number of observed values of data and $P_J(x_k)$ is the calculated value of the J^{th} order orthogonal polynomial at the value x_k.

Additionally, using the corresponding values for Y_k, multiplier coefficients.

$$A_J = \frac{\sum_{k=1}^{n} Y_k P_J(x_k)}{\sum_{k=1}^{n} P^2_J(x_k)} \qquad \text{(eq. C.4)}$$

can be calculated to minimize the least square error for the polynomial

$$\sum_{J=0}^{m} A_J P_J \qquad \text{(eq. C.5)}$$

That is, for a given order m and a given set of n data points (m<n)

$$\sum_{k=1}^{n} \left[Y(k) - \sum_{J=0}^{m} A_J P_J (k) \right]^2$$

is a minimum.

A simple example will illustrate the workings of this method. Assume the n values of x and y are determined by the equation

$$y = 1+x+x^2$$

Assume n = 5 in the internal $0 \leq x \leq 4$, then

$x = 0, 1, 2, 3, 4$

$y = 1, 3, 7, 13, 21$

from eq. C.1, $P_0 = 1$

from eq. C.2,

$$\alpha_1 = \frac{\sum_{k=1}^{5} x_k \cdot 1}{\sum_{k=1}^{5} 1} = \frac{10}{5} = 2$$

then, from eq. C.1, $P_1 = x-2$

from eq. C.4

$$A_0 = \frac{\sum_{k=1}^{5} Y_K \cdot 1}{\sum_{k=1}^{5} 1} = \frac{45}{5} = 9$$

and,

$$A_1 = \frac{\sum_{k=1}^{5} Y_k(x_k - 2)}{\sum_{k=1}^{5} (x_k - 2)^2} = \frac{50}{10} = 5$$

therefore, the least squares polynomial for order 1 by equation C.5 is:

$$9 \cdot (1) + 5(x-2) = 5x - 1$$

Continuing the same calculations for J=2,

$$P_2 = x^2 - 4x + 2$$

and

$$A_2 = 1$$

with the result that the least squared polynomial for order 2 by eq. C.5 is:

$$9 \cdot (1) + 5 \cdot (x-2) + 1 \cdot (x^2 - 4x + 2)$$

$$= x^2 + x + 1$$

which, of course, is exact as it should be. If higher orders were desired, the routine would calculate

$$P_3 = x^3 - 6x^2 + 8.6x - 1.2$$

but with $A_3 = 0$, thus producing the same equation as above.

As seen by the equations and as illustrated in the example, this method calculates the orders of polynomials in sequence. This allows for a best fit methodology. The least squares fit for order zero is calculated, then modified for order one, then modified for order two, etc. By comparing two consecutive residues, the best fit can be defined as having order m where the residue of order m+1 is larger than order m. In computer terms, this means that round off error has occurred at order m+1, making the

resulting polynomial worse in the least square sense than that found for order m. This has advantages in determining if double precision calculations are needed in order to obtain a fit of a desired ordered polynomial on a given computer. It also allows for best fit polynomials with only slightly more computation than a straight fit.

The program listing follows as Figure C-1. User instructions for this curve fitting routine are found in the comments preceding the program listing.

```
C TITLE  ORTHOGONAL POLYNOMIAL LEAST SQUARES
C
C     SUBROUTINE OPLSQ
C
C     PURPOSE
C        TO FIT A POLYNOMIAL TO A SET OF DATA POINTS IN THE
C        LEAST SQUARE SENSE BY USE OF THE GENERALIZED ORTHOGONAL
C        POLYNOMIALS WHICH ARE GENERATED FROM THE DATA.
C
C
C
C     USAGE
C        CALL OPLSQ(X,Y,N,M,POL,RES,P,M23,E)
C
C     DESCRIPTION OF PARAMETER
C
C        X     -INPUT VECTOR OF ARGUMENT VALUES.
C        Y     -INPUT VECTOR OF FUNCTION VALUES.
C        N     -NUMBER OF X AND Y VALUES.
C        M     -DEGREE OF POLYNOMIAL DESIRED.
C                 IF M IS NEGATIVE OUTPUT WILL BE BEST FIT UP TO ORDER M,
C                 IN THIS CASE M WILL BE SET EQUAL TO ORDER FIT AT OUTPUT.
C        POL   -RESULTING VECTOR OF THE COEFFICIENTS OF POWERS OF X
C                 ORDER FROM LOW TO HIGH.
C                 DIMENSION OF POL MUST BE AT LEAST M+1.
C        RES   -OUTPUT SUM OF SQUARE OF DIFFERENCES AT THE DATA POINTS.
C                 IF -999. AT INPUT, CALCULATION IS SUPPRESED.
C        P     -2 DIMENSIONAL WORK AREA WITH DIMENSIONS (M23,N)
C        M23   -CONSTANT  = 2*M + 3
C        E     -OUTPUT VECTOR OF FUNCTION VALUES
C                 E HAS DIMENSIONS  N
C                 IF E(1) = -999 AT INPUT, CALCULATION IS SUPPRESED.
C
C     COMMENTS
C        ALL REAL VARIABLES ARE DOUBLE PRECISION.
C        RUN TIME FOR NEGATIVE N IS SLIGHTLY LONGER THAN POS N.
C        OBJECT TIME EXAMPLES
C             N=100, M=5 (TIME=1.54 SEC),  M=-5 (TIME=2.15 SEC)
C             N=100, M=10(TIME=3.80 SEC),  M=-10(TIME=5.75 SEC)
C                TIME VARIES LINEARLY WITH N
C             N=200, M=5 (TIME=3.12 SEC),  M=-5 (TIME=4.40 SEC)
C
      SUBROUTINE OPLSQ(X,Y,N,M,POL,RES,P,M23,E)
      IMPLICIT REAL*8 (A-H,O-Z)
      DIMENSION E(1)
      DIMENSION  P(M23,N),X(1),Y(1),POL(1)
      DIMENSION A(50),AS(500)
      KSW=0
      STRES=1.E30
      M1=M+1
      IF (M .LT. 0) M1=-M1+2
      M2=M1+1
      DO 3 I=1,M1
      DO 2 J=1,N
      P(M2,J)=1.0
    2 P(I,J)=0.0
      A(I)=0.0
    3 P(I,I)=1.0
C
C     INTIALIZATION FINISHED
C
```

Figure C-1. Program Listing - Orthogonal Polynomial Least Squared Error Curve Fitting Routine

```
      ALP= X(1)
      A(1)=Y(1)
      DO 4 K=2,N
      ALP=ALP+X(K)
    4 A(1)=A(1)+ Y(K)
      A(1)=A(1)/N
      ALP=ALP/N
      P(2,1)=-ALP
      VOT=N
      IF (M .EQ. 0) GO TO 16
      J=2
      MM=2*M1+1
      IF (M .LT. 0) GO TO 17
    9 CONTINUE
C
C     FIND VALUE OF P(J) AT X(K)
C
      BTM=VOT
      VOT=0.0
      JJ=M1+J
      DO 6 K=1,N
      P(JJ,K)=1.0
      DO 5 JL=2,J
      L=J-JL+1
    5 P(JJ,K)=P(JJ,K)*X(K)+P(J,L)
      P(MM,K)=P(JJ,K)*P(JJ,K)
      VOT=VOT+P(MM,K)
C
C     COMPUTE A(J)
C
    6 A(J)=A(J)+P(JJ,K)*Y(K)
      A(J)=A(J)/VOT
      IF(J .EQ. M1) GO TO 10
      J=J+1
      BET=0
      ALP=0.
C
C     COMPUTE NEXT ALPHA AND BETA
C
      DO 7 K=1,N
      ALP=ALP+X(K)*P(MM,K)
    7 BET= BET + X(K)*P(JJ-1,K)*P(JJ,K)
      ALP=ALP/VOT
      BET=BET/BTM
C
C     COMPUTE  P(J,IT)
C
      JM1=J-1
      P(J,1)=-ALP*P(J-1,1)-BET*P(J-2,1)
      DO 8 IT=2,JM1
    8 P(J,IT)=P(J-1,IT-1)-ALP*P(J-1,IT)-BET*P(J-2,IT)
      IF (M .LT. 0) GO TO 17
      GO TO 9
   10 IF (M .LT. 0) M=-M
      DO 14 I=1,M1
      POL(I)=0.
      DO 14 J=1,M1
   14 POL(I)=POL(I)+P(J,I)*A(J)
      IF ((E(1) .EQ. -999.) .AND. (RES .EQ. -999.)) GO TO 22
      IF(KSW .EQ. 1) GO TO 22
      DO 16 K=1,N
```

Figure C-1. Program Listing - Orthogonal Polynomial Least Squared Error Curve Fitting Routine (Continued)

```
      E(K)=POL(M1)
      DO 15 JL=2,M1
      L=M1-JL+1
   15 E(K)=E(K)*X(K)+POL(L)
   16 CONTINUE
      IF (RES .EQ. -999.) GO TO 22
      IF (KSW .EQ. 1) GO TO 23
      RES=0.0
      DO 21 I=1,N
   21 RES=RES+(E(I)-Y(I))**2
   22 RETURN
   23 RES=STRES
      GO TO 22
   17 RES=0.
      JM1=J-1
      IUP=0
      DO 18 K=1,N
      VL=0.
      DO 20 L=1,JM1
      JM=M1+L
   20 VL=VL+P(JM,K)*A(L)
      E(K)=ES(K)
      ES(K)=VL
      IF(K .EQ. 1 .OR. K .EQ. 2) GO TO 18
      IF(ES(K-2) .LT. ES(K-1) .AND. ES(K-1) .GT. ES(K)) IUP=IUP+1
      IF(ES(K-2) .GT. ES(K-1) .AND. ES(K-1) .LT. ES(K)) IUP=IUP+1
   18 RES=RES+(VL-Y(K))**2
      IF (RES .GT. STRES) GO TO 19
      IF(IUP .GT. 28) GO TO 19
      STRES=RES+1.E-18
      GO TO 9
   19 M=J-3
      M1=M+1
      KSW=1
      GO TO 10
      END
```

Figure C-1. Program Listing - Orthogonal Polynomial Least Squared Error Curve Fitting Routine (Concluded)


HE
18.5
.A34
no.
DOT
TSC
NHTSA
75-2
BORROWER
Form DOT F 172
FORMERLY FORM DO
Dept. OST
Library

00347304

Analysis of automobile crash test data and recommendations for ac
DiMasi, Frank P;United States. National Highway Traffic Safety A
National Transportation Library, United States Department of Tran
[156] analysisofautomo00dima
DOT-TSC-NHTSA-75-2
Aug 17, 2015